

**INNATE IMMUNE ANTAGONISM BY DIVERSE  
CORONAVIRUS PHOSPHODIESTERASES**

Stephen A. Goldstein

A DISSERTATION

in

Cell and Molecular Biology

Presented to the Faculties of the University of Pennsylvania

in

Partial Fulfillment for the

Degree of Doctor of Philosophy

2019

Supervisor of Dissertation

---

Susan R. Weiss, Ph.D.  
Professor of Microbiology

Graduate Group Chairperson

---

Daniel Kessler, Ph.D.  
Associate Professor of Cell and Developmental Biology

Dissertation Committee:

Paul Bates, Professor of Microbiology

Sara Cherry, Professor of Microbiology

Matthew Weitzman, Professor of Microbiology

Carolina Lopez, Associate Professor of Microbiology and Immunology

## ACKNOWLEDGEMENTS

I have been fortunate and privileged to do this work under the mentorship of Dr. Susan Weiss. Together I think we have struck a perfect balance of close guidance and support while allowing me a great deal of latitude to pursue my ideas. Aside from support for my work at the bench, Susan has provided invaluable mentorship in grant and manuscript writing. Most importantly perhaps, Susan fosters a collegial, healthy work environment conducive to scientific progress.

My thesis committee has been indispensable as well and I'm sure will remain valuable mentors in the future. Thank you to Dr. Paul Bates, Dr. Sara Cherry, Dr. Matthew Weitzman, and Dr. Carolina Lopez who have been available to me at any time throughout my years here.

The other members of the Weiss lab also have my thanks for their scientific support and valuable personal relationships. Ruth Elliott taught me many of the things I've needed to have success and Yize (Henry) Li has been an unparalleled sounding board and source of ideas. Every member of the lab during my time here has in some way contributed to my success. This is especially true of my co-authors Dr. Joshua Thornbrough, Dr. Rong Zhang, and Courtney Comar. I'm also grateful for valuable collaborations with Dr. Robert Silverman and Dr. Ralph Baric.

Looking further back, Dr. Diane Griffin at the Johns Hopkins University gave me my first research opportunity as a fairly clueless Masters student.

Without my mentors in her lab, this dissertation wouldn't exist. I'm eternally grateful to Dr. Kimberly Schultz, Dr. Kirsten Kulcsar, and Dr. Victoria Baxter.

I've also been fortunate enough to have supportive and generous friends, especially Dr. Katie and Chris Wetzel, Dr. Adam SanMiguel and Dr. Jen Myers SanMiguel, and Dr. Suzi Shapira and Dr. Jeffrey Rosa. Despite conventional wisdom, in some ways grad school gets harder as it goes on. Thank you as well to frequent running partners Sophie Trefely and Katie Strelau who helped make my time outside the lab conducive to success in the lab over this last challenging year of graduate school (and in one instance alerted me to a rattlesnake).

My family has been enormously supportive since I made what must have seemed a very strange decision to pursue a career in scientific research. My parents Michael and Linda Goldstein and my sister Melissa Goldstein have nevertheless never doubted me and instead supported me in whatever way I needed. I wouldn't be here without them and I am lucky to be able to count on their continued support.

Last but most significantly, my wife Jaclyn has been a better partner than I'd ever thought I would find. She has backed me from the very beginning of my scientific journey and never doubted for a second that I would have success or failed to tell me that, despite confronting enormous personal challenges of her own. There is no way to express what she and her support have meant to me or the degree to which they've enabled my success until now and will foster it going forward. I am so looking forward to our next adventure together and hope I will continue to be as good a partner to her as she has been to me.

## ABSTRACT

Coronaviruses comprise a large family of viruses within the order *Nidovirales* containing single-stranded positive-sense RNA genomes of 27-32 kilobases. Divided into four genera (alpha, beta, gamma, delta) and multiple newly defined subgenera, coronaviruses include a number of important human and livestock pathogens responsible for a range of diseases. Historically, human coronaviruses OC43 and 229E have been associated with up to 30% of common colds, while the 2002 emergence of severe acute respiratory syndrome-associated coronavirus (SARS-CoV) first raised the specter of these viruses as possible pandemic agents. Although the SARS-CoV pandemic was quickly contained and the virus has not returned, the 2012 discovery of Middle East respiratory syndrome-associated coronavirus (MERS-CoV) once again elevated coronaviruses to a list of global public health threats. The genetic diversity of these viruses has resulted in their utilization of both conserved and unique mechanisms of interaction with infected host cells. Like all viruses, coronaviruses encode multiple mechanisms for evading, suppressing, or otherwise circumventing host antiviral responses. Specifically, our lab has studied coronavirus interactions with antiviral pathways activated by the presence of cytoplasmic viral double-stranded RNA (dsRNA) such as OAS-RNase L and interferons (IFN). Previous work from our lab demonstrated that the murine coronavirus mouse hepatitis virus (MHV) uses a phosphodiesterase (PDE) to suppress RNase L activation. We have also now shown that additional viruses within *Nidovirales* encode similar PDEs that suppress RNase L activation in the

context of chimeric MHV, and that a PDE encoded by MERS-CoV, the NS4b accessory protein, inhibits RNase L in its native context. I have further shown that MERS-CoV NS4b is a unique PDE with additional functions inhibiting the IFN response, a role dependent on both nuclear localization and its catalytic activity.

# TABLE OF CONTENTS

ACKNOWLEDGEMENTS.....	ii
ABSTRACT .....	iv
LIST OF FIGURES.....	vii
CHAPTER 1: GENERAL INTRODUCTION.....	1
CHAPTER 2: LINEAGE A <i>BETACORONAVIRUS</i> NS2 PROTEINS AND HOMOLOGOUS TOROVIRUS PP1A-CARBOXYTERMINAL DOMAIN ARE PHOSPHODIESTERASES THAT ANTAGONIZE ACTIVATION OF RNASE L..	45
CHAPTER 3: ANTAGONISM OF dsRNA-INDUCED INNATE IMMUNE PATHWAYS BY NS4A AND NS4B ACCESSORY PROTEINS DURING MERS- COV INFECTION .....	70
CHAPTER 4: PRELIMINARY NS4B MECHANISTIC INSIGHTS.....	109
CHAPTER 5: GENERAL DISCUSSION.....	137

## LIST OF FIGURES

FIGURE 1.1 SIMPLIFIED VIEW OF CORONAVIRUS TAXONOMY .....	4
FIGURE 1.2 MAJOR ANTIVIRAL PATHWAYS INDUCED BY dsRNA.....	20
FIGURE 1.3 VIRAL ANTAGONISM OF OAS-RNASE L .....	22
FIGURE 1.4 VIRAL PDE INTERACTIONS WITH THE INNATE IMMUNE RESPONSE .....	26
FIGURE 2.1 ALIGNMENT OF LINEAGE A <i>BETACORONAVIRUS</i> AND BERNE TOROVIRUS PDEs .....	56
FIGURE 2.2 STRUCTUREs OF NIDOVIRUS PDEs.....	57
FIGURE 2.3 PDE ACTIVITY ASSAY OF CORONAVIRUS AND TOROVIRUS PDEs .....	57
FIGURE 2.4 NS2 ORGANIZATION AND CONSTRUCTION OF CHIMERIC VIRUSES.....	58
FIGURE 2.5 EXPRESSION OF EXOGENOUS PDEs FROM CHIMERIC VIRUSES.....	59
FIGURE 2.6 REPLICATION AND ACTIVATION OF RNASE L BY CHIMRIC VIRUSES IN BONE MARROW DERIVED MACROPHAGES.....	60
FIGURE 2.7 REPLICATION AND PATHOGENESIS OF CHIMERIC VIRUSES <i>IN VIVO</i> .....	61
FIGURE 3.1 MERS-CoV NS4A AND NS4B RECOMBINANT MUTANTS.....	84
FIGURE 3.2 SUBCELLULAR LOCALIZATION OF MERS-CoV NS4B EXPRESSION .....	86
FIGURE 3.3 NS4A COLOCALIZES WITH dsRNA AND REPLICATION/TRANSCRIPTION COMPLEXES DURING MERS-CoV INFECTION .....	87

FIGURE 3.4 MERS-CoV NS4A AND NS4B MUTANTS ARE ATTENUATED IN IFN-COMPETENT CELLS.....	88
FIGURE 3.5 NS4A AND NS4B ANTAGONIZE IFN EXPRESSION .....	89
FIGURE 3.6 MERS-CoV NS4B NLS AND PDE CATALYTIC MUTANTS ARE ATTENUATED IN A549 CELLS AND EXHIBIT INCREASED TYPE III IFN EXPRESSION .....	90
FIGURE 3.7 NS4B ANTAGONIZES IFN EXPRESSION INDEPENDENTLY OF RNASE L ACTIVATION.....	91
FIGURE 3.8 LOSS OF NS4A DOES NOT ACTIVATE RNASE L DURING MERS-CoV INFECTION .....	93
FIGURE 3.9 LOSS OF NS4A ACTIVATES PKR BUT DOES NOT LEAD TO eIF2 $\alpha$ PHOSPHORYLATION OF TRANSLATION ARREST IN A549 <sup>DPP4</sup> CELLS .....	94
FIGURE 4.1 WT AND NS4B MUTANT MERS-CoV DO NOT INDUCE IRF3 PHOSPHORYLATION.....	122
FIGURE 4.2 WT AND NS4B MUTANT MERS-CoV DO NOT INDUCE NUCLEAR LOCALIZATION OF IRF3.....	123
FIGURE 4.3 MUTATION OF MERS-CoV NS4B DOES NOT ALTER ANTIVIRAL mRNA STABILITY .....	124
FIGURE 4.4 ABLATION OF MERS-CoV NS4B CATALYTIC ACTIVITY RESULTS IN INCREASED ABUNDANCE OF INTRON-DERIVED RNA .....	125
FIGURE 5.1 HYPOTHESIZED MODEL FOR NS4B ACCELERATION OF LARIAT DEBRANCHING .....	148

**Chapter 1**

**INTRODUCTION:**

**HUMAN CORONAVIRUSES AND INTERACTIONS WITH  
INNATE IMMUNITY**

## General Introduction to Coronavirus Biology

### ***Coronavirus genome structure, replication, and transcription***

Coronaviruses fall within the *Cornidovirineae* suborder, family *Coronaviridae*, and subfamily *Orthocoronavirinae* of the order *Nidovirales*. These viruses are grouped together for their unique genome organization, ribosomal frameshift in the first open reading frame, and expression of 3' structural and accessory genes via transcription of nested, subgenomic mRNAs (1). Also within the order *Nidovirales* is the suborder *Tornidovirineae* which includes the genus *Torovirus*, that includes the toroviruses, which are distinguished from coronaviruses primarily by differences in their accessory genes. The most notable feature of coronaviruses is their extraordinary genome size of up to 32 kilobases, among the largest RNA genomes, which is capped at the 5' end and 3' polyadenylated. Recently, two nidoviruses have been discovered with genomes of 36 and 41 kilobases in length, highlighting the increase in coding capacity afforded by the expression of a viral proofreading exonuclease and a non-icosahedral nucleocapsid (1-4).

The 5' ~20 kb of the coronavirus genome comprises the replicase gene (ORF1ab), which is translated from the genome as a single polyprotein and proteolytically processed into up to 16 constituent non-structural proteins (nsp). In the majority of translation events, protein synthesis terminates at the end of ORF1a while a low-frequency ribosomal frameshift allows translation of the full length ORF1ab. Downstream of the conserved replicase gene, in the 3' 10 kb of

the genome, are the coronavirus structural genes. The four major structural genes, in their 5'→3' order are spike (S), membrane (M), envelope (E), and nucleocapsid (N). Some viruses within the *Betacoronavirus* genus contain a fifth structural gene, hemagglutinin-esterase (HE) (1). Interspersed in the 3' region are genes encoding non-structural (NS) accessory proteins, which are unique to distinct genera and subgenera of coronaviruses and often mediate critical interactions between the virus and host innate immune pathways. As such, these genes and the proteins they encode have been of particular interest to the Weiss laboratory.

As with other positive sense ssRNA viruses, coronavirus replication and transcription occurs at ER-derived and localized replication-transcription complexes (RTCs) that are formed by several of the non-structural proteins and contain the RNA-dependent RNA polymerase (nsp12), RNA primase (nsp8), RNA helicase (nsp13), and RNA proofreading exonuclease (nsp15) among other viral and host proteins (1). While ORF1ab translation occurs directly from the genome, synthesis of all other proteins requires transcription of nested subgenomic mRNAs which is regulated by a transcription regulatory sequence (TRS) upstream of each structural and accessory gene (5). The first step in this unusual process is transcription of a negative-sense subgenomic (sg) RNA corresponding to each gene. The negative-sense sgRNA is joined to a leader sequence from the 5' end of the genome and used as a template for viral mRNA

synthesis, with in most cases only the 5' gene of each subgenomic mRNA being translated.

### **Coronaviridae phylogeny**

The taxonomic organization of the order *Nidovirales* was substantially revised in July 2018 by the International Committee on the Taxonomy of Viruses. Previously, the family *Coronaviridae* comprised two sub-families, *Coronavirinae* and *Torovirinae* which contained the coronaviruses and toroviruses, respectively. Under the 2018 revision, *Nidovirales* is now divided into seven sub-orders with the coronaviruses reclassified into the sub-order *Cornidovirineae*, family *Coronaviridae*, sub-family *Orthocoronavirinae* (Fig 1.1). Subordinate to this sub-family, they are further divided into four genera: *Alphacoronavirus*, *Betacoronavirus*, *Gammacoronavirus*, and *Deltacoronavirus* that are further separated into numerous subgenera (Fig 1.1). The majority of human and agricultural pathogens among the coronaviruses fall within *Alphacoronavirus* and *Betacoronavirus*, divided into twelve and five subgenera, respectively.

The human upper respiratory tract pathogen human coronavirus 229E (HCoV-229E) and HCoV-NL63 are among the alphacoronaviruses,

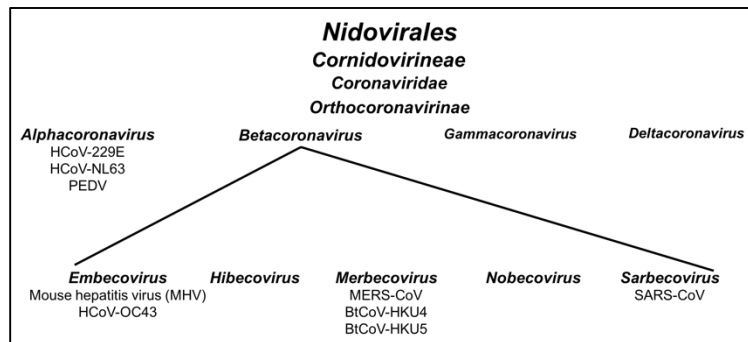


**Figure 1.1 Simplified view of coronavirus taxonomy.**

along with the highly virulent agricultural pathogen porcine epidemic diarrhea virus (PEDV) (6, 7). *Betacoronavirus* had previously been divided into four lineages (A-D), but now consists of the subgenera *Embecovirus* (HCoV-OC43, HCoV-HKU1, mouse hepatitis virus/MHV), *Hibecovirus* (bat Hp-betacoronavirus Zhejiang 2013), *Merbecovirus* (MERS-CoV, MERS-like bat coronaviruses), *Nobecovirus* (*Rousettus* bat coronavirus HKU9), and *Sarbecovirus* (SARS-CoV, SARS-like bat coronaviruses). The distinction between the *Betacoronavirus* subgenera lies in the degree of sequence similarity between their replicase genes and the suite of accessory genes they contain, while the basic genomic organization is highly conserved. Aside from providing taxonomic classification, the accessory genes likely underlie virus-host interactions that are unique between subgenera. Further, they are likely acquired from host organisms or via horizontal gene transfer with other coronaviruses or unrelated viruses, as appears to have occurred with a recently discovered deltacoronavirus that contains a small reovirus-derived open reading frame (8).

The toroviruses, previously grouped into *Coronaviridae* with the coronaviruses, are now in their own suborder *Tornidovirineae*, family *Tobaniviridae*, and subfamily *Torovirinae*, which contains the genus *Torovirus*. These viruses are primarily characterized as agricultural pathogens, the best studied of which is equine torovirus, with the most intensively studied variant known as Berne virus (BEV) (9).

## History and Origin of Human Coronaviruses

### ***Common cold-causing coronaviruses***

For several decades preceding the 2002 emergence of SARS-CoV human coronaviruses were understood as etiological agents of the common cold. HCoV-229E, an *Alphacoronavirus*, was first isolated from the respiratory tract of common cold patients in 1966 (10) while HCoV-OC43 was isolated the following year from patients with similarly mild respiratory disease (11). Though viral taxonomy was in its infancy at this time, both viruses were quickly recognized as morphologically highly similar to avian infectious bronchitis virus (IBV) (11, 12), now classified as a gammacoronavirus. HCoV-OC43 was identified as serologically related to MHV while HCoV-229E was found to be serologically distinct, a classification that is borne out by the genetic similarity between MHV and HCoV-OC43 as betacoronaviruses of the same subgenus (*Embecovirus*) (11). While the isolation conditions of both HCoV-OC43 and HCoV-229E suggested they cause a cold-like disease, experimental infection of healthy volunteers confirmed these original observations (13).

Although these viruses have been known and studied for several decades, recent work has begun to shed light on their origins, which appear to have similarities with the more recent zoonotic emergence of SARS-CoV and MERS-CoV. While HCoV-OC43 was initially classified serologically as closely related to MHV, later studies identified an even greater degree of antigenic similarity with bovine coronavirus (BCoV) (14). Subsequent studies of HCoV-OC43, MHV, and

BCoV partial genome sequences revealed that HCoV-OC43 is most closely related to BCoV and that the two viruses likely diverged relatively recently (15, 16). The HCoV-OC43 complete genomic sequence was reported in 2005 and firmly established its close genetic relationship with BCoV (17). In all ORFs, BCoV is the closest relative to HCoV-OC43 with the exception of the E gene, which is more closely related to its ortholog from porcine hemagglutinating encephalomyelitis virus (PHEV), suggesting a recombination event between BCoV and PHEV may have preceded the emergence of HCoV-OC43 (17). This study further suggested that although HCoV-OC43 has circulated throughout the human population for several decades, its origin bears more in common with SARS-CoV and MERS-CoV than previously understood. A molecular clock analysis suggested that BCoV and HCoV-OC43 may have had a common ancestor as recently as the year 1890, and that HCoV-OC43 originated through zoonotic transmission from a livestock source, similar to the spillover of MERS-CoV from dromedary camels to humans (17). Since its zoonotic transmission, HCoV-OC43 has become a globally ubiquitous cause of common colds and exhibits considerable genetic diversity indicative of its continuous transmission among humans (18, 19).

As with HCoV-OC43, recent work has illuminated a relatively recent zoonotic origin for HCoV-229E, which with HCoV-OC43 and the *Alphacoronavirus* HCoV-NL63 is responsible for 10-30% of common colds (20). The ecological origins of HCoV-229E now appear to have much in common with

those of SARS-CoV and particularly MERS-CoV. The clarification of these origins began with the 2005 report of partial genome sequences of a novel alphacoronavirus recovered from bats of the species *Miniopterus pusillus* in Hong Kong (21). Subsequently, RNA was detected from bats in Ghana representing a different novel alphacoronavirus closely related to HCoV-229E, suggesting that like numerous other emerging zoonotic viruses, HCoV-229E may have originated in bats (22). Most recently, several HCoV-229E-like viruses were successfully isolated from dromedary camels (23). The best available evidence suggests that the HCoV-229E lineage originated among African bats and entered the human population via an intermediate reservoir in dromedaries, where an ORF8 deletion that distinguishes bat from human variants appears to have emerged (24, 25).

In the 21<sup>st</sup> century, between the SARS-CoV pandemic and discovery of MERS-CoV, two additional human coronaviruses were discovered. The first of these, HCoV-NL63, was isolated in 2003 in the Netherlands from a hospitalized child (26) and characterized as a novel alphacoronavirus. That study and others (20, 26) have identified HCoV-NL63 as a continuously circulating cause of frequently mild respiratory infection, though like HCoV-OC43 and HCoV-229E it is capable of causing moderate to severe disease in particularly susceptible hosts (20). As with HCoV-229E, recent work has uncovered a close evolutionary relationship with currently circulating alphacoronaviruses of bats (27), bolstering the emerging consensus that the *Alphacoronavirus* and *Betacoronavirus* genera

have their origins in bats (28, 29). Interestingly, given the dramatic differences in virulence between HCoV-NL63 and SARS-CoV, they both utilize the cell-surface protease ACE-2 as an entry receptor (30, 31).

A fourth human coronavirus, the novel betacoronavirus HCoV-HKU1, was isolated from a hospital patient in Hong Kong in 2004 (32). A rapid follow-up study in Hong Kong determined that HCoV-HKU1 circulates throughout the year, causing primarily mild respiratory disease (33). Continued molecular epidemiology and surveillance studies have revealed similar patterns of HCoV-HKU1 infection in Europe (34) and the United States (35, 36). Overall, it appears to cause a similar percentage of respiratory infections as HCoV-229E, and both are somewhat less prevalent than HCoV-OC43 (36). Like HCoV-NL63, HCoV-HKU1 clinical isolates replicate in primary human airway epithelial (HAE) cell cultures (37, 38) but the inability to propagate these viruses on established cell lines has limited efforts to understand their basic biology.

Collectively, in addition to being responsible for 10-30% of common colds, these four viruses cause or contribute to an unknown burden of severe disease among the very young, very old, or immunocompromised. Thus, even before consideration of the potential threat posed by more virulent zoonotic coronaviruses, the endemic human coronaviruses are responsible for a significant disease burden. Despite this, surprisingly little is known about their basic biology beyond that which is likely conserved with more extensively studied

coronaviruses. Partly this is a result of difficulties in culturing them. More significant, however, is the attention that has been committed to SARS-CoV and MERS-CoV since their emergence.

### ***SARS-CoV – First pandemic of the 21<sup>st</sup> century***

For over forty years after the discoveries of HCoV-OC43 and HCoV-229E, coronaviruses were considered only mildly important to human health. The discovery of SARS-CoV in 2003 and its rapid global spread dramatically changed this paradigm. The first indications that a new infectious threat had emerged came from reports of a large outbreak of atypical pneumonia in Guangdong Province, southern China, in November 2002 (39). This disease, termed severe acute respiratory syndrome (SARS) before its etiological agent had been identified, spread from Guangdong to Hong Kong, where a remarkable “super spreader” event took place on February 21, 2003 that led to large outbreaks in Canada, Vietnam, and Singapore (39-42). Ultimately, 8,096 cases and 774 deaths were recorded in 27 countries by the time the outbreak was declared to be over on July 31, 2003 (43).

Upon the recognition of a novel respiratory disease efforts began to identify the etiological agent and its source. By May 2003 three independent groups, in Hong Kong, Germany, and the United States (44-46) had identified a novel coronavirus as the likely cause of SARS. This determination was made based on morphology of the virus, partial genome sequencing, and virus isolation

in cell culture. The rapid identification of SARS-CoV and its receptor, angiotensin converting enzyme-2 (ACE-2) (47) would ultimately serve as a model for later studies that rapidly identified MERS-CoV and its cellular receptor. While the outbreak was still ongoing, numerous SARS-CoV isolates were fully sequenced and characterized (48, 49), representing one of the first examples of modern molecular biology being brought to bear against a novel infectious disease threat.

Modern molecular biology techniques were combined with classic epidemiology to identify the source of the outbreak, a critical step in bringing it to an end. Experts quickly suspected that SARS-CoV was a zoonotic agent, transmitted from animals to humans. As early SARS-CoV cases were particularly common among restaurant workers who handled exotic game animals, suspicions about the source turned to live animal markets in southern China. SARS-CoV was isolated from palm civets and raccoon dogs in a single market, and there was a high prevalence of SARS-CoV antibodies found in animal handlers working in the same market (50). A second, and the last known SARS-CoV outbreak at the end of 2003 provided further evidence for civet-to-human transmission, as employees and civets from the same restaurant were found to be infected with virtually identical SARS-CoV isolates (51). Although a strong link was drawn between civet and human SARS-CoV infections, extensive surveys failed to find SARS-CoV in civets outside animal markets, suggesting they were not the true wild reservoir (52), as did the observation that SARS-CoV infection of civets results in overt disease (53). Nevertheless, the live animal markets clearly

served to amplify transmission between civets and humans, and shutting down these markets was critical to ending the epidemic.

Because various species of bat had previously been identified as reservoirs of zoonotic viruses such as Ebola (54), Marburg (55), Nipah (56, 57), and Hendra (57) viruses, they were also considered possible reservoirs of SARS-CoV. A 2004 survey of more than 400 bats from four different regions of China found high seroprevalence and wide geographical distribution of anti-SARS-CoV antibodies in bats from the genus *Rhinolophus*, or horseshoe bats (58), as did a contemporary study conducted in Hong Kong (59). Both reported the first full genome sequences of SARS-like coronaviruses (SL-CoVs), showing a much greater degree of genetic diversity among these viruses than among civet and human SARS-CoV isolates. Notably, the bat SL-CoV genomes have an intact ORF8, similar to civet and early human isolates, while later human isolates feature a 29 nucleotide deletion in this region (49, 50).

Continued studies into the prevalence of SL-CoVs in Chinese bats has provided significant insight into the potential for a re-emergence of SARS-CoV or spillover of SL-CoVs into the human population. SARS-CoV is unusual among zoonotic viruses in that has not caused any additional human outbreaks, aside from a small cluster of cases in late 2003. However, SL-CoVs with the potential to infect humans continue to circulate among bat populations in China. In 2013 the first bat SL-CoV that can infect human cells via ACE-2 was isolated from

*Rhinolophus sinicus* bats (60) and genome sequences of other viruses predicted to do were found in the same population. Serological evidence from humans in southern China suggests that SL-CoVs do infect humans (61) without erupting into large outbreaks. Whether these infections result in any clinical disease is unclear, but experimental evidence suggests that ACE-2 utilizing SL-CoVs, while capable of infecting human cells, may be less virulent than SARS-CoV (62, 63). The potential for SARS-CoV itself to re-emerge remains unclear. Unlike Marburg (64) or Nipah (56) viruses, SARS-CoV itself has not been found in a wild reservoir. The simplest explanation for why it has not re-emerged may be that it is extinct in the wild, and recent evidence suggests it arose due to a series of recombination events in a bat population rich with SL-CoVs (65) that may only rarely recombine to produce a virus with the potential to cause human outbreaks. Whatever the reason for the apparent disappearance of SARS-CoV, the diversity of SL-CoVs in the wild makes clear that the threat of such viruses remains, and the emergence of MERS-CoV in 2012 demonstrates that this threat is far from geographically isolated.

### ***Emergence and ecology of MERS-CoV***

For nearly a decade following the disappearance of SARS-CoV, coronaviruses receded as a public health concern. In September 2012 a novel coronavirus was isolated from a patient in the Kingdom of Saudi Arabia with fatal atypical pneumonia (66). Subsequently, infections by the same virus in Jordan were retrospectively identified dating to April 2012 (67). Rapid sequencing and

genomic characterization (68) of this virus quickly established that it was a novel betacoronavirus of lineage C (recently reclassified as *Betacoronavirus* subgenus *Merbecovirus*), most closely related to Asian bat coronaviruses that had been previously identified only by sequence (69). Subsequently, this virus was formally named Middle East respiratory syndrome-associated coronavirus (MERS-CoV). As of January 19, 2019 MERS-CoV has been responsible for 2,266 documented infections and 804 deaths, with the vast majority of these occurring in the Kingdom of Saudi Arabia, as well as a large travel-associated outbreak in the Republic of Korea (70). Like SARS-CoV, MERS-CoV causes severe disease primarily in older patients, with severe respiratory symptoms being the most common manifestation of documented infections (71). Also like SARS-CoV is the propensity of MERS-CoV to infect healthcare workers (72) and in fact the largest outbreaks have occurred in hospital settings. In contrast, and perhaps linked to its failure to cause a global pandemic, large MERS-CoV outbreaks in the community have not been documented, though unrecognized subclinical infections almost certainly occur (73).

As with SARS-CoV, identifying the reservoir and source of MERS-CoV infections has been a major focus of research efforts since 2012. Due to the previous identification of related bat coronaviruses (69) and SL-CoVs in bats, it was quickly suspected that MERS-CoV originated in bats. A 2013 survey of bats in the vicinity of a small outbreak in Saudi Arabia recovered a small, 190 nucleotide fragment with 100% identity to the MERS-CoV replicase gene in a

single bat (74). Though suggestive of a MERS-CoV bat reservoir, the fragment was isolated from just a single bat and no further evidence for MERS-CoV circulation in Arabian bats has emerged. Despite this early indication that MERS-CoV might have a bat reservoir on the Arabian peninsula, a 2013 study from Ithete *et. al.* first suggested that bats from sub-Saharan Africa harbor viruses most closely related to MERS-CoV. This study identified an 816 nucleotide fragment from a South African *Neoromicia capensis* bat with 89.7% identity to the equivalent sequence from MERS-CoV (75). Characterization of the complete genome sequence of this virus showed 85% nucleotide identity to MERS-CoV across the entire genome with 97% amino acid identity, placing this virus (NeoCoV) in the same species as MERS-CoV (76). NeoCoV has recently been detected again in the wild (77) as has another virus (designated PREDICT/PDF-2180) with a similarly close relationship to NeoCoV and MERS-CoV (78).

Despite the overall close relationship of these viruses and MERS-CoV, the S1 subunit of the spike proteins of NeoCov and PREDICT/PDF-2180 that contains the receptor binding domain is highly divergent from that of MERS-CoV (79), and does not bind to or mediate infection of human cells (78). These findings support the hypothesis that, like SARS-CoV, MERS-CoV arose as a result of recombination events between different bat coronaviruses (76). Further supporting this hypothesis is the identification of currently circulating bat coronaviruses that can mediate entry into human cells using DPP4 (80-82). The spike protein of bat coronavirus HKU4 (BtCoV-HKU4) binds to human DPP4 and

can mediate entry when exogenous trypsin is added, suggesting the emergence of MERS-CoV may have required the acquisition of a DPP4-binding spike by a NeoCoV-like virus, as well as further adaptation in the fusion domain (80, 81). Later research has determined that two amino acid substitutions in the BtCoV-HKU4 spike allow proteolytic processing of spike by human proteases and entry into human cells without the addition of trypsin (83). More recently, two MERS-like bat coronaviruses identified in China show evidence of having acquired the S1 subunit of their spike proteins from HKU4-like viruses that bind human DPP4, providing further evidence for intra-spike recombination as essential in the emergence of MERS-CoV, and evidence that such events may not be particularly infrequent (82).

Although these studies have illuminated the evolutionary history of MERS-CoV, the lack of an epidemiological link between bats and human infection suggested the possibility of an intermediate reservoir. Within a short period of the discovery of MERS-CoV, extensive serological surveys of Omani livestock identified a seroprevalence in dromedary camels of 100% (84). Similarly high seroprevalence and active MERS-CoV infection has been detected in dromedary camels across the Middle East, including Qatar (85), Egypt (86-88), the United Arab Emirates (89-91), Jordan (92), and Saudi Arabia (93, 94). By 2014, MERS-CoV in camels had been convincingly linked to human outbreaks (85, 94-96). Continued studies have demonstrated that MERS-CoV isolates circulating in camels exhibit significantly greater genetic diversity than human isolates,

suggesting that camels are a source of human infection, rather than humans infecting camels (97-100).

Further supporting the link between camels and human infection is growing evidence that intense exposure to camels is a significant risk factor for MERS-CoV infection. A 2015 nationwide serological survey in Saudi Arabia found an overall seroprevalence rate of 0.15% for anti-MERS-CoV antibodies, with camel shepherds being fifteen times and slaughterhouse workers twenty-three times more likely to test positive than individuals without occupational exposure to camels (101). Notably, however, the low overall seropositive rate meant that although the total sample size was large (10,009 individuals) the absolute number of positive individuals was small (15, including just 2 shepherds and 3 slaughterhouse workers), leading the authors to call for a warranted degree of caution in interpretation. Despite the limitations of this particular study, it contributes to a compelling body of evidence that individuals with occupational exposure to camels are an entry point for zoonotic transmission of MERS-CoV into humans. One 2014 study of a human outbreak linked to a Qatari slaughterhouse found a high proportion of camels at the facility were actively shedding infectious virus (102), while another study in Qatar of a limited sample size found an elevated likelihood of seropositivity among workers with daily occupational exposure to camels (103). Additional serosurveys have further bolstered the link between occupational exposure to camels and human MERS-CoV infection while also shedding light on an enduring mystery in the human

history of MERS-CoV; why a significant percentage of primary cases report no exposure to camels. A 2015 study identified two camel workers with active but asymptomatic MERS-CoV infection (104) and a 2018 study found that 50% of Saudi camel workers show evidence of previous MERS-CoV infection without a history of severe respiratory disease (105). The possibility of frequent asymptomatic infections among camel workers suggests a plausible route for MERS-CoV to enter the human population, where it may not be recognized until it causes severe disease, primarily in older individuals.

Despite only being discovered recently, abundant evidence indicates that MERS-CoV has been circulating in Arabian camels for decades (93, 106, 107). While it remains unclear whether MERS-CoV infection of humans was unrecognized prior to 2012 or did not occur, the high camel seroprevalence in this region overlaps with the vast majority of known human infections. In addition to ubiquitous infection of dromedary camels on the Arabian peninsula, serosurveys of camels in sub-Saharan Africa have also demonstrated evidence of MERS-CoV infection dating back to at least 1983 (108-112). Contemporary studies continue to find evidence of widespread active dromedary infection in this expansive region (112). Despite this, no human MERS-CoV infections have been detected south of Egypt, and serosurveys produce evidence of only extremely limited human infection (113), even among individuals with extensive occupational exposure to camels positive for MERS-CoV RNA indicative of active infection (114). The absence of human MERS-CoV cases in Africa remains an

mystery which may be ascribed to genetic factors in potentially susceptible humans or genetic differences between African and Arabian MERS-CoV variants. There is a robust, unidirectional trade in dromedary camels from East Africa to the Arabian peninsula, but the MERS-CoV clades in these two regions appear to have diverged some time ago (115). The genetic diversity of African MERS-CoV variants coupled with the detection of the closest MERS-CoV relatives in sub-Saharan African bats suggests MERS-CoV first evolved in Africa and was introduced to the Arabian peninsula by imported camels, after which genetic drift may have given rise to variants with a greater ability to infect humans. Bolstering this hypothesis is a recent study that found African MERS-CoV isolates replicate less robustly in both immortalized Calu-3 human airway epithelial cells and primary human respiratory tract *ex vivo* cultures compared to isolates from Saudi Arabia (116). Notably, the attenuation of these isolates was not linked to greater activation of antiviral immune responses, indicating genetic drift throughout the MERS-CoV genome may be responsible for its relatively emergence into humans.

## **Coronavirus interactions with the OAS-RNase L antiviral pathway**

### ***OAS-RNase L activation by viral dsRNA***

Like all viruses, coronaviruses employ mechanisms to evade, suppress or otherwise counteract host innate immune responses. The most important aspect of this response early in infection is the interferon (IFN)-dependent antiviral

response, which is triggered by host sensing of viral dsRNA. Without evasion or antagonism of this pathway, a virus is unlikely to establish a productive infection and replicate to a sufficient level that transmission to new hosts can occur. IFNs are a large class of cytokines, with type I (IFN $\alpha$  and IFN $\beta$ ) and type III (IFN $\lambda$ ) IFNs being most critical for initiating innate antiviral immune responses (117, 118).

Though both classes of IFNs induce expression of a similar suite of IFN stimulated genes (ISGs), IFN $\lambda$  plays a dominant role

at mucosal barriers such as the airway and intestinal tract (119, 120), where it is preferentially produced by and acts upon epithelial cells (121, 122). In the context of human coronavirus infections which primarily occur in the airway, IFN $\lambda$  may therefore play a predominant role in the early antiviral response.

The expression of these IFN genes occurs downstream of viral dsRNA sensing by host RIG-I-like receptors (Fig 1.2) (123, 124), specifically MDA5 in the context of coronavirus infection (125). Cytoplasmic dsRNA is a hallmark activator

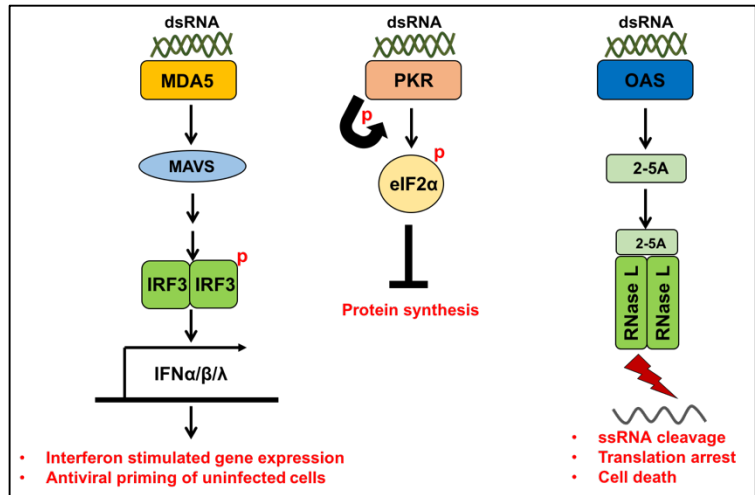


**Figure 1.2 Major antiviral pathways induced by dsRNA.** dsRNA activates three major classes of cytoplasmic pattern recognition receptors, The RIG-I like receptors (represented by MDA5, PKR, and OAS). **MDA5** signals through the adaptor protein MAVS to induce phosphorylation of the transcription factor IRF3, which drives interferon gene expression. **PKR** activation results in auto-phosphorylation and phosphorylation of the translation initiation factor eIF2 $\alpha$ , which arrests nascent protein synthesis. **OAS** proteins bind dsRNA and synthesize the second messenger 2-5A, consisting of linear multimeric ATP molecules linked by 2',5' phosphodiester bonds. 2-5A binds RNase L monomers, inducing their dimerization and activation.

of the antiviral response because it is rare in uninfected cells or modified by the cellular adenosine deaminase ADAR1 such that it loses the capacity to activate antiviral signaling (126-128). IFN signaling induces the expression of up to several hundred ISGs, including other dsRNA binding proteins such as protein kinase R (PKR), and oligoadenylate synthetases (OAS), though high basal expression of PKR and OAS genes in some cell types allows their activation in the absence of additional IFN (129, 130). OAS proteins, upon binding dsRNA, catalyze the synthesis of a small second-messenger molecule 2',5'-oligoadenylate (2-5A) which binds to ribonuclease L (RNase L) monomers, inducing their dimerization and activation. Activated RNase L targets single-stranded (ss) RNA of both cellular and viral origin and as such can have direct antiviral effects (131), cause translational arrest (132, 133), and lead to cell death (128).

Through the combination of these events downstream of its activation, RNase L can potently restrict the replication of diverse RNA and DNA viruses (131). These include flaviviruses such as West Nile virus (134, 135), hepatitis C virus (136), and Sindbis virus (SINV) (130). Consequently, numerous viruses encode well characterized antagonists of this pathway. These include dsRNA binding proteins such as E3L encoded by Vaccinia virus (VACV) (137) and the NS1 protein of influenza A viruses (138). Other known RNase L antagonists include the L\* protein encoded by Theiler's murine encephalomyelitis virus (139, 140) and the VACV D9 protein, an mRNA decapping enzyme (141).

The Weiss lab has extensively studied another class of OAS-RNase L antagonists, the host-derived phosphodiesterases (PDEs) encoded by select rotaviruses and, most significantly, by mouse hepatitis virus (MHV).

### ***OAS-RNase L antagonism by viral phosphodiesterases***

As with many antiviral pathways, OAS-RNase L is vulnerable to evasion or antagonism at different points. While viruses such as Vaccinia and Influenza A use dsRNA binding proteins to prevent OAS activation, other viruses

have acquired the ability to prevent RNase L activation downstream of OAS through cleavage of 2-5A (Fig 1.3). The prototypical viral protein acting by this mechanism is the MHV accessory protein NS2, which was first identified as a putative phosphodiesterase (PDE) in a 2002 computational analysis (142).

Specifically, MHV NS2 belongs to a large family of phosphodiesterases called the LigT-like 2H-phosphoesterases (2H-PE), named for

the prototypical *E. coli* LigT protein, a 2',5' tRNA ligase, and characteristic catalytic HxS/Tx (x is typically a hydrophobic residue) motifs spaced 80-100 residues apart (142-144). Although first identified in prokaryotes, 2H-PEs are ubiquitous throughout all three kingdoms of life and include numerous eukaryotic representatives. The 2H-PE central domain of mammalian A-kinase anchoring

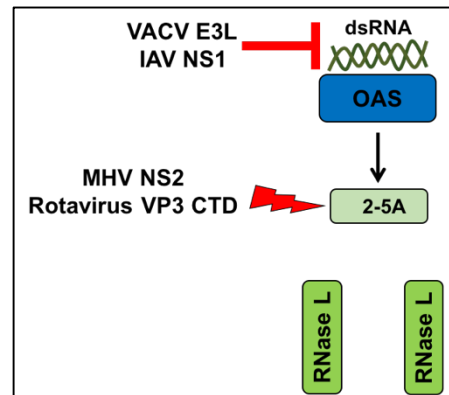


**Figure 1.3 Viral antagonism of OAS-RNase L.** Viruses such as vaccinia and influenza A use dsRNA binding proteins E3L and NS1, respectively, to prevent dsRNA sensing by OAS proteins. Viral phosphodiesterases such as MHV NS2 and rotavirus VP3, in contrast, degrade 2-5A via 2',5' phosphodiesterase activity to prevent dimerization and activation of RNase L.

protein 7 (AKAP7) binds cAMP but the function of its catalytic activity remains unknown (145, 146), while USB1 has known exoribonuclease activity and processes the 3' poly(U) tract of the U6 snRNA to protect it from exosomal degradation (147-151). Another eukaryotic 2H-PE, CGI-18, is a component of the large transcriptional co-activator complex Asc-1; its exact role in this complex remains undefined but may involve co-transcriptional or post-transcriptional RNA processing (142, 152, 153).

The Weiss laboratory has extensively studied 2H-PEs encoded by diverse RNA viruses that exhibit 2',5' phosphodiesterase (PDE) activity. The 2002 computational analysis of 2H-PEs that identified the MHV NS2 accessory protein as a 2H-PE also identified an orthologous domain in the C-terminus of group A rotavirus (RVA) VP3 protein (142). An early study of MHV NS2 found that it was not essential for MHV replication in immortalized cell lines (154). However, a 2009 study found that mutation of either NS2 catalytic histidine (NS2<sup>H46A</sup> or NS2<sup>H126R</sup>) crippled viral replication in the liver though it did not impact MHV replication in the brain (155), suggesting NS2 inhibits a component of the antiviral response that is active in the liver but not the brain. Further work demonstrated that MHV-NS2<sup>H126R</sup> is attenuated in bone marrow-derived macrophages (BMMs) from wild-type (WT) B6 mice but replicates normally in BMMs generated from mice that lack expression of the type I IFN receptor (IFNAR) (156). Subsequent work demonstrated that MHV NS2 has specific 2',5' phosphodiesterase activity, enabling it to degrade 2-5A synthesized by OAS

proteins in response to viral dsRNA and linking the attenuation of MHV-NS2<sup>H126R</sup> explicitly to a failure to antagonize RNase L (157).

Work in the Weiss laboratory on the interaction of 2H-PEs with the OAS-RNase L pathway has extended beyond MHV NS2 to other viral and cellular members of the family. In a 2013 study the RVA VP3 C-terminal domain (CTD) 2H-PE, either WT or inactive VP3-CTD<sup>H798R</sup> was inserted in place of MHV NS4 in an MHV-NS2<sup>H126R</sup> background (158). In addition to exhibiting 2',5' PDE activity in biochemical assays, chimeric MHV-NS2<sup>H126R</sup> expressing RVA VP3-CTD inhibited RNase L activation and replicated equivalently to WT MHV in BMMs. Additionally, VP3-CTD restored replication and pathogenesis of MHV-NS2<sup>H126R</sup> in the mouse liver (158-160). A 2015 study confirmed that VP3 is involved in RNase L antagonism during bona-fide RVA infection (161).

In addition to this work on viral LigT-like 2H-PEs, the Weiss laboratory has investigated whether cellular homologs exhibit the same catalytic activity and have the potential to interact with the OAS-RNase L pathway. The central domain (CD) of long isoforms of AKAP7 contains a putative PDE domain with the expected HxS/Tx catalytic motifs. In biochemical assays the AKAP7 CD exhibits equivalent 2',5' PDE activity to MHV NS2, and like RVA VP3-CTD, can functionally replace NS2 in recombinant MHV-NS2<sup>H126R</sup> (162). Notably, the ability of AKAP7-CD to function in place of inactive NS2 required removal of its nuclear localization sequence (NLS), providing strong evidence that antagonism of

RNase L requires 2H-PEs be localized at least partly to the cytoplasm. This finding makes it unlikely that AKAP7 is involved in OAS-RNase L regulation in host cells. Rather, its exclusively nuclear localization (162) makes it more likely to participate in RNA processing like other cellular 2H-PEs. However, the observation that it has the same catalytic activity as MHV NS2 suggests that the ability to inhibit OAS-RNase L need not have been acquired through genetic drift of viral 2H-PEs after their acquisition from the host, but could have been present in the cellular ancestor. Following these findings, our work studying encounters between viruses and the OAS-RNase L pathway has continued. Additionally, we have expanded these studies to explore interactions between viral 2H-PEs and other arms of the innate antiviral response

This work has explored the function of viral 2H-PEs from diverse viruses within the order *Nidovirales*. In addition to MHV, other viruses within the subgenus *Embecovirus* (formerly lineage A) encode an NS2 protein that is a putative PDE, the lone exception being HCoV-HKU1. Although these NS2 proteins are predicted to have similar structure and function to MHV NS2, it was unknown whether they exhibit the same ability to inhibit the activation of OAS-RNase L. Chapter 3 of this thesis, published in 2016 in the *Journal of Virology*, describes our characterization of the interaction between 2H-PEs encoded by other embecoviruses, as well as a related torovirus, and the OAS-RNase L response (163). We found that in all but one case, the proteins we studied had equivalent enzymatic activity to MHV NS2 and were able to rescue replication of

MHV-NS2<sup>H126R</sup>. The lone exception, however, the NS2 protein of porcine hemagglutinating encephalomyelitis virus (PHEV), demonstrates that structure

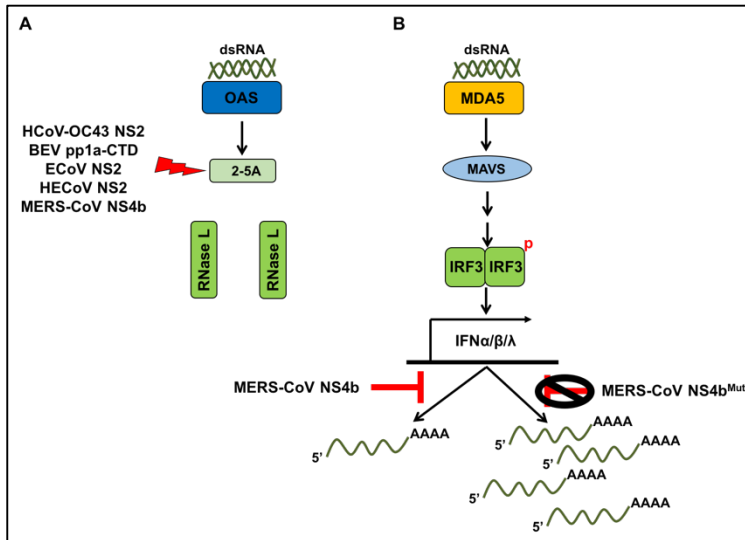


**Figure 1.4 Viral PDE interactions with the innate immune response.** A) PDEs encoded by MHV-like betacoronaviruses (OC43, ECoV, HECoV), torovirus strain Berne (BEV), and MERS-CoV inhibit activation of RNase L through cleavage of the 2-5A second messenger produced by OAS. B) MERS-CoV NS4b suppresses the abundance of antiviral mRNAs, with IFN and ISG transcript increasing in abundance in the context of mutant NS4b. IRF3 nuclear translocation is unaffected by mutation of NS4b, indicating the interaction likely occurs downstream of this point, while the specific underlying mechanism remains unknown.

and function predictions are not sufficient for ascertaining biological activity. In the course of this study, we also identified the NS4b protein of MERS-CoV as a putative PDE and demonstrated that it too degrades 2-5A and inhibits RNase L activation by the same

mechanism as MHV NS2 (Fig 1.4) (164). However, as described in Chapter 4, NS4b localizes primarily to the nucleus unlike other viral 2H-PEs, which spurred us to investigate additional functions. Due to this continuation of our work, we have demonstrated that in addition to inhibiting the OAS-RNase L pathway, MERS-CoV NS4b also inhibits the interferon response, as IFN and other antiviral transcripts are more abundant during infection with recombinant MERS-CoV containing targeted mutations in the NS4b catalytic site or nuclear localization sequence (Fig 1.4) (165). Although the specific mechanism of NS4b interaction with the IFN response remains unclear, it is clear that this work has uncovered

previously unrecognized interactions between viral 2H-PEs and host antiviral responses. Continued work in the Weiss laboratory will include a focus on elucidating the mechanistic nature of these interactions.

## References

1. **Fehr AR, Perlman S.** 2015. Coronaviruses: An Overview of Their Replication and Pathogenesis, pp. 1–23. *In* Randell, SH, Fulcher, ML (eds.), *Epithelial Cell Culture Protocols*. Springer New York, New York, NY.
2. **Saberi A, Gulyaeva AA, Brubacher J, Newmark PA, Gorbalenya A.** 2018. A planarian nidovirus expands the limits of RNA genome size.
3. **Debat HJ.** 2018. Expanding the size limit of RNA viruses: Evidence of a novel divergent nidovirus in California sea hare, with a ~35.9 kb virus genome.
4. **Wolf YI, Kazlauskas D, Iranzo J, Lucía-Sanz A, Kuhn JH, Krupovic M, Dolja VV, Koonin EV.** 2018. Origins and Evolution of the Global RNA Virome. *mBio* **9**:e02329–18.
5. **Sawicki SG, Sawicki DL, Siddell SG.** 2006. A Contemporary View of Coronavirus Transcription. *Journal of Virology* **81**:20–29.
6. **Song D, Moon H, Kang B.** 2015. Porcine epidemic diarrhea: a review of current epidemiology and available vaccines. *Clinical and experimental vaccine research* **4**:166–176.
7. **Lee C.** 2015. Porcine epidemic diarrhea virus: An emerging and re-emerging epizootic swine virus. *Virology Journal* **12**:193–193.
8. **Huang C, Liu WJ, Xu W, Jin T, Zhao Y, Song J, Shi Y, Ji W, Jia H, Zhou Y, Wen H, Zhao H, Liu H, Li H, Wang Q, Wu Y, Wang L, Liu D, Liu G, Yu H, Holmes EC, Lu L, Gao GF.** 2016. A Bat-Derived Putative Cross-Family Recombinant Coronavirus with a Reovirus Gene. *PLOS Pathogens* **12**:e1005883.
9. **Maestre AM, Garzón A, Rodríguez D.** 2011. Equine Torovirus (BEV) Induces Caspase-Mediated Apoptosis in Infected Cells. *PLoS ONE* **6**:e20972.

10. **Hamre D, Procknow JJ.** 1966. A new virus isolated from the human respiratory tract. *Proc Soc Exp Biol Med* **121**:190–193.
11. **McIntosh K, Becker WB, Chanock RM.** 1967. Growth in suckling-mouse brain of “IBV-like” viruses from patients with upper respiratory tract disease. *Proc Natl Acad Sci USA* **58**:2268–2273.
12. **Almeida JD, Tyrrell DA.** 1967. The morphology of three previously uncharacterized human respiratory viruses that grow in organ culture. *J Gen Virol* **1**:175–178.
13. **Bradburne AF, Somerset BA.** 1972. Coronative antibody titres in sera of healthy adults and experimentally infected volunteers. *J Hyg (Lond)* **70**:235–244.
14. **Hogue BG, King B, Brian DA.** 1984. Antigenic relationships among proteins of bovine coronavirus, human respiratory coronavirus OC43, and mouse hepatitis coronavirus A59. *Journal of Virology* **51**:384–388.
15. **Lapps W, Brian DA.** 1985. Oligonucleotide fingerprints of antigenically related bovine coronavirus and human coronavirus OC43. *Archives of Virology* **86**:101–108.
16. **Kamahora T, Soe LH, Lai MM.** 1989. Sequence analysis of nucleocapsid gene and leader RNA of human coronavirus OC43. *Virus Research* **12**:1–9.
17. **Vijgen L, Keyaerts E, Moes E, Thoelen I, Wollants E, Lemey P, Vandamme AM, Van Ranst M.** 2005. Complete Genomic Sequence of Human Coronavirus OC43: Molecular Clock Analysis Suggests a Relatively Recent Zoonotic Coronavirus Transmission Event. *Journal of Virology* **79**:1595–1604.
18. **Vijgen L, Keyaerts E, Lemey P, Moës E, Li S, Vandamme A-M, Van Ranst M.** 2005. Circulation of genetically distinct contemporary human coronavirus \OC43\ strains. *Virology* **337**:85–92.
19. **Hu Q, Lu R, Peng K, Duan X, Wang Y, Zhao Y, Wang W, Lou Y, Tan W.** 2014. Prevalence and Genetic Diversity Analysis of Human Coronavirus OC43 among Adult Patients with Acute Respiratory Infections in Beijing, 2012. *PLoS ONE* **9**:e100781.
20. **Gerna G, Campanini G, Rovida F, Percivalle E, Sarasini A, Marchi A, Baldanti F.** 2006. Genetic variability of human coronavirus OC43-, 229E-, and NL63-like strains and their association with lower respiratory tract infections of hospitalized infants and immunocompromised patients. *Journal of Medical Virology* **78**:938–

949.

21. **Poon LLM, Chu DKW, Chan KH, Wong OK, Ellis TM, Leung YHC, Lau SKP, Woo PCY, Suen KY, Yuen KY, Guan Y, Peiris JSM.** 2005. Identification of a novel coronavirus in bats. *Journal of Virology* **79**:2001–2009.
22. **Pfefferle S, Oppong S, Drexler JF, Gloza-Rausch F, Ipsen A, Seebens A, Müller MA, Annan A, Vallo P, Adu-Sarkodie Y, Kruppa TF, Drosten C.** 2009. Distant relatives of severe acute respiratory syndrome coronavirus and close relatives of human coronavirus 229E in bats, Ghana. *Emerging Infectious Diseases* **15**:1377–1384.
23. **Corman VM, Eckerle I, Memish ZA, Liljander AM, Dijkman R, Jonsdottir H, Juma Ngeiywa KJZ, Kamau E, Younan M, Masri Al M, Assiri A, Gluecks I, Musa BE, Meyer B, Müller MA, Hilali M, Bornstein S, Wernery U, Thiel V, Jores J, Drexler JF, Drosten C.** 2016. Link of a ubiquitous human coronavirus to dromedary camels. *Proceedings of the National Academy of Sciences* **113**:9864–9869.
24. **Corman VM, Baldwin HJ, Tateno AF, Zerbinati RM, Annan A, Owusu M, Nkrumah EE, Maganga GD, Oppong S, Adu-Sarkodie Y, Vallo P, da Silva Filho LVR, Leroy EM, Thiel V, van der Hoek L, Poon LLM, Tschapka M, Drosten C, Drexler JF.** 2015. Evidence for an Ancestral Association of Human Coronavirus 229E with Bats. *Journal of Virology* **89**:11858–11870.
25. **Corman VM, Eckerle I, Memish ZA, Liljander AM, Dijkman R, Jonsdottir H, Juma Ngeiywa KJZ, Kamau E, Younan M, Masri Al M, Assiri A, Gluecks I, Musa BE, Meyer B, Müller MA, Hilali M, Bornstein S, Wernery U, Thiel V, Jores J, Drexler JF, Drosten C.** 2016. Link of a ubiquitous human coronavirus to dromedary camels. *Proc Natl Acad Sci USA* **113**:9864–9869.
26. **van der Hoek L, Pyrc K, Jebbink MF, Vermeulen-Oost W, Berkhout RJM, Wolthers KC, Wertheim-van Dillen PME, Kaandorp J, Spaargaren J, Berkhout B.** 2004. Identification of a new human coronavirus. *Nat Med* **10**:368–373.
27. **Huynh J, Li S, Yount B, Smith A, Sturges L, Olsen JC, Nagel J, Johnson JB, Agnihothram S, Gates JE, Frieman MB, Baric RS, Donaldson EF.** 2012. Evidence supporting a zoonotic origin of human coronavirus strain NL63. *Journal of Virology*, 5 ed. **86**:12816–12825.
28. **Anthony SJ, Johnson CK, Greig DJ, Kramer S, Che X, Wells H, Hicks AL, Joly DO, Wolfe ND, Daszak P, Karesh W, Lipkin WI,**

- Morse SS, Mazet JAK, Goldstein T.** 2017. Global patterns in coronavirus diversity. *Virus Evol* **3**:vex012–vex012.
29. **Lau SKP, Li KSM, Poon RWS, Wong BHL, Tsoi H-W, Yip BCK, Huang Y, Chan K-H, Yuen K-Y.** 2006. Molecular diversity of coronaviruses in bats. *Virology* **351**:180–187.
30. **Hofmann H, Pyrc K, van der Hoek L, Geier M, Berkhout B, Pöhlmann S.** 2005. Human coronavirus NL63 employs the severe acute respiratory syndrome coronavirus receptor for cellular entry. *Proc Natl Acad Sci USA* **102**:7988–7993.
31. **Lin HX, Feng Y, Wong G, Wang L, Li B, Zhao X, Li Y, Smaill F, Zhang C.** 2008. Identification of residues in the receptor-binding domain (RBD) of the spike protein of human coronavirus NL63 that are critical for the RBD-ACE2 receptor interaction. *J Gen Virol* **89**:1015–1024.
32. **Woo PCY, Lau SKP, Chu CM, Chan KH, Tsoi HW, Huang Y, Wong BHL, Poon RWS, Cai JJ, Luk WK, Poon LLM, Wong SSY, Guan Y, Peiris JSM, Yuen KY.** 2004. Characterization and Complete Genome Sequence of a Novel Coronavirus, Coronavirus HKU1, from Patients with Pneumonia. *Journal of Virology* **79**:884–895.
33. **Lau SKP, Woo PCY, Yip CCY, Tse H, Tsoi H-W, Cheng VCC, Lee P, Tang BSF, Cheung CHY, Lee RA, So L-Y, Lau Y-L, Chan K-H, Yuen K-Y.** 2006. Coronavirus HKU1 and other coronavirus infections in Hong Kong. *Journal of Clinical Microbiology* **44**:2063–2071.
34. **Heimdal I, Moe N, Krokstad S, Christensen A, Skanke LH, Nordbø SA, Døllner H.** 2018. Human Coronavirus in Hospitalized Children with Respiratory Tract Infections: A Nine-year-long, Population-based Study from Norway. *Journal of Infectious Diseases*.
35. **Kanwar A, Selvaraju S, Esper F.** 2017. Human Coronavirus-HKU1 Infection Among Adults in Cleveland, Ohio. *Open Forum Infect Dis* **4**:ofx052.
36. **Killerby ME, Biggs HM, Haynes A, Dahl RM, Mustaquim D, Gerber SI, Watson JT.** 2018. Human coronavirus circulation in the United States 2014-2017. *J Clin Virol* **101**:52–56.
37. **Pyrc K, Sims AC, Dijkman R, Jebbink M, Long C, Deming D, Donaldson E, Vabret A, Baric R, van der Hoek L, Pickles R.** 2010. Culturing the unculturable: human coronavirus HKU1 infects, replicates, and produces progeny virions in human ciliated airway epithelial cell cultures. *Journal of Virology* **84**:11255–11263.

38. **Dijkman R, Jebbink MF, Koekkoek SM, Deijs M, Jonsdottir HR, Molenkamp R, Ieven M, Goossens H, Thiel V, van der Hoek L.** 2013. Isolation and Characterization of Current Human Coronavirus Strains in Primary Human Epithelial Cell Cultures Reveal Differences in Target Cell Tropism. *Journal of Virology* **87**:6081–6090.
39. **Tsang KW, Ho PL, Ooi GC, Yee WK, Wang T, Chan-Yeung M, Lam WK, Seto WH, Yam LY, Cheung TM, Wong PC, Lam B, Ip MS, Chan J, Yuen KY, Lai KN.** 2003. A cluster of cases of severe acute respiratory syndrome in Hong Kong. *N Engl J Med* **348**:1977–1985.
40. **Peiris JSM, Yuen KY, Osterhaus ADME, Stöhr K.** 2003. The Severe Acute Respiratory Syndrome. *The New England Journal of Medicine* **349**:2431–2441.
41. **Lee N, Hui D, Wu A, Chan P, Cameron P, Joynt GM, Ahuja A, Yung MY, Leung CB, To KF, Lui SF, Szeto CC, Chung S, Sung JJY.** 2003. A major outbreak of severe acute respiratory syndrome in Hong Kong. *N Engl J Med* **348**:1986–1994.
42. **Poutanen SM, Low DE, Henry B, Finkelstein S, Rose D, Green K, Tellier R, Draker R, Adachi D, Ayers M, Chan AK, Skowronski DM, Salit I, Simor AE, Slutsky AS, Doyle PW, Kraiden M, Petric M, Brunham RC, McGeer AJ, National Microbiology Laboratory, Canada, Canadian Severe Acute Respiratory Syndrome Study Team.** 2003. Identification of severe acute respiratory syndrome in Canada. *N Engl J Med* **348**:1995–2005.
43. **World Health Organization.** 2003. Global Alert and Response (GAR) Summary of probable SARS cases with onset of illness from 1 November 2002 to 31 July 2003. [www.who.int](http://www.who.int).
44. **Peiris JSM, Lai ST, Poon LLM, Guan Y, Yam LYC, Lim W, Nicholls J, Yee WKS, Yan WW, Cheung MT, Cheng VCC, Chan KH, Tsang DNC, Yung RWH, Ng TK, Yuen KY, SARS study group.** 2003. Coronavirus as a possible cause of severe acute respiratory syndrome. *Lancet* **361**:1319–1325.
45. **Ksiazek TG, Erdman D, Goldsmith CS, Zaki SR, Peret T, Emery S, Tong S, Urbani C, Comer JA, Lim W, Rollin PE, Dowell SF, Ling A-E, Humphrey CD, Shieh W-J, Guarner J, Paddock CD, Rota P, Fields B, DeRisi J, Yang J-Y, Cox N, Hughes JM, LeDuc JW, Bellini WJ, Anderson LJ.** 2003. A Novel Coronavirus Associated with Severe Acute Respiratory Syndrome. *The New England Journal of Medicine* **348**:1953–1966.
46. **Drosten C, Günther S, Preiser W, van der Werf S, Brodt H-R, Becker S, Rabenau H, Panning M, Kolesnikova L, Fouchier RAM,**

- Berger A, Burguière A-M, Cinatl J, Eickmann M, Escriou N, Grywna K, Kramme S, Manuguerra J-C, Müller S, Rickerts V, Stürmer M, Vieth S, Klenk H-D, Osterhaus ADME, Schmitz H, Doerr HW.** 2003. Identification of a Novel Coronavirus in Patients with Severe Acute Respiratory Syndrome. *The New England Journal of Medicine* **348**:1967–1976.
47. **Li W, Moore MJ, Vasilieva N, Sui J, Wong SK, Berne MA, Somasundaran M, Sullivan JL, Luzuriaga K, Greenough TC, Choe H, Farzan M.** 2003. Angiotensin-converting enzyme 2 is a functional receptor for the SARS coronavirus. *Nature* **426**:450–454.
48. **Marra MA, Jones SJM, Astell CR, Holt RA, Brooks-Wilson A, Butterfield YSN, Khattra J, Asano JK, Barber SA, Chan SY, Cloutier A, Coughlin SM, Freeman D, Girn N, Griffith OL, Leach SR, Mayo M, McDonald H, Montgomery SB, Pandoh PK, Petrescu AS, Robertson AG, Schein JE, Siddiqui A, Smailus DE, Stott JM, Yang GS, Plummer F, Andonov A, Artsob H, Bastien N, Bernard K, Booth TF, Bowness D, Czub M, Drebot M, Fernando L, Flick R, Garbutt M, Gray M, Grolla A, Jones S, Feldmann H, Meyers A, Kabani A, Li Y, Normand S, Stroher U, Tipples GA, Tyler S, Vogrig R, Ward D, Watson B, Brunham RC, Kraiden M, Petric M, Skowronski DM, Upton C, Roper RL.** 2003. The Genome sequence of the SARS-associated coronavirus. *Science* **300**:1399–1404.
49. **Ruan YJ, Wei CL, Ee AL, Vega VB, Thoreau H, Su STY, Chia J-M, Ng P, Chiu KP, Lim L, Zhang T, Peng CK, Lin EOL, Lee NM, Yee SL, Ng LFP, Chee RE, Stanton LW, Long PM, Liu ET.** 2003. Comparative full-length genome sequence analysis of 14 SARS coronavirus isolates and common mutations associated with putative origins of infection. *Lancet* **361**:1779–1785.
50. **Guan Y, Zheng BJ, He YQ, Liu XL, Zhuang ZX, Cheung CL, Luo SW, Li PH, Zhang LJ, Guan YJ, Butt KM, Wong KL, Chan KW, Lim W, Shortridge KF, Yuen KY, Peiris JSM, Poon LLM.** 2003. Isolation and characterization of viruses related to the SARS coronavirus from animals in southern China. *Science* **302**:276–278.
51. **Wang M, Yan M, Xu H, Liang W, Kan B, Zheng B, Chen H, Zheng H, Xu Y, Zhang E, Wang H, Ye J, Li G, Li M, Cui Z, Liu Y-F, Guo R-T, Liu X-N, Zhan L-H, Zhou D-H, Zhao A, Hai R, Yu D, Guan Y, Xu J.** 2005. SARS-CoV infection in a restaurant from palm civet. *Emerging Infectious Diseases* **11**:1860–1865.
52. **Kan B, Wang M, Jing H, Xu H, Jiang X, Yan M, Liang W, Zheng H, Wan K, Liu Q, Cui B, Xu Y, Zhang E, Wang H, Ye J, Li G, Li M, Cui Z, Qi X, Chen K, Du L, Gao K, Zhao Y-T, Zou X-Z, Feng Y-J, Gao**

- Y-F, Hai R, Yu D, Guan Y, Xu J.** 2005. Molecular evolution analysis and geographic investigation of severe acute respiratory syndrome coronavirus-like virus in palm civets at an animal market and on farms. *Journal of Virology* **79**:11892–11900.
53. **Wu D, Tu C, Xin C, Xuan H, Meng Q, Liu Y, Yu Y, Guan Y, Jiang Y, Yin X, Crameri G, Wang M, Li C, Liu S, Liao M, Feng L, Xiang H, Sun J, Chen J, Sun Y, Gu S, Liu N, Fu D, Eaton BT, Wang L-F, Kong X.** 2005. Civets Are Equally Susceptible to Experimental Infection by Two Different Severe Acute Respiratory Syndrome Coronavirus Isolates. *Journal of Virology* **79**:2620–2625.
54. **Leroy EM, Kumulungui B, Pourrut X, Rouquet P, Hassanin A, Yaba P, Délicat A, Paweska JT, Gonzalez J-P, Swanepoel R.** 2005. Fruit bats as reservoirs of Ebola virus. *Nature* **438**:575–576.
55. **Towner JS, Amman BR, Sealy TK, Carroll SAR, Comer JA, Kemp A, Swanepoel R, Paddock CD, Balinandi S, Khristova ML, Formenty PBH, Albarino CG, Miller DM, Reed ZD, Kayiwa JT, Mills JN, Cannon DL, Greer PW, Byaruhanga E, Farnon EC, Atimnedi P, Okware S, Katongole-Mbidde E, Downing R, Tappero JW, Zaki SR, Ksiazek TG, Nichol ST, Rollin PE.** 2009. Isolation of Genetically Diverse Marburg Viruses from Egyptian Fruit Bats. *PLOS Pathogens* **5**:e1000536.
56. **Yob JM, Field H, Rashdi AM, Morrissy C, van der Heide B, Rota P, bin Adzhar A, White J, Daniels P, Jamaluddin A, Ksiazek T.** 2001. Nipah virus infection in bats (order Chiroptera) in peninsular Malaysia. *Emerging Infectious Diseases* **7**:439–441.
57. **Han H-J, Wen H-L, Zhou C-M, Chen F-F, Luo L-M, Liu J-W, Yu X-J.** 2015. Bats as reservoirs of severe emerging infectious diseases. *Virus Research* **205**:1–6.
58. **Li W, Shi Z, Yu M, Ren W, Smith C, Epstein JH, Wang H, Crameri G, Hu Z, Zhang H, Zhang J, McEachern J, Field H, Daszak P, Eaton BT, Zhang S, Wang L-F.** 2005. Bats are natural reservoirs of SARS-like coronaviruses. *Science* **310**:676–679.
59. **Lau SKP, Li KSM, Huang Y, Tsoi H-W, Wong BHL, Wong SSY, Leung S-Y, Chan K-H, Yuen K-Y.** 2005. Severe acute respiratory syndrome coronavirus-like virus in Chinese horseshoe bats. *Proceedings of the National Academy of Sciences of the United States of America* **102**:14040–14045.
60. **Ge X-Y, Li J-L, Yang X-L, Chmura AA, Zhu G, Epstein JH, Mazet JK, Ben Hu, Zhang W, Peng C, Zhang Y-J, Luo C-M, Tan B, Wang N, Zhu Y, Crameri G, Zhang S-Y, Wang L-F, Daszak P, Shi Z-L.**

2013. Isolation and characterization of a bat SARS-like coronavirus that uses the ACE2 receptor. *Nature* **503**:535–538.
61. **Wang N, Li S-Y, Yang X-L, Huang H-M, Zhang Y-J, Guo H, Luo C-M, Miller M, Zhu G, Chmura AA, Hagan E, Zhou J-H, Zhang Y-Z, Wang L-F, Daszak P, Shi Z-L.** 2018. Serological Evidence of Bat SARS-Related Coronavirus Infection in Humans, China. *Viol Sin*, 6 ed. **33**:104–107.
62. **Menachery VD, Yount BL, Debbink K, Agnihothram S, Gralinski LE, Plante JA, Graham RL, Scobey T, Ge X-Y, Donaldson EF, Randell SH, Lanzavecchia A, Marasco WA, Shi Z-L, Baric RS.** 2015. A SARS-like cluster of circulating bat coronaviruses shows potential for human emergence. *Nat Med* **21**:1508–1513.
63. **Menachery VD, Yount BL, Sims AC, Debbink K, Agnihothram SS, Gralinski LE, Graham RL, Scobey T, Plante JA, Royal SR, Swanstrom J, Sheahan TP, Pickles RJ, Corti D, Randell SH, Lanzavecchia A, Marasco WA, Baric RS.** 2016. SARS-like WIV1-CoV poised for human emergence. *Proceedings of the National Academy of Sciences* **113**:3048–3053.
64. **Towner JS, Amman BR, Sealy TK, Carroll SAR, Comer JA, Kemp A, Swanepoel R, Paddock CD, Balinandi S, Khristova ML, Formenty PBH, Albarino CG, Miller DM, Reed ZD, Kayiwa JT, Mills JN, Cannon DL, Greer PW, Byaruhanga E, Farnon EC, Atimnedi P, Okware S, Katongole-Mbidde E, Downing R, Tappero JW, Zaki SR, Ksiazek TG, Nichol ST, Rollin PE.** 2009. Isolation of genetically diverse Marburg viruses from Egyptian fruit bats. *PLOS Pathogens* **5**:e1000536.
65. **Hu B, Zeng L-P, Yang X-L, Ge X-Y, Zhang W, Li B, Xie J-Z, Shen X-R, Zhang Y-Z, Wang N, Luo D-S, Zheng X-S, Wang M-N, Daszak P, Wang L-F, Cui J, Shi Z-L.** 2017. Discovery of a rich gene pool of bat SARS-related coronaviruses provides new insights into the origin of SARS coronavirus. *PLOS Pathogens* **13**:e1006698.
66. **Zaki AM, van Boheemen S, Bestebroer TM, Osterhaus ADME, Fouchier RAM.** 2012. Isolation of a Novel Coronavirus from a Man with Pneumonia in Saudi Arabia. *The New England Journal of Medicine* **367**:1814–1820.
67. **Hijawi B, Abdallat M, Sayaydeh A, Alqasrawi S, Haddadin A, Jaarour N, Alsheikh S, Alsanouri T.** 2013. Novel coronavirus infections in Jordan, April 2012: epidemiological findings from a retrospective investigation. *East Mediterr Health J* **19 Suppl 1**:S12–8.
68. **van Boheemen S, de Graaf M, Lauber C, Bestebroer TM, Raj VS,**

- Zaki AM, Osterhaus ADME, Haagmans BL, Gorbalenya AE, Snijder EJ, Fouchier RAM.** 2012. Genomic Characterization of a Newly Discovered Coronavirus Associated with Acute Respiratory Distress Syndrome in Humans. *mBio* **3**:e00473–12.
69. **Wang M, Lau SKP, Xu H, Poon RWS, Guo R, Wong BHL, Gao K, Tsoi H-W, Huang Y, Li KSM, Lam CSF, Chan K-H, Zheng B-J, Yuen K-Y.** 2007. Comparative Analysis of Twelve Genomes of Three Novel Group 2c and Group 2d Coronaviruses Reveals Unique Group and Subgroup Features. *Journal of Virology* **81**:1574–1585.
70. **Kim KH, Tandi TE, Choi JW, Moon JM, Kim MS.** Middle East respiratory syndrome coronavirus (MERS-CoV) outbreak in South Korea, 2015: epidemiology, characteristics and public health implications. *J Hosp Infect* **95**:207–213.
71. **Saad M, Omrani AS, Baig K, Bahloul A, Elzein F, Matin MA, Selim MAA, Mutairi AI M, Nakhli AI D, Aidaroos AI AY, Sherbeeni AI N, Al-Khashan HI, Memish ZA, Albarrak AM.** 2014. Clinical aspects and outcomes of 70 patients with Middle East respiratory syndrome coronavirus infection: a single-center experience in Saudi Arabia. *Int J Infect Dis* **29**:301–306.
72. **Assiri A, Al-Tawfiq JA, Rabeeah AI AA, Al-Rabiah FA, Al-Hajjar S, Al-Barrak A, Flemban H, Al-Nassir WN, Balkhy HH, Al-Hakeem RF, Makhdoom HQ, Zumla AI, Memish ZA.** 2013. Epidemiological, demographic, and clinical characteristics of 47 cases of Middle East respiratory syndrome coronavirus disease from Saudi Arabia: a descriptive study. *Lancet Infect Dis* **13**:752–761.
73. **Omrani AS, Matin MA, Haddad Q, Nakhli AI D, Memish ZA, Albarrak AM.** 2013. A family cluster of Middle East Respiratory Syndrome Coronavirus infections related to a likely unrecognized asymptomatic or mild case. *Int J Infect Dis* **17**:e668–72.
74. **Memish ZA, Mishra N, Olival KJ, Fagbo SF, Kapoor V, Epstein JH, AlHakeem R, Durosinsloun A, Asmari AI M, Islam A, Kapoor A, Briese T, Daszak P, Rabeeah AI AA, Lipkin WI.** 2013. Middle East Respiratory Syndrome Coronavirus in Bats, Saudi Arabia. *Emerging Infectious Diseases* **19**.
75. **Ithete NL, Stoffberg S, Corman VM, Cottontail VM, Richards LR, Schoeman MC, Drosten C, Drexler JF, Preiser W.** 2013. Close Relative of Human Middle East Respiratory Syndrome Coronavirus in Bat, South Africa. *Emerging Infectious Diseases* **19**:1697–1699.
76. **Corman VM, Ithete NL, Richards LR, Schoeman MC, Preiser W, Drosten C, Drexler JF.** 2014. Rooting the Phylogenetic Tree of

Middle East Respiratory Syndrome Coronavirus by Characterization of a Conspecific Virus from an African Bat. *Journal of Virology* **88**:11297–11303.

77. **Geldenhuys M, Mortlock M, Weyer J, Bezuidt O, Seamark ECJ, Kearney T, Gleasner C, Erkkila TH, Cui H, Markotter W.** 2018. A metagenomic viral discovery approach identifies potential zoonotic and novel mammalian viruses in *Neoromicia* bats within South Africa. *PLoS ONE* **13**:e0194527.
78. **Anthony SJ, Gilardi K, Menachery VD, Goldstein T, Ssebide B, Mbabazi R, Navarrete-Macias I, Liang E, Wells H, Hicks A, Petrosov A, Byarugaba DK, Debbink K, Dinnon KH, Scobey T, Randell SH, Yount BL, Cranfield M, Johnson CK, Baric RS, Lipkin WI, Mazet JAK.** 2017. Further Evidence for Bats as the Evolutionary Source of Middle East Respiratory Syndrome Coronavirus. *mBio* **8**:e00373–17.
79. **Raj VS, Mou H, Smits SL, Dekkers DHW, Müller MA, Dijkman R, Muth D, Demmers JAA, Zaki A, Fouchier RAM, Thiel V, Drosten C, Rottier PJM, Osterhaus ADME, Bosch B-J, Haagmans BL.** 2013. Dipeptidyl peptidase 4 is a functional receptor for the emerging human coronavirus-EMC. *Nature* **495**:251–254.
80. **Wang Q, Qi J, Yuan Y, Xuan Y, Han P, Wan Y, Ji W, Li Y, Wu Y, Wang J, Iwamoto A, Yuen K-Y, Yan J, Lu G, Gao GF.** 2014. Bat Origins of MERS-CoV Supported by Bat Coronavirus HKU4 Usage of Human Receptor CD26. *Cell Host and Microbe* **16**:328–337.
81. **Yang Y, Du L, Liu C, Wang L, Ma C, Tang J, Baric RS, Jiang S, Li F.** 2014. Receptor usage and cell entry of bat coronavirus HKU4 provide insight into bat-to-human transmission of MERS coronavirus. *Proceedings of the National Academy of Sciences* **111**:12516–12521.
82. **Luo C-M, Wang N, Yang X-L, Liu H-Z, Zhang W, Li B, Hu B, Peng C, Geng Q-B, Zhu G-J, Li F, Shi Z-L.** 2018. Discovery of novel bat coronaviruses in south China that use the same receptor as MERS coronavirus. *Journal of Virology* **JVI.00116–18**.
83. **Yang Y, Liu C, Du L, Jiang S, Shi Z, S Baric R, Li F.** 2015. Two mutations were critical for bat-to-human transmission of MERS coronavirus. *Journal of Virology* **JVI.01279–15**.
84. **Reusken CB, Haagmans BL, Müller MA, Gutierrez C, Godeke G-J, Meyer B, Muth D, Raj VS, Vries LS-D, Corman VM, Drexler JF, Smits SL, Tahir El YE, De Sousa R, van Beek J, Nowotny N, van Maanen K, Hidalgo-Hermoso E, Bosch B-J, Rottier P, Osterhaus A, Gortázar-Schmidt C, Drosten C, Koopmans MP.** 2013. Middle

East respiratory syndrome coronavirus neutralising serum antibodies in dromedary camels: a comparative serological study. *Lancet Infect Dis* **13**:859–866.

85. **Haagmans BL, Dhahiry AI SHS, Reusken CBEM, Raj VS, Galiano M, Myers R, Godeke G-J, Jonges M, Farag E, Diab A, Ghobashy H, AlHajri F, Al-Thani M, Al-Marri SA, Al-Romaihi HE, Khal AI A, Bermingham A, Osterhaus ADME, AlHajri MM, Koopmans MPG.** 2014. Middle East respiratory syndrome coronavirus in dromedary camels: an outbreak investigation. *Lancet Infect Dis* **14**:140–145.
86. **Chu DK, Poon LL, Gomaa MM, Shehata MM, Perera RA, Abu Zeid D, Rifay El AS, Siu LY, Guan Y, Webby RJ, Ali MA, Peiris M, Kayali G.** 2014. MERS Coronaviruses in Dromedary Camels, Egypt. *Emerging Infectious Diseases* **20**:1049–1053.
87. **Ali M, El-Shesheny R, Kandeil A, Shehata M, Elsokary B, Gomaa M, Hassan N, Sayed El A, El-Taweel A, Sobhy H, Oludayo FF, Dauphin G, Masry El I, Wolde AW, Daszak P, Miller M, VonDobschuetz S, Gardner E, Morzaria S, Lubroth J, Makonnen YJ.** 2017. Cross-sectional surveillance of Middle East respiratory syndrome coronavirus (MERS-CoV) in dromedary camels and other mammals in Egypt, August 2015 to January 2016. *Euro Surveill* **22**:30487.
88. **Perera R, Wang P, Gomaa M, El-Shesheny R, Kandeil A, Bagato O, Siu L, Shehata M, Kayed A, Moatasim Y, Li M, Poon L, Guan Y, Webby R, Ali M, Peiris J, Kayali G.** 2013. Seroepidemiology for MERS coronavirus using microneutralisation and pseudoparticle virus neutralisation assays reveal a high prevalence of antibody in dromedary camels in Egypt, June 2013. *Euro Surveill* **18**:20574.
89. **Wernery U, Rasoul IE, Wong EY, Joseph M, Chen Y, Jose S, Tsang AK, Patteril NAG, Chen H, Elizabeth SK, Yuen K-Y, Joseph S, Xia N, Wernery R, Lau SK, Woo PC.** 2015. A phylogenetically distinct Middle East respiratory syndrome coronavirus detected in a dromedary calf from a closed dairy herd in Dubai with rising seroprevalence with age. *Emerg Microbes Infect* **4**:e74 EP –.
90. **Meyer B, Müller MA, Corman VM, Reusken CBEM, Ritz D, Godeke G-J, Lattwein E, Kallies S, Siemens A, van Beek J, Drexler JF, Muth D, Bosch B-J, Wernery U, Koopmans MPG, Wernery R, Drosten C.** 2014. Antibodies against MERS Coronavirus in Dromedary Camels, United Arab Emirates, 2003 and 2013. *Emerging Infectious Diseases* **20**:552–559.
91. **Wernery U, Corman VM, Wong EYM, Tsang AKL, Muth D, Lau**

- SKP, Khazanehdari K, Zirkel F, Ali M, Nagy P, Juhasz J, Wernery R, Joseph S, Syriac G, Elizabeth SK, Patteril NAG, Drosten C.** 2015. Acute Middle East Respiratory Syndrome Coronavirus Infection in Livestock Dromedaries, Dubai, 2014. *Emerging Infectious Diseases* **21**:1019–1022.
92. **van Doremalen N, Hijazeen ZSK, Holloway P, Omari AI B, McDowell C, Adney D, Talafha HA, Guitian J, Steel J, Amarin N, Tibbo M, Abu-Basha E, Al-Majali AM, Munster VJ, Richt JA.** 2017. High Prevalence of Middle East Respiratory Coronavirus in Young Dromedary Camels in Jordan. *Vector-Borne and Zoonotic Diseases* **17**:155–159.
93. **Alagaili AN, Briese T, Mishra N, Kapoor V, Sameroff SC, Burbelo PD, de Wit E, Munster VJ, Hensley LE, Zalmout IS, Kapoor A, Epstein JH, Karesh WB, Daszak P, Mohammed OB, Lipkin WI.** 2014. Middle East respiratory syndrome coronavirus infection in dromedary camels in Saudi Arabia. *mBio* **5**:e00884–14.
94. **Khalafalla AI, Lu X, Al-Mubarak AIA, Dalab AHS, Al-Busadah KAS, Erdman DD.** 2015. MERS-CoV in Upper Respiratory Tract and Lungs of Dromedary Camels, Saudi Arabia, 2013–2014. *Emerging Infectious Diseases* **21**:1153–1158.
95. **Memish ZA, Cotten M, Meyer B, Watson SJ, Alshafiqi AJ, Rabeeah AI AA, Corman VM, Sieberg A, Makhdoom HQ, Assiri A, Masri AI M, Aldabbagh S, Bosch B-J, Beer M, Müller MA, Kellam P, Drosten C.** 2014. Human Infection with MERS Coronavirus after Exposure to Infected Camels, Saudi Arabia, 2013. *Emerging Infectious Diseases* **20**:1012–1015.
96. **Azhar EI, El-Kafrawy SA, Farraj SA, Hassan AM, Al-Saeed MS, Hashem AM, Madani TA.** 2014. Evidence for Camel-to-Human Transmission of MERS Coronavirus. *The New England Journal of Medicine* **370**:2499–2505.
97. **Kiambi S, Corman VM, Sitawa R, Githinji J, Ngoci J, Ozomata AS, Gardner E, Dobschuetz von S, Morzaria S, Kimutai J, Schroeder S, Njagi O, Simpkin P, Rugalema G, Tadesse Z, Lubroth J, Makonnen Y, Drosten C, Müller MA, Fasina FO.** 2018. Detection of distinct MERS-Coronavirus strains in dromedary camels from Kenya, 2017. *Emerg Microbes Infect* **7**:195.
98. **Sabir JSM, Lam TTY, Ahmed MMM, Li L, Shen Y, E M Abo-Aba S, Qureshi MI, Abu-Zeid M, Zhang Y, Khiyami MA, Alharbi NS, Hajrah NH, Sabir MJ, Mutwakil MHZ, Kabli SA, Alsulaimany FAS, Obaid AY, Zhou B, Smith DK, Holmes EC, Zhu H, Guan Y.** 2015.

Co-circulation of three camel coronavirus species and recombination of MERS-CoVs in Saudi Arabia. *Science* **351**:81–84.

99. **Briese T, Mishra N, Jain K, Zalmout IS, Jabado OJ, Karesh WB, Daszak P, Mohammed OB, Alagaili AN, Lipkin WI.** 2014. Middle East Respiratory Syndrome Coronavirus Quasispecies That Include Homologues of Human Isolates Revealed through Whole-Genome Analysis and Virus Cultured from Dromedary Camels in Saudi Arabia. *mBio* **5**.
100. **Lau SKP, Wernery R, Wong EYM, Joseph S, Tsang AKL, Patteril NAG, Elizabeth SK, Chan K-H, Muhammed R, Kinne J, Yuen K-Y, Wernery U.** 2016. Polyphyletic origin of MERS coronaviruses and isolation of a novel clade A strain from dromedary camels in the United Arab Emirates. *Emerg Microbes Infect* **5**:e128.
101. **Müller MA, Meyer B, Corman VM, Al-Masri M, Turkestani A, Ritz D, Sieberg A, Aldabbagh S, Bosch B-J, Lattwein E, Alhakeem RF, Assiri AM, Albarrak AM, Al-Shangiti AM, Al-Tawfiq JA, Wikramaratna P, Alrabeeh AA, Drosten C, Memish ZA.** 2015. Presence of Middle East respiratory syndrome coronavirus antibodies in Saudi Arabia: a nationwide, cross-sectional, serological study. *Lancet Infect Dis* **15**:559–564.
102. **Farag EABA, Reusken CBEM, Haagmans BL, Mohran KA, Stalin Raj V, Pas SD, Voermans J, Smits SL, Godeke G-J, Al-Hajri MM, Alhajri FH, Al-Romaihi HE, Ghobashy H, El-Maghraby MM, El-Sayed AM, Thani Al MHJ, Al-Marri S, Koopmans MPG.** 2015. High proportion of MERS-CoV shedding dromedaries at slaughterhouse with a potential epidemiological link to human cases, Qatar 2014. *Infect Ecol Epidemiol* **5**:28305.
103. **Reusken CBEM, Farag EABA, Haagmans BL, Mohran KA, Godeke G-J, Raj S, AlHajri F, Al-Marri SA, Al-Romaihi H, Al-Thani M, Bosch B-J, van der Eijk AA, El-Sayed AM, Ibrahim AK, Al-Molawi N, Müller MA, Pasha SK, Park SS, AlHajri MM, Koopmans MPG.** 2015. Occupational Exposure to Dromedaries and Risk for MERS-CoV Infection, Qatar, 2013–2014. *Emerging Infect Dis* **21**:1422.
104. **Hammadi Al ZM, Chu DKW, Eltahir YM, Hosani Al F, Mulla Al M, Tarnini W, Hall AJ, Perera RAPM, Abdelkhalek MM, Peiris JSM, Muhairi Al SS, Poon LLM.** 2015. Asymptomatic MERS-CoV Infection in Humans Possibly Linked to Infected Dromedaries Imported from Oman to United Arab Emirates, May 2015. *Emerging Infect Dis* **21**:2197.

105. **Alshukairi AN, Zheng J, Zhao J, Nehdi A, Baharoon SA, Layqah L, Bokhari A, Johani AI SM, Samman N, Boudjelal M, Eyck Ten P, Al-Mozaini MA, Zhao J, Perlman S, Alagaili AN.** 2018. High Prevalence of MERS-CoV Infection in Camel Workers in Saudi Arabia. *mBio* **9**:PE217.
106. **Meyer B, Müller MA, Corman VM, Reusken CB, Ritz D, Godeke G-J, Lattwein E, Kallies S, Siemens A, van Beek J, Drexler JF, Muth D, Bosch B-J, Wernery U, Koopmans MP, Wernery R, Drosten C.** 2014. Antibodies against MERS Coronavirus in Dromedary Camels, United Arab Emirates, 2003 and 2013. *Emerging Infectious Diseases* **20**:552–559.
107. **Yusof MF, Eltahir YM, Serhan WS, Hashem FM, Elsayed EA, Marzoug BA, Abdelazim AS, Bensalah OKA, Muhairi AI SS.** 2015. Prevalence of Middle East respiratory syndrome coronavirus (MERS-CoV) in dromedary camels in Abu Dhabi Emirate, United Arab Emirates. *Virus Genes* **50**.
108. **Corman VM, Jores J, Meyer B, Younan M, Liljander A, Said MY, Gluecks I, Lattwein E, Bosch B-J, Drexler JF, Bornstein S, Drosten C, Müller MA.** 2014. Antibodies against MERS Coronavirus in Dromedary Camels, Kenya, 1992–2013. *Emerging Infectious Diseases* **20**:1319.
109. **Deem SL, Fèvre EM, Kinnaird M, Browne AS, Muloi D, Godeke G-J, Koopmans M, Reusken CB.** 2015. Serological Evidence of MERS-CoV Antibodies in Dromedary Camels (*Camelus dromedaries*) in Laikipia County, Kenya. *PLoS ONE* **10**:e0140125.
110. **Reusken CBEM, Messadi L, Feyisa A, Ularamu H, Godeke G-J, Danmarwa A, Dawo F, Jemli M, Melaku S, Shamaki D, Woma Y, Wungak Y, Gebremedhin EZ, Zutt I, Bosch B-J, Haagmans BL, Koopmans MPG.** 2014. Geographic Distribution of MERS Coronavirus among Dromedary Camels, Africa. *Emerging Infectious Diseases* **20**:1370–1374.
111. **Müller MA, Corman VM, Jores J, Meyer B, Younan M, Liljander A, Bosch B-J, Lattwein E, Hilali M, Musa BE, Bornstein S, Drosten C.** 2014. MERS Coronavirus Neutralizing Antibodies in Camels, Eastern Africa, 1983–1997. *Emerging Infectious Diseases* **20**:2093–2095.
112. **Miguel E, Chevalier V, Ayelet G, Ben Bencheikh MN, Boussini H, Chu DK, Berbri EI, Fassi-Fihri O, Faye B, Fekadu G, Grosbois V, Ng BC, Perera RA, So TY, Traore A, Roger F, Peiris M.** 2017. Risk factors for MERS coronavirus infection in dromedary camels in

- Burkina Faso, Ethiopia, and Morocco, 2015. *Euro Surveill* **22**:30498–10.
113. **Liljander A, Meyer B, Jores J, Müller MA, Lattwein E, Njeru I, Bett B, Drosten C, Corman VM.** 2016. MERS-CoV Antibodies in Humans, Africa, 2013–2014. *Emerging Infectious Diseases* **22**:1086–1089.
114. **So RT, Perera RA, Oladipo JO, Chu DK, Kuranga SA, Chan K-H, Lau EH, Cheng SM, Poon LL, Webby RJ, Peiris M.** 2018. Lack of serological evidence of Middle East respiratory syndrome coronavirus infection in virus exposed camel abattoir workers in Nigeria, 2016. *Euro Surveill* **23**:30086.
115. **Younan M, Bornstein S, Gluecks IV.** 2016. MERS and the dromedary camel trade between Africa and the Middle East. *Tropical Animal Health and Production* **48**:1277–1282.
116. **Chu DKW, Hui KPY, Perera RAPM, Miguel E, Niemeyer D, Zhao J, Channappanavar R, Dudas G, Oladipo JO, Traore A, Fassi-Fihri O, Ali A, Demissié GF, Muth D, Chan MCW, Nicholls JM, Meyerholz DK, Kuranga SA, Mamo G, Zhou Z, So RTY, Hemida MG, Webby RJ, Roger F, Rambaut A, Poon LLM, Perlman S, Drosten C, Chevalier V, Peiris M.** 2018. MERS coronaviruses from camels in Africa exhibit region-dependent genetic diversity. *Proceedings of the National Academy of Sciences* **115**:3144–3149.
117. **Takeuchi O, Akira S.** 2009. Innate immunity to virus infection. *Immunological Reviews* **227**:75–86.
118. **Ank N, West H, Bartholdy C, Eriksson K, Thomsen AR, Paludan SR.** 2006. Lambda Interferon (IFN- $\lambda$ ), a Type III IFN, Is Induced by Viruses and IFNs and Displays Potent Antiviral Activity against Select Virus Infections In Vivo. *Journal of Virology* **80**:4501–4509.
119. **Lazear HM, Nice TJ, Diamond MS.** 2015. Interferon- $\lambda$ : Immune Functions at Barrier Surfaces and Beyond. *Immunity* **43**:15–28.
120. **Wells AI, Coyne CB.** 2018. Type III Interferons in Antiviral Defenses at Barrier Surfaces. *Trends in Immunology*.
121. **Sommereyns C, Paul S, Staeheli P, Michiels T.** 2008. IFN-Lambda (IFN- $\lambda$ ) Is Expressed in a Tissue-Dependent Fashion and Primarily Acts on Epithelial Cells In Vivo. *PLOS Pathogens* **4**:e1000017 EP –.
122. **Mordstein M, Neugebauer E, Ditt V, Jessen B, Rieger T, Falcone V, Sorgeloos F, Ehl S, Mayer D, Kochs G, Schwemmler M, Günther S, Drosten C, Michiels T, Staeheli P.** 2010. Lambda Interferon Renders Epithelial Cells of the Respiratory and

Gastrointestinal Tracts Resistant to Viral Infections. *Journal of Virology* **84**:5670–5677.

123. **Kato H, Takahasi K, Fujita T.** 2011. RIG-I-like receptors: cytoplasmic sensors for non-self RNA  
. *Immunological Reviews* **243**:91–98.
124. **Jensen S, Thomsen AR.** 2012. Sensing of RNA Viruses: a Review of Innate Immune Receptors Involved in Recognizing RNA Virus Invasion. *Journal of Virology* **86**:2900–2910.
125. **Roth-Cross JK, Bender SJ, Weiss SR.** 2008. Murine Coronavirus Mouse Hepatitis Virus Is Recognized by MDA5 and Induces Type I Interferon in Brain Macrophages/Microglia. *Journal of Virology* **82**:9829–9838.
126. **Liddicoat BJ, Piskol R, Chalk AM, Ramaswami G, Higuchi M, Hartner JC, Li JB, Seeburg PH, Walkley CR.** 2015. RNA editing by ADAR1 prevents MDA5 sensing of endogenous dsRNA as nonself. *Science* **349**:1115.
127. **Chung H, Calis JJA, Wu X, Sun T, Yu Y, Sarbanes SL, Dao Thi VL, Shilvock AR, Hoffmann HH, Rosenberg BR, Rice CM.** 2018. Human ADAR1 Prevents Endogenous RNA from Triggering Translational Shutdown. *Cell* **172**:811–824.e14.
128. **Li Y, Banerjee S, Goldstein SA, Dong B, Gaughan C, Rath S, Donovan J, Korennykh A, Silverman RH, Weiss SR.** 2017. Ribonuclease L mediates the cell-lethal phenotype of double-stranded RNA editing enzyme ADAR1 deficiency in a human cell line. *eLife* **6**:e00856–14.
129. **Birdwell LD, Zalinger ZB, Li Y, Wright PW, Elliott R, Rose KM, Silverman RH, Weiss SR.** 2016. Activation of RNase L by Murine Coronavirus in Myeloid Cells Is Dependent on Basal Oas Gene Expression and Independent of Virus-Induced Interferon. *Journal of Virology* **90**:3160–3172.
130. **Li Y, Banerjee S, Wang Y, Goldstein SA, Dong B, Gaughan C, Silverman RH, Weiss SR.** 2016. Activation of RNase L is dependent on OAS3 expression during infection with diverse human viruses. *Proc Natl Acad Sci USA* 201519657.
131. **Silverman RH.** 2007. Viral encounters with 2′,5′-oligoadenylate synthetase and RNase L during the interferon antiviral response. *Journal of Virology* **81**:12720–12729.

132. **Burke JM, Moon SL, Lester ET, Matheny T, Parker R.** 2018. RNase L reprograms translation by widespread mRNA turnover escaped by antiviral mRNAs. *bioRxiv* 486530.
133. **Donovan J, Rath S, Kolet-Mandrikov D, Korennykh A.** 2017. Rapid RNase L-Driven Arrest of Protein Synthesis in the dsRNA Response without Degradation of Translation Machinery. *RNA*.
134. **Samuel MA, Whitby K, Keller BC, Marri A, Barchet W, Williams BRG, Silverman RH, Gale M, Diamond MS.** 2006. PKR and RNase L contribute to protection against lethal West Nile Virus infection by controlling early viral spread in the periphery and replication in neurons. *Journal of Virology* **80**:7009–7019.
135. **Scherbik SV, Paranjape JM, Stockman BM, Silverman RH, Brinton MA.** 2006. RNase L plays a role in the antiviral response to West Nile virus. *Journal of Virology* **80**:2987–2999.
136. **Washenberger CL, Han J-Q, Kechris KJ, Jha BK, Silverman RH, Barton DJ.** 2007. Hepatitis C virus RNA: dinucleotide frequencies and cleavage by RNase L. *Virus Research* **130**:85–95.
137. **Rivas C, Gil J, Mělková Z, Esteban M, Díaz-Guerra M.** 1998. Vaccinia Virus E3L Protein Is an Inhibitor of the Interferon (IFN)-Induced 2-5A Synthetase Enzyme. *Virology* **243**:406–414.
138. **Min JY, Krug RM.** 2006. The primary function of RNA binding by the influenza A virus NS1 protein in infected cells: Inhibiting the 2<sup>′</sup>-5<sup>′</sup> oligo (A) synthetase/RNase L pathway. *Proc Natl Acad Sci USA* **103**:7100–7105.
139. **Drappier M, Jha BK, Stone S, Elliott R, Zhang R, Vertommen D, Weiss SR, Silverman RH, Michiels T.** 2018. A novel mechanism of RNase L inhibition: Theiler's virus L\* protein prevents 2-5A from binding to RNase L. *PLOS Pathogens* **14**:e1006989.
140. **Sorgeloos F, Jha BK, Silverman RH, Michiels T.** 2013. Evasion of antiviral innate immunity by Theiler's virus L\* protein through direct inhibition of RNase L. *PLOS Pathogens* **9**:e1003474.
141. **Liu S-W, Katsafanas GC, Liu R, Wyatt LS, Moss B.** 2015. Poxvirus Decapping Enzymes Enhance Virulence by Preventing the Accumulation of dsRNA and the Induction of Innate Antiviral Responses. *Cell Host and Microbe* **17**:320–331.
142. **Mazumder R, Iyer LM, Vasudevan S, Aravind L.** 2002. Detection of novel members, structure–function analysis and evolutionary classification of the 2H phosphoesterase superfamily. *Nucleic Acids*

Research **30**:5229–5243.

143. **Mylykoski M, Kursula P.** 2017. Structural aspects of nucleotide ligand binding by a bacterial 2H phosphoesterase. *PLoS ONE* **12**:e0170355.
144. **Arn EA, Abelson JN.** 1996. The 2'-5' RNA Ligase of *Escherichia coli* PURIFICATION, CLONING, AND GENOMIC DISRUPTION. *Journal of Biological Chemistry* **271**:31145–31153.
145. **Gold MG, Smith FD, Scott JD, Barford D.** 2008. AKAP18 Contains a Phosphoesterase Domain that Binds AMP. *Journal of Molecular Biology* **375**:1329–1343.
146. **Frasher IDC, Tavalin SJ, Lester LB, Langeberg LK, Westphal AM, Dean RA, Marrion NV, Scott JD.** 1998. A novel lipid-anchored A-kinase Anchoring Protein facilitates cAMP-responsive membrane events. *The EMBO Journal* **17**:2261–2272.
147. **Didychuk AL, Montemayor EJ, Carrocci TJ, DeLaitsch AT, Lucarelli SE, Westler WM, Brow DA, Hoskins AA, Butcher SE.** 2017. Usb1 controls U6 snRNP assembly through evolutionarily divergent cyclic phosphodiesterase activities. *Nat Commun* **8**:497.
148. **Nomura Y, Roston D, Montemayor EJ, Cui Q, Butcher SE.** 2018. Structural and mechanistic basis for preferential deadenylation of U6 snRNA by Usb1. *Nucleic Acids Research* **46**:11488–11501.
149. **Mroczek S, Krwawicz J, Kutner J, Lazniewski M, Kuciński I, Ginalski K, Dziembowski A.** 2012. C16orf57, a gene mutated in poikiloderma with neutropenia, encodes a putative phosphodiesterase responsible for the U6 snRNA 3' end modification. *Genes & Development* **26**:1911–1925.
150. **Hilcenko C, Simpson PJ, Finch AJ, Bowler FR, Churcher MJ, Jin L, Packman LC, Shlien A, Campbell P, Kirwan M, Dokal I, Warren AJ.** 2013. Aberrant 3' oligoadenylation of spliceosomal U6 small nuclear RNA in poikiloderma with neutropenia. *Blood* **121**:1028–1038.
151. **Shchepachev V, Azzalin CM.** 2013. The Mpn1 RNA exonuclease: Cellular functions and implication in disease. *FEBS Lett* **587**:1858–1862.
152. **Kim H-J, Yi J-Y, Sung H-S, Moore DD, Jhun BH, Lee YC, Lee JW.** 1999. Activating Signal Cointegrator 1, a Novel Transcription Coactivator of Nuclear Receptors, and Its Cytosolic Localization under Conditions of Serum Deprivation. *Molecular and Cellular Biology* **19**:6323–6332.

153. **Jung D-J, Sung H-S, Goo Y-W, Lee HM, Park OK, Jung S-Y, Lim J, Kim H-J, Lee S-K, Kim TS, Lee JW, Lee YC.** 2002. Novel Transcription Coactivator Complex Containing Activating Signal Cointegrator 1. *Molecular and Cellular Biology* **22**:5203–5211.
154. **Schwarz B, Routledge E, Siddell SG.** 1990. Murine coronavirus nonstructural protein ns2 is not essential for virus replication in transformed cells. *Journal of Virology* **64**:4784–4791.
155. **Roth-Cross JK, Stokes H, Chang G, Chua MM, Thiel V, Weiss SR, Gorbalenya AE, Siddell SG.** 2009. Organ-Specific Attenuation of Murine Hepatitis Virus Strain A59 by Replacement of Catalytic Residues in the Putative Viral Cyclic Phosphodiesterase ns2. *Journal of Virology* **83**:3743–3753.
156. **Zhao L, Rose KM, Elliott R, Van Rooijen N, Weiss SR.** 2011. Cell-Type-Specific Type I Interferon Antagonism Influences Organ Tropism of Murine Coronavirus. *Journal of Virology* **85**:10058–10068.
157. **Zhao L, Jha BK, Wu A, Elliott R, Ziebuhr J, Gorbalenya AE, Silverman RH, Weiss SR.** 2012. Antagonism of the Interferon-Induced OAS-RNase L Pathway by Murine Coronavirus ns2 Protein Is Required for Virus Replication and Liver Pathology. *Cell Host and Microbe* **11**:607–616.
158. **Zhang R, Jha BK, Ogden KM, Dong B, Zhao L, Elliott R, Patton JT, Silverman RH, Weiss SR.** 2013. Homologous 2',5'-phosphodiesterases from disparate RNA viruses antagonize antiviral innate immunity. *Proceedings of the National Academy of Sciences* **110**:13114–13119.
159. **Brandmann T, Jinek M.** 2015. Crystal structure of the C-terminal 2',5'-phosphodiesterase domain of group a rotavirus protein VP3. *Proteins* **83**:997–1002.
160. **Ogden KM, Hu L, Jha BK, Sankaran B, Weiss SR, Silverman RH, Patton JT, Prasad BVV.** 2015. Structural Basis for 2'-5'-Oligoadenylate Binding and Enzyme Activity of a Viral RNase L Antagonist. *Journal of Virology* **89**:6633–6645.
161. **Sánchez-Tacuba L, Rojas M, Arias CF, López S.** 2015. Rotavirus Controls Activation of the 2'-5'-Oligoadenylate Synthetase/RNase L Pathway Using at Least Two Distinct Mechanisms. *Journal of Virology*, 5 ed. **89**:12145–12153.
162. **Gusho E, Zhang R, Jha BK, Thornbrough JM, Dong B, Gaughan C, Elliott R, Weiss SR, Silverman RH.** 2014. Murine AKAP7 Has a 2',5'-Phosphodiesterase Domain That Can Complement an Inactive

Murine Coronavirus ns2 Gene. *mBio* **5**.

163. **Goldstein SA, Thornbrough JM, Zhang R, Jha BK, Li Y, Elliott R, Quiroz-Figueroa K, Chen AI, Silverman RH, Weiss SR.** 2016. Lineage A Betacoronavirus NS2 proteins and homologous Torovirus Berne pp1a-carboxyterminal domain are phosphodiesterases that antagonize activation of RNase L. *Journal of Virology* JVI.02201–16.
164. **Thornbrough JM, Jha BK, Yount B, Goldstein SA, Li Y, Elliott R, Sims AC, Baric RS, Silverman RH, Weiss SR.** 2016. Middle East Respiratory Syndrome Coronavirus NS4b Protein Inhibits Host RNase L Activation. *mBio* **7**:e00258–16.
165. **Comar CE, Goldstein SA, Li Y, Yount B, Baric RS, Weiss SR, Palese P, Perlman S, Hogue B.** 2019. Antagonism of dsRNA-Induced Innate Immune Pathways by NS4a and NS4b Accessory Proteins during MERS Coronavirus Infection. *mBio* **10**:e00319–19.

## Chapter 2

# **LINEAGE A *BETACORONAVIRUS* NS2 PROTEINS AND HOMOLOGOUS TOROVIRUS PP1A- CARBOXYTERMINAL DOMAIN ARE PHOSPHODIESTERASES THAT ANTAGONIZE ACTIVATION OF RNASE L**

This chapter appeared as the published article “Lineage A *Betacoronavirus* NS2 proteins and homologous torovirus pp1a-carboxyterminal domain are phosphodiesterases that antagonize activation of RNase L” by Stephen A. Goldstein\*, Joshua M. Thornbrough\*, Rong Zhang\*, Babal K. Jha\*, Yize Li, Ruth Elliott, Katherine Quiroz-Figueroa, Annie I. Chen, Robert H. Silverman, Susan R. Weiss. *Journal of Virology*, **91**: p.e 02201-15 (2016)

\* These authors made equivalent contributions

## Abstract

Viruses in the family *Coronaviridae*, within the order *Nidovirales*, are etiologic agents of a range of human and animal diseases, including both mild and severe respiratory disease in humans. These viruses encode conserved replicase and structural proteins, and more diverse accessory proteins in the 3' end of their genomes that often act as host cell antagonists. We have previously shown that 2',5' phosphodiesterases (PDE) encoded by the prototypical *Betacoronavirus*, mouse hepatitis virus (MHV) and Middle East respiratory syndrome-associated coronavirus (MERS-CoV) antagonize the oligoadenylate synthetase – ribonuclease L (OAS-RNase L) pathway. Here we report that additional coronavirus superfamily members including lineage A betacoronaviruses and toroviruses infecting both humans and animals encode 2',5' PDEs capable of antagonizing RNase L. We used a chimeric MHV system, in which exogenous PDEs were expressed from an MHV backbone lacking a functional NS2 protein (MHV<sup>Mut</sup>), its endogenous RNase L antagonist to test the ability of these PDEs to antagonize RNase L. In this system, we found that 2',5' PDEs encoded by human coronavirus HCoV-OC43 (OC43), an agent of the common cold, human enteric coronavirus (HECoV), equine coronavirus (ECoV), and equine torovirus-Berne (BEV) are enzymatically active, rescue replication of MHV<sup>Mut</sup> in bone marrow-derived macrophages and inhibit RNase L-mediated rRNA degradation in these cells. Additionally, PDEs encoded by OC43 and BEV rescue MHV<sup>Mut</sup> replication and restore pathogenesis in WT B6 mice. This finding expands the range of viruses known to encode antagonists of the potent OAS-RNase L

antiviral pathway, highlighting its importance in a range of species, as well as the selective pressures exerted on viruses to antagonize it.

### **Importance**

Viruses in the family *Coronaviridae* include important human and animal pathogens, including the recently emerged SARS-CoV and MERS-CoV. We have shown previously that two viruses within the genus *Betacoronavirus*, mouse hepatitis virus (MHV) and MERS-CoV, encode 2',5' phosphodiesterases (PDEs) that antagonize the OAS-RNase L pathway and report here that these proteins are furthermore conserved among additional coronavirus superfamily members including lineage A betacoronaviruses and toroviruses, suggesting they may play critical roles in pathogenesis. As there are no licensed vaccines or effective antivirals against human coronaviruses and few against those infecting animals, identifying viral proteins contributing to virulence can inform therapeutic development. Thus, this work demonstrates that a potent antagonist of host antiviral defenses is encoded by multiple and diverse viruses within *Coronaviridae*, presenting a possible broad-spectrum therapeutic target.

## Introduction

Coronaviruses (CoV) and closely related toroviruses (ToV) are well known agents of disease in mammals, including humans. Coronaviruses and toroviruses, members of the family *Coronaviridae* within the order *Nidovirales*, contain positive sense single stranded (ss)RNA genomes ranging from 28-31 kilobases in length, among the longest known RNA genomes (1-3). The first two thirds of their genomes encode the replicase proteins, which include the viral RNA-dependent RNA polymerase and numerous non-structural proteins (NSPs), which are required for replication and in some cases have host immune antagonist activities (4). The structural proteins are encoded in the 3' third of the genome and consist of spike (S), small membrane protein (E), membrane (M), nucleocapsid (N) and sometimes hemagglutinin-esterase (HE). Interspersed among the structural genes are diverse genes encoding accessory proteins that are not essential for replication but are believed to be required for virulence *in vivo* (1).

Mouse hepatitis virus (MHV) is a lineage A *Betacoronavirus* and the prototypical CoV. MHV encodes the accessory protein NS2 which was previously identified as a 2-His (H) phosphoesterase (2H-PE) superfamily member (5), and that we have demonstrated has 2',5'-phosphodiesterase (PDE) activity that antagonizes the host 2',5'-oligoadenylate synthetase (OAS)-ribonuclease (RNase) L pathway (6). Upon sensing double stranded (ds)RNA, OAS proteins synthesize 2',5'-oligoadenylates (2-5A) which catalyze the activation of RNase L

via homodimerization. RNase L subsequently cleaves host and viral ssRNA leading to termination of protein synthesis and subsequent apoptosis (7). NS2 cleaves 2-5A thus preventing the activation of RNase L. NS2 is a critical determinant of MHV strain A59 (A59) liver tropism in C57BL/6 (B6) mice and is required for the virus to cause hepatitis. Mutant MHV A59 (MHV<sup>Mut</sup>) expressing NS2 with an inactive phosphodiesterase domain (NS2<sup>H126R</sup>) is unable to antagonize the OAS-RNase L pathway in mouse bone marrow-derived macrophages (BMMs) or the mouse liver. Infection with this virus does not result in hepatitis and MHV<sup>Mut</sup> replication is reduced at least 10,000 fold compared to wild-type (WT) MHV A59. However, in mice genetically deficient for RNase L (RNase L<sup>-/-</sup>), MHV<sup>Mut</sup> replicates to wild-type levels and causes hepatitis (6).

As might be expected of antagonists of a potent innate antiviral pathway, 2',5' PDEs are not a host evasion mechanism unique to MHV. We recently showed that the NS4b accessory protein of MERS-CoV and related bat coronaviruses, all lineage C betacoronaviruses, exhibit 2',5'-PDE activity (8). Additionally, unrelated group A rotaviruses encode a PDE in the C-terminal domain of the VP3 structural protein (9). We show here that lineage A betacoronaviruses closely related to MHV, including the human respiratory HCoV-OC43 (OC43), human enteric CoV-4408 (HECoV), equine ECoV-NC99 (ECoV), and porcine hemagglutinating encephalomyelitis virus (PHEV), as well as the more distantly related equine torovirus (EToV)-Berne (BEV) also encode NS2 homologs with predicted PDE activity. We found that these proteins do

possess enzymatic 2',5'-PDE activity that is capable of antagonizing RNase L (with the exception of PHEV NS2) and thus countering a potent host antiviral response, suggesting that PDE mediated OAS-RNase L antagonism is an important virulence strategy for lineage A betacoronaviruses and toroviruses.

## **Material and Methods**

**Cell lines and mice.** Murine fibroblast L2 (L2), murine 17 clone 1 (17C11) and baby hamster kidney cells expressing MHV receptor (BHK-R) were cultured as previously described (10, 11). C57BL/6 (B6) mice were originally procured from the National Cancer Institute mouse repository, and RNase L<sup>-/-</sup> mice on a B6 genetic background were derived by Dr. Robert Silverman (12) and subsequently bred in the University of Pennsylvania animal facility. All experiments involving mice were approved by the Institutional Animal Care and Use Committee at the University of Pennsylvania. Primary bone marrow-derived macrophages (BMM) were generated from marrow harvested from the hind limbs (tibia and femur) of four to six week old B6 or RNase L<sup>-/-</sup> mice as described previously (6, 13). Cells were cultured in DMEM (Gibco) supplemented with 10% FBS (Hyclone) and 20% L929 cell-conditioned media for 6 days before infection.

**Plasmids.** NS2 genes from lineage A betacoronaviruses OC43, HECV-4408, ECoV-NC99 NC99, PHEV and pp1a-carboxyterminal domain (CTD) from the torovirus Berne were synthesized and cloned into pUC57 by BioBasic yielding

pUC-OC43NS2, pUC-HECVNS2, pUC-ECovNS2, pUC-PHEVNS2 and pUC-pp1a. The second catalytic His to Arg substitutions were made by site directed mutagenesis in all plasmids resulting in pUC-OC43-NS2<sup>H129R</sup>, pUC-HECV-NS2<sup>H129R</sup>, pUC-NC99-NS2<sup>H129R</sup>, pUC-PHEV-NS2<sup>H129R</sup> and pUC-pp1a<sup>H4516R</sup>. Select genes were subsequently sub-cloned into the pMal parallel-2 expression vector resulting in pMAL-OC43-NS2, pMAL-OC43-NS2<sup>H129R</sup>, pMAL-PHEV-NS2, pMAL-PHEV-NS2<sup>H129R</sup>, pMAL-pp1a and pMAL-pp1a<sup>H4516R</sup>. MHV NS2 and NS2<sup>H126R</sup> had been previously cloned into pMAL-c2 (6).

**Purification of recombinant PDEs from E. coli and FRET assay.** MBP-PDE fusion proteins were expressed from pMAL-plasmids in BL21 T7 expression competent *E. coli* (NEB, Inc., Ipswich, MA) and purified by affinity chromatography followed by ion exchange chromatography on MonoQ GL10/100 using a NaCl gradient from 0 to 1 M in 20 mM NaCl as previously described (6, 14). The integrity and the purity of the purified MBP fusion proteins were determined by SDS-PAGE electrophoresis and Coomassie Blue R250 staining. The extent of purity was similar for all of the enzymes as assessed by SDS-PAGE analysis. To assess enzymatic activity, purified proteins [10  $\mu$ M MBP (420  $\mu$ g/ml) as control or 1  $\mu$ M OC43 (75  $\mu$ g/ml); BEV (60  $\mu$ g/ml) PHEV (65  $\mu$ g/ml) or MHV (70 $\mu$ g/ml) MBP-PDE fusion proteins] in 150  $\mu$ l of assay buffer (20 uM HEPES [pH 7.2], 10 mM MgCl<sub>2</sub>, 1 mM dithiothreitol) were incubated at 30° with (2'-5')p<sub>3</sub>A<sub>3</sub> (2-5A). After one hour, reactions were stopped by heat inactivation at 95° for 3 min followed by 30 min centrifugation at 20,000 X g (4°) and

supernatants carefully removed. A fluorescent resonance energy transfer (FRET) assay was used to assess enzymatic activity by measuring the amount of uncleaved, intact 2-5A left in the reaction, as previously described (15). The abilities of recombinant enzyme to degrade 2-5A were determined by a FRET based RNase L activation assay using an authentic 2-5A (2',5'-p<sub>3</sub>A<sub>3</sub>) trimer as described earlier (6, 8, 16, 17). Assays were performed three times in triplicate using two separate enzyme preparations.

**Viruses and chimeric recombinant virus construction.** Wild-type MHV strain A59 and mutant NS2<sup>H126R</sup> (referred to as MHV and MHV<sup>Mut</sup> in the data shown herein) were described previously (6, 9). The chimeric viruses were constructed based on the infectious cDNA clone icMHV-A59 (10, 18). The wild-type and mutant PDEs genes were PCR amplified from the pUC plasmids constructed above with primers bearing Sall and NotI restricting sites. After purification and digestion with Sall and NotI, the fragments were cloned into icMHV-A59 fragment G, with an NS2<sup>H126R</sup> mutation, as previously described (9) and confirmed by DNA sequencing. The full-length A59 genome cDNA was assembled, and the recombinant viruses were recovered in BHK-R cells as previously described (9, 10, 17, 18). When virus cytopathology was observed, virus was plaque purified from the supernatant and amplified on 17CL-1 cells for use. The pairs of chimeric viruses expressing WT and mutant PDEs were named by the source of the PDE, OC43 & OC43<sup>Mut</sup>, HECoV & HECoV<sup>Mut</sup>, PHEV & PHEV<sup>Mut</sup>, ECoV<sup>Mut</sup> & ECoV and BEV & BEV<sup>Mut</sup>. The PDE gene and flanking regions were amplified by

PCR from the cloned chimeric virus genomes and the sequences verified. The primers used for sequencing were Fns4 (5'-TTGTTGTGATGAGTATGGAG) which maps 136 nucleotides upstream of the ATG start codon for the PDE and Rns4 (5'-GCGTAACCATGCATCACTCAC) which maps 139 nucleotides downstream of the PDE ORF. The regions sequenced include the Sall and NotI restriction sites as well as the transcription regulatory sequence (TRS) for ORF4 and ORF5a.

#### **Chimeric MHV infections of bone marrow derived macrophages (BMM).**

BMMs were mock infected or infected at a multiplicity of infection (MOI) of 1 PFU/cell (in triplicate) and allowed to adsorb for 1 hour at 37 °C. Cultures were washed with PBS (3 times) and fed with medium. At the times indicated, cells were lysed and analyzed for degradation of RNA (described below) or supernatants were harvested for quantification of viral titers by plaque assay on L2 cells (6, 9).

**Immunoblotting.** L2 cells were infected with MHV or chimeric viruses (MOI=1 PFU/cell). At 10 hours post-infection, cells were lysed in nonidet P-40 (NP-40) buffer (1% NP-40, 2 mM EDTA, 10% glycerol, 150 mM NaCl and 50 mM Tris pH 8.0) containing protease inhibitors (Roche). Protein concentrations were measured using a DC protein assay kit (Bio-Rad). Supernatants were mixed 3:1 with 4X SDS-PAGE sample buffer. Samples were boiled, separated by 4-15% SDS-PAGE and transferred to polyvinylidene difluoride (PVDF) membranes.

Blots were blocked with 5% nonfat milk and probed with the following antibodies: anti-Flag M2 mouse monoclonal antibody (Agilent, 1:1000); anti MHV nucleocapsid mouse monoclonal antibody (a gift from Dr. Julian Leibowitz; 1:400) and anti GAPDH mouse monoclonal antibody (Thermo Scientific, 1:1000). Anti-mouse HRP (Santa Cruz; 1:5000) secondary antibodies were used to detect the primary antibodies. The blots were visualized using Super Signal West Dura Extended Duration Substrate (Thermo Scientific). Blots were probed sequentially with antibodies with stripping between antibody treatments.

**Analysis of RNase L mediated rRNA degradation.** RNA was harvested from B6 WT BMMs infected with MHV and chimeric viruses encoding WT and catalytically inactive PDEs at the indicated time points using a Qiagen RNeasy kit. RNase was denatured at 70° for 2 min and analyzed with an Agilent BioAnalyzer 2100 on a eukaryotic total RNA nanochip. The BioAnalyzer converts the electropherogram generated for each sample into the pseudogel as depicted in Fig 2.6 (6).

**Replication in mice.** Four week old B6 or RNase L<sup>-/-</sup> mice (5-7) were anesthetized with isoflurane (Abbott Laboratories; Chicago, IL) and inoculated intrahepatically with 2000 PFU in 50 µL of DPBS (Gibco) containing 0.75% bovine serum albumin (Sigma). Mice were euthanized with CO<sub>2</sub>, perfused with DPBS (Gibco) and livers harvested at day five post inoculation. Part of the liver was fixed for histology and the rest was homogenized and viral titers were

determined by plaque assay of liver homogenates on L2 cells (19). A piece of each liver was fixed overnight in 4% paraformaldehyde, embedded in paraffin and sectioned. Sections were stained with hematoxylin and eosin (H&E) or alternatively blocked with 10% normal donkey serum and immunostained with a 1:20 dilution of a monoclonal antibody against MHV nucleocapsid (N) protein (1:1000 dilution). Staining was developed using avidin-biotin-immunoperoxidase (Vector Laboratories).

## Results

**Alignment and modeling of coronavirus and torovirus NS2 proteins.** To determine whether the MHV-related betacoronaviruses encode proteins with 2',5'-PDE activity we first analyzed the primary amino acid sequence of the NS2 proteins from OC43, HECoV, ECoV-NC99, PHEV and the pp1a-CTD of BEV. While the NS2 homologs are encoded within ORF2, the PDE of BEV is encoded at the 3' end of the ORF1a and processed from the pp1a polyprotein (4). All of these proteins contain two conserved HxS/Tx motifs spaced by ~80 residues, where x is any hydrophobic residue, characteristic of 2H-phosphoesterase superfamily proteins (5, 6, 9) (Fig 2.1). Interestingly the carboxytermini of the PHEV and BEV PDEs are truncated relative to the other NS2 proteins, similar to the group A rotavirus VP3-CTD PDE (9, 25, 26). We further entered the primary amino acid sequence of these proteins into Phyre<sup>2</sup> to predict their tertiary structures (Fig 2.2). All of these proteins scored highly for homology with the

published structure of the A-kinase anchoring protein 7 (AKAP7) central domain (CD) (27), a

previously

identified host-

encoded 2H-PE

with 2',5'-PDE

activity (17). We

have previously

shown that the

MHV NS2 and

group A rotavirus

(RVA) VP3

proteins, also structural homologs of AKAP7 CD, exhibit 2',5' PDE activity and can antagonize RNase L (6, 9, 17).

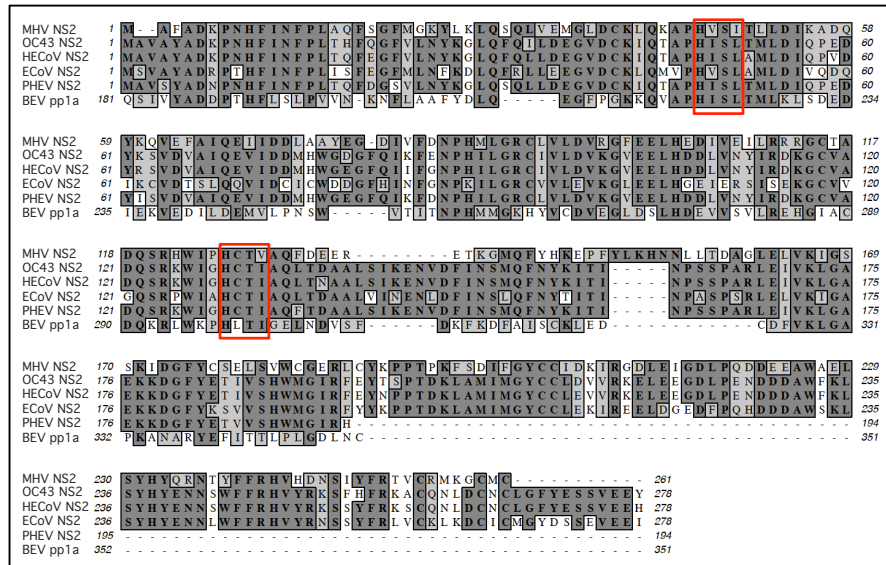


**Figure 2.1. Alignment of lineage A betacoronavirus and Berne torovirus PDEs.** PDEs with Genbank accession numbers are MHV NS2 (P19738.1) (20), OC43 NS2 (AAT84352.1) (21), HCoV NS2 (ACJ35484.1), ECoV NS2 (ABP87988.1) (22), PHEV NS2 (AAY68295.1) (23) and BEV (CAA36600.1) (24). Conserved catalytic HxS/Tx motifs are indicated by boxes. **Contributor:** JMT

## Coronavirus and torovirus putative 2',5' PDEs are enzymatically active and

**cleave 2-5A.** To determine whether the predicted nidovirus PDEs (OC43 NS2,

BEV pp1a-CTD, PHEV NS2) are enzymatically active, the genes encoding them

as well as their corresponding mutants with an Arg substitution of the second

predicted catalytic His residue were expressed in *Escherichia coli* as maltose

binding protein (MBP) fusion proteins and purified by affinity chromatography

followed by ion exchange chromatography and size exclusion chromatography

as described in Materials and Methods (6). Purified wild type or catalytic mutant

proteins were incubated with 2-5A substrate and an indirect fluorescent resonance energy transfer (FRET) assay was used to assess activation of RNase L, in which higher RLUs represent active RNase L as described in Materials and Methods and in detail previously (15). MHV NS2 was utilized as a positive control for inhibition of RNase L (Fig 2.3). OC43 and BEV proteins reduced RNase L activation to a similar degree as MHV NS2, while PHEV NS2 was significantly less active. The mutant proteins containing a His → Arg mutation in the second catalytic motif did not inhibit RNase L, as expected and consistent with previously results describing MHV NS2 (6).

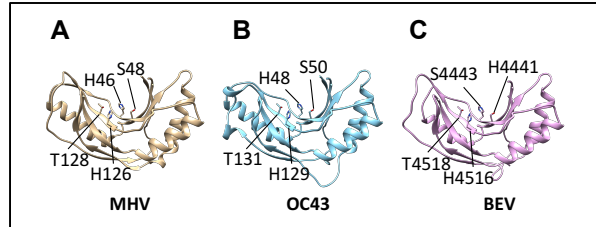


**Figure 2.2. Known and predicted structures of nidovirus PDEs.** (A) Crystal structure of MHV NS2 (PDB: 4Z5V) and predicted structures of OC43 NS2 (B) and BEV pp1a-CTD (C). Predicted structures were generated using Phyre<sup>2</sup> then visualized and annotated using UCSF Chimera 1.8. Catalytic His and conserved Ser/Thr residues are indicated. **Contributors:** JMT and SAG

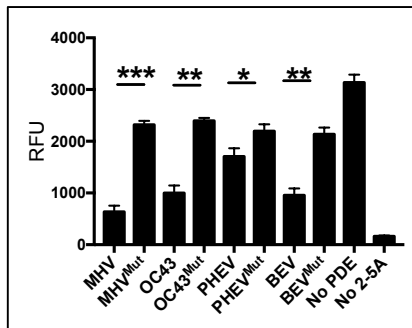


**Figure 2.3. PDE activity assay of coronavirus and torovirus PDEs.** Recombinant WT and mutant PDEs were incubated with 2-5A for 60 minutes and the remaining substrate was quantified using an indirect FRET based assay as described in Materials and Methods. RFU= relative fluorescence units, is proportional to 2-5A remaining. Data shown are from one representative of three independent experiments, each carried out in triplicate with separate enzyme preparations and are expressed as means ± SEM; \*,  $P < 0.05$ , \*\*,  $P < 0.01$ , \*\*\*,  $P < 0.001$ . **Contributors:** BKJ and JMT

**Coronavirus and Torovirus PDEs inhibit RNase L when expressed from a chimeric MHV NS2 mutant backbone.** To investigate whether the NS2 proteins of OC43, HECov, ECoV, PHEV, and BEV pp1a-CTD can antagonize RNase L during infection, we constructed chimeric viruses expressing each exogenous

PDE from ORF4 (encoding NS4a, 4b) of an MHV backbone (Fig 2.4). The MHV-A59 backbone we utilized encodes the H126R substitution in NS2 (MHV<sup>Mut</sup>, referred to in literature as NS2<sup>H126R</sup>) that abrogates its enzymatic activity and ability to antagonize RNase L. MHV<sup>Mut</sup> exhibits minimal replication in primary bone marrow-derived macrophages (BMM) or *in vivo* (6). The chimeric viruses we constructed express either the exogenous PDE protein or its catalytic mutant from the ORF4 locus of MHV, which is dispensable for MHV replication *in vitro* and *in vivo* (28). Each exogenous protein was constructed with a C-terminal Flag-tag to allow verification of expression from the chimeric viruses. To assess expression of PDEs by western blot, we infected L2 cells with the chimeric viruses and harvested protein lysates 10 hours post-infection (hpi). We probed for the exogenous PDEs using a primary antibody directed against the Flag-tag, and utilized GAPDH as a loading control (Fig 2.5). The OC43, HECV and ECov PDEs were detectable by western blot at a high level of abundance, while detection of BEV pp1-CTD expression was less robust.

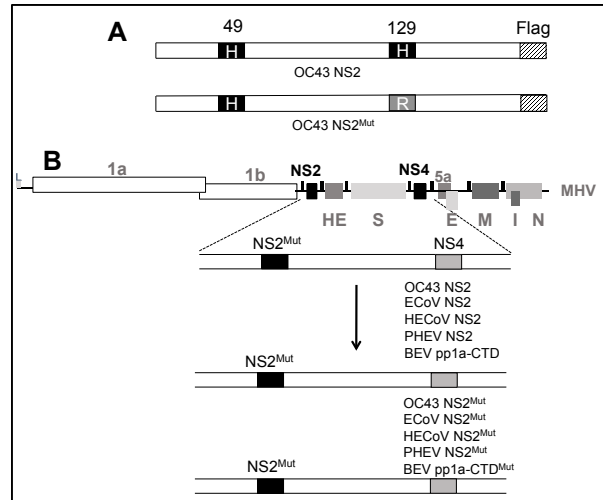


**Figure 2.4. NS2 organization and construction of chimeric viruses.** (A) Depiction of the NS2 protein of HCoV-OC43. Shown are the catalytic His residues at positions 49 and 129, with the His->Arg mutation shown below. (B) Genome organization of MHV with NS2 and NS4 loci indicated. Also shown are replicate open reading frames 1a and 1b, genes encoding structural proteins HE, S, E, M, N and I as well as nonstructural protein 5a. In chimeric viruses MHV NS2 residue 126 is mutated from H->R, rendering NS2 catalytically inactive (NS2<sup>Mut</sup>). The gene encoding the exogenous PDE or its catalytically inactive mutant is inserted in place of MHV NS4. **Contributor:** SAG

PHEV NS2 expression from multiple viral clones as well as the swarm of uncloned recombinant virus could not be detected by western blot.

**Exogenous coronavirus and torovirus PDEs rescue replication of MHV<sup>Mut</sup> in primary B6 BMMs through inhibition of RNase L activation.** To determine if the exogenous PDEs can antagonize RNase L in the context of infection, we

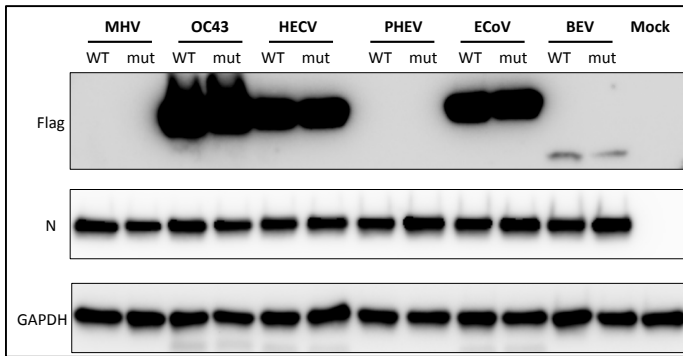


**Figure 2.5. Expression of exogenous PDEs from chimeric viruses.** L2 cells were infected with MHV or chimeric viruses and protein harvested 10 hpi and analyzed by western immunoblotting. Blots were probed with antibody against Flag to detect PDEs, anti-nucleocapsid antibody to assess chimeric viral infection and GAPDH as a protein loading control. MHV NS2 (lanes 1-2) is not Flag-tagged. Flag-tagged WT and mutant PDEs of OC43, HECV, PHEV, ECoV and BEV are detected as indicated. This blot was performed two times using proteins from independent infections with similar results.  
**Contributor:** JMT

infected BMMs from WT B6 and RNase L<sup>-/-</sup> mice with MHV, MHV<sup>Mut</sup> and the chimeric viruses and measured replication by plaque assay at 6, 9, 12, and 24 hpi. As expected, MHV<sup>Mut</sup> is significantly attenuated in WT BMMs but replicates to equivalent titers as MHV in

RNase L<sup>-/-</sup> BMMs (Fig 2.6A). All of the chimeric viruses encoding WT exogenous PDEs from OC43, HECov, ECoV and BeV, replicated to a similar extent as WT A59 in B6 BMMs, indicating that these proteins effectively compensate for an inactive NS2<sup>H126R</sup> in MHV (Fig 2.6B-E). In contrast, and similarly to MHV<sup>Mut</sup>, the chimeras expressing catalytically inactive exogenous PDEs fail to replicate robustly in B6 BMMs but do replicate efficiently in RNase L<sup>-/-</sup> BMMs (Fig 2.6A-E).

The chimeric virus encoding PHEV NS2 were not assessed for replication in BMMs due to our inability to confirm its expression (Figure 2.5).

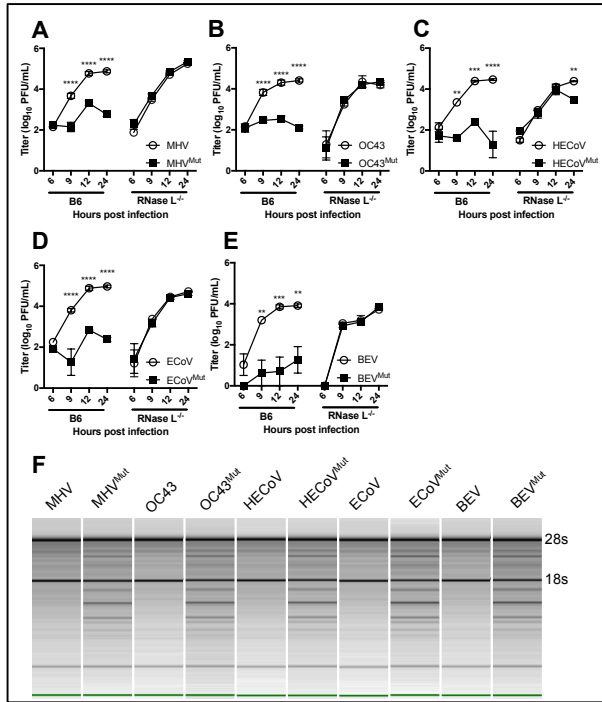


**Figure 2.6. Replication and activation of RNase L by chimeric viruses in bone marrow derived macrophages (BMM).** (A-E) BMMs derived from WT B6 or RNase L<sup>-/-</sup> mice were infected with (A) MHV or chimeric MHV viruses expressing WT or mutant (B) OC43 NS2, (C) HECoV NS2, (D) ECoV NS2 and (E) BEV pp1a-CTD. Virus at each time point was titrated by plaque assay. Each time point is represented by three biological replicates, titrated in duplicate and variance expressed as SEM. Statistical significance was calculated by 2-way ANOVA in GraphPad Prism. \*\*, *P* < 0.01; \*\*\*, *P* < 0.001. (F) Total RNA was isolated from WT B6 BMMs 9 hpi and rRNA integrity assayed using an Agilent BioAnalyzer. These data are from one of at least two independent experiments with similar results. **Contributors:** JMT, RZ, RE, SAG, and YL

To directly link antagonism of RNase L to the ability of the exogenous PDEs to rescue MHV<sup>Mut</sup> replication, we assessed rRNA degradation in infected cells by Bioanalyzer. We have previously used this assay to demonstrate that MHV NS2, but not NS2<sup>H126R</sup>, inhibits RNase L-mediated RNA degradation, and that a deficiency in RNase L obviates the requirement for NS2 in MHV replication (6). We infected B6 WT and RNase L<sup>-/-</sup> BMMs with MHV and the chimeric viruses and harvested

total RNA 9 hpi. We ran the total RNA on a Bioanalyzer to visualize the integrity of rRNA during infection with MHV and the chimeric viruses. MHV and the chimeric viruses encoding exogenous PDEs encoded by MHV, OC43, HECoV, ECoV and BEV prevented rRNA degradation in B6 WT BMMs, while the corresponding catalytically inactive PDEs failed to do so (Fig 2.6F). This directly

links the ability of the exogenous PDEs to rescue MHV<sup>Mut</sup> replication to their antagonism of RNase L activation.

### OC43 NS2 and BEV pp1a-CTD restore MHV<sup>Mut</sup> replication and pathogenesis

**in vivo.** MHV causes profound hepatitis and associated liver pathology in B6 mice, with its liver replication and pathogenesis dependent on NS2-mediated antagonism of RNase L (Fig 2.7) (6). To determine whether exogenous viral PDEs can rescue replication and restore pathogenesis to MHV<sup>Mut</sup>, we infected B6 and RNase L<sup>-/-</sup> mice with MHV, MHV<sup>Mut</sup> and the chimeric viruses expressing either WT or catalytic mutant PDEs from OC43 (NS2) and BEV (pp1a-CTD). Five

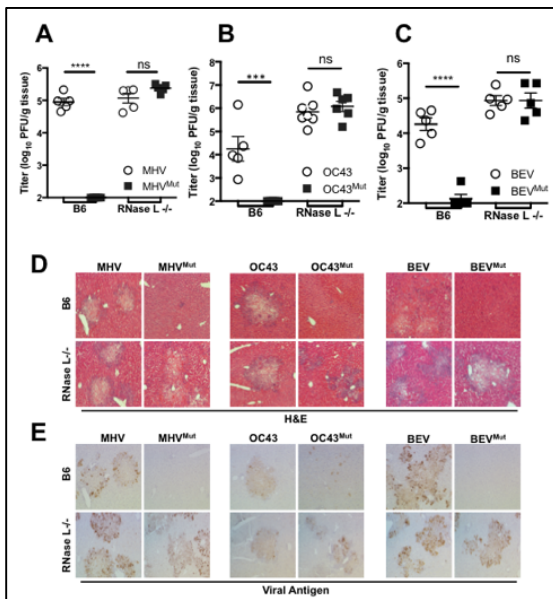


**Figure 2.7. Replication and pathogenesis of chimeric viruses *in vivo*.** (A-C) WT B6 or RNase L<sup>-/-</sup> mice (n= 5-7) were infected intrahepatically with (A) MHV and MHV<sup>Mut</sup> or chimeric viruses encoding WT or mutant (B) OC43 NS2 or (C) BEV pp1a-CTD. Five days post-infection livers were harvested and virus titrated by plaque assay. Each data point represents a single mouse liver, titrated in duplicate with variance expressed as SEM. Statistical significance determined by 1-way ANOVA in GraphPad Prism. \*\*\*\*, *P* < 0.001. Liver sections from infected mice were stained with (D) H&E to identify hepatic pathology or (E) antibody to detect MHV nucleocapsid protein. **Contributors:** JMT, RZ, RE, and SAG

days post-infection, at the time of peak titer, the mice were sacrificed and livers harvested for virus titration by plaque assay. In WT B6 mice chimeric viruses expressing either WT OC43 NS2 or BEV pp1-CTD replicated robustly in the liver, similarly to MHV.

In contrast, and like MHV<sup>Mut</sup>, the chimeric viruses expressing mutant OC43 NS2 (Fig 2.7B) or BEV pp1a-CTD (Fig 2.7C) are dramatically restricted, replicating only to titers below

or just above the limit of detection, whereas all of the chimeric viruses replicated robustly in the livers of RNase L<sup>-/-</sup> mice (Fig 2.7A-C). To assess hepatitis in these infected mice, liver sections were assessed for viral antigen and pathological changes. Like A59, chimeric viruses expressing WT OC43 NS2 or BEV pp1a-CTD caused hepatitis in B6 mice, indicated by pathologic foci in H&E stained livers, with viral antigen staining widely observed (Fig 2.7D,E). Chimeric viruses expressing catalytically inactive OC43 NS2 or BEV pp1a-CTD did not cause liver pathology in B6 mice and viral antigen was absent, consistent with the lack of replication (Fig 2.7D,E). In RNase L<sup>-/-</sup> mice, all of the chimeric viruses replicated robustly and caused pathology similar to MHV A59 (Fig 2.7D,E), further demonstrating that the restriction of the viruses expressing mutant PDEs in B6 mice is RNase L-mediated and that the exogenous PDEs function equivalently to MHV NS2.

## **Discussion**

We have previously demonstrated 2-5A cleavage and RNase L antagonism by 2',5' PDEs encoded by a lineage A and a lineage C betacoronavirus (MHV and MERS-CoV respectively) and group A rotaviruses as well as by cellular AKAP7 CD (6, 8, 9, 17). Here, we extend these findings to show that additional lineage A betacoronaviruses as well as a related torovirus family member encode 2',5' PDEs capable of antagonizing RNase L by cleaving 2-5A. The presence of genes encoding these proteins in multiple lineage A betacoronaviruses suggests that this gene was acquired by an ancient common

ancestor of this lineage. Whether this virus was also ancestral to toroviruses and lineage C betacoronaviruses, or whether 2',5' PDEs were acquired by viruses in multiple independent events is unclear. The maintenance of this highly conserved protein throughout lineage A betacoronaviruses supports the idea that this protein mediates an essential function in the diverse natural hosts of these viruses, spanning multiple mammalian families. Our finding of a homologous PDE in some groups of rotaviruses (9), a virus family unrelated to coronaviruses is intriguing. A coronavirus recently isolated from bats was found to encode a protein likely to have originated from a bat orthoreovirus, which like rotaviruses has a dsRNA genome, suggesting the possibility of recombination between coronaviruses and a dsRNA virus (29). Further support for this idea comes from a recent report of isolation of a MERS-like coronavirus and a rotavirus in the feces of Korean bats (30). Additionally, the viruses encoding the PDEs we have described here infect different tissues within their hosts (1, 31, 32), indicating that RNase L antagonism may be required for robust replication in diverse cell types. For example, although MHV is hepatotropic, OC43 infects the upper airway, while other PDEs described here are encoded by enterotropic viruses (1, 31, 32).

The PDEs encoded by OC43, HECov, ECoV and BEV antagonized RNase L and rescued replication of MHV<sup>Mut</sup> in primary WT B6 BMMs, indicating that not only are they enzymatically active 2',5' PDEs, but that they functionally compensate for an inactive MHV NS2 (Fig 2.3, 2.6, 2.7). Interestingly the BEV encoded PDE was able to antagonize RNase L and rescue MHV<sup>Mut</sup> replication

both *in vitro* and *in vivo* despite the apparently low level of expression (Fig 2.5, 2.6, 2.7). This is not entirely surprising as the MERS-CoV NS4b PDE can rescue MHV<sup>Mut</sup> despite its low abundance in the cytoplasm (8). PHEV NS2 is less enzymatically active than the other PDEs (Fig 2.3), suggesting it may be less able to antagonize RNase L. However, since we could not detect expression by western blot of the PHEV PDE from a chimeric virus (Fig 2.5), further work will be needed to determine if it has RNase L antagonist activity in the context of infection. Interestingly both the BEV and PHEV PDEs are truncated at the carboxytermini similar to the rotavirus PDE (Fig 2.3) (9); clearly the carboxyterminal sequences are not required for cleavage of 2-5A or RNase L antagonism as the rotavirus VP3-CTD and BEV PDEs have similar activity to MHV NS2 (Fig 2.3) (9). Nevertheless, the diminished enzymatic activity of PHEV NS2 relative to the other PDEs, suggests that while a PDE may have been essential in the PHEV ancestor, it may not be required in the cells targeted by PHEV in its porcine host. However, RNase L is likely actively antiviral in other porcine tissues or stages of development, as suggested by the presence of an RNase L antagonist in protein 7 of transmissible gastroenteritis virus (33).

Although the chimeric MHVs encoding OC43-NS2 and BEV pp1a-CTD do not replicate quite as well as MHV *in vivo* (Fig 2.6), this is unlikely due to disruption of the ORF4 gene by insertion of the exogenous PDEs as ablation of ORF4 expression within the genome of MHV strain JHM had no effect on replication *in vitro* and *in vivo* pathogenesis and the MHV strain A59 ORF4 is

disrupted by a termination codon (34). Nevertheless, these chimeric viruses replicated robustly *in vivo* causing hepatitis and their respective mutants replicated to wild-type titers in the livers of RNase L<sup>-/-</sup> mice, indicating that restriction of the mutants in WT B6 mice is due to RNase L activity.

Overall, we have demonstrated that active 2',5' PDEs are a conserved feature of lineage A *Betacoronavirus* genomes, and that a homologous domain is encoded in the first open reading frame of a related nidovirus, BEV. This suggests that RNase L is a potent antiviral effector in diverse species and tissues, due to the wide host range represented by the viruses encoding these now-characterized PDEs. This thus far includes the lineage A and lineage C betacoronaviruses as well as the related toroviruses and the unrelated group A Rotaviruses (6, 9). Finally since 2',5' PDEs are potent antagonists of host antiviral defenses encoded by multiple and diverse viruses within *Coronaviridae*, this class of protein may have the potential to be a broad-spectrum therapeutic target for human viruses including HCoV-OC43, a ubiquitous agent of the common cold, and MERS-CoV.

### **Author contributions**

**Manuscript and figure preparation:** SAG, RSH, and SRW

**Figure 2.1:** JMT

**Figure 2.2:** JMT and SAG

**Figure 2.3:** BKJ and JMT

**Figure 2.4:** SAG

**Figure 2.5:** JMT

**Figure 2.6:** JMT, RZ, RE, SAG, and YL

**Figure 2.7:** JMT, RZ, RE, and SAG

**Acknowledgments.** Research reported in this publication was supported by National Institute of Allergy and Infectious Disease of the National Institutes of Health (NIH) under award number F32AI114143 to JMT, R21AI114920 to SRW and R01AI104887 to SRW and RHS.

## References

1. **Weiss SR, Leibowitz JL.** 2011. Coronavirus pathogenesis. *Adv Virus Res* **81**:85–164.
2. **Debat HJ.** 2018. Expanding the size limit of RNA viruses: Evidence of a novel divergent nidovirus in California sea hare, with a ~35.9 kb virus genome.
3. **Saberi A, Gulyaeva AA, Brubacher JL, Newmark PA, Gorbalenya AE.** 2018. A planarian nidovirus expands the limits of RNA genome size. *PLOS Pathogens* **14**:e1007314.
4. **Snijder EJ, Bredenbeek PJ, Dobbe JC, Thiel V, Ziebuhr J, Poon LLM, Guan Y, Rozanov M, Spaan WJM, Gorbalenya AE.** 2003. Unique and conserved features of genome and proteome of SARS-coronavirus, an early split-off from the coronavirus group 2 lineage. *Journal of Molecular Biology* **331**:991–1004.
5. **Mazumder R, Iyer LM, Vasudevan S, Aravind L.** 2002. Detection of novel members, structure–function analysis and evolutionary classification of the 2H phosphoesterase superfamily. *Nucleic Acids Research* **30**:5229–5243.
6. **Zhao L, Jha BK, Wu A, Elliott R, Ziebuhr J, Gorbalenya AE, Silverman RH, Weiss SR.** 2012. Antagonism of the Interferon-Induced OAS-RNase L Pathway by Murine Coronavirus ns2 Protein Is Required for Virus Replication and Liver Pathology. *Cell Host and Microbe* **11**:607–616.
7. **Silverman RH.** 2007. Viral encounters with 2′,5′-oligoadenylate synthetase and RNase L during the interferon antiviral response. *Journal of Virology* **81**:12720–12729.
8. **Thornbrough JM, Jha BK, Yount B, Goldstein SA, Li Y, Elliott R, Sims AC, Baric RS, Silverman RH, Weiss SR.** 2016. Middle East Respiratory Syndrome Coronavirus NS4b Protein Inhibits Host RNase

L Activation. *mBio* **7**:e00258–16.

9. **Zhang R, Jha BK, Ogden KM, Dong B, Zhao L, Elliott R, Patton JT, Silverman RH, Weiss SR.** 2013. Homologous 2',5'-phosphodiesterases from disparate RNA viruses antagonize antiviral innate immunity. *Proceedings of the National Academy of Sciences* **110**:13114–13119.
10. **Yount B, Denison MR, Weiss SR, Baric RS.** 2002. Systematic assembly of a full-length infectious cDNA of mouse hepatitis virus strain A59. *Journal of Virology* **76**:11065–11078.
11. **Roth-Cross JK, Stokes H, Chang G, Chua MM, Thiel V, Weiss SR, Gorbalenya AE, Siddell SG.** 2009. Organ-specific attenuation of murine hepatitis virus strain A59 by replacement of catalytic residues in the putative viral cyclic phosphodiesterase ns2. *Journal of Virology* **83**:3743–3753.
12. **Zhou A, Paranjape J, Brown TL, Nie H, Naik S, Dong B, Chang A, Trapp B, Fairchild R, Colmenares C, Silverman RH.** 1997. Interferon action and apoptosis are defective in mice devoid of 2',5'-oligoadenylate-dependent RNase L. *EMBO J* **16**:6355–6363.
13. **Caamaño J, Alexander J, Craig L, Bravo R, Hunter CA.** 1999. The NF-kappa B family member RelB is required for innate and adaptive immunity to *Toxoplasma gondii*. *J Immunol* **163**:4453–4461.
14. **Sheffield P, Garrard S, Derewenda Z.** 1999. Overcoming expression and purification problems of RhoGDI using a family of “parallel” expression vectors. *Protein Expr Purif* **15**:34–39.
15. **Thakur CS, Xu Z, Wang Z, Novince Z, Silverman RH.** 2005. A convenient and sensitive fluorescence resonance energy transfer assay for RNase L and 2',5' oligoadenylates. *Methods Mol Med* **116**:103–113.
16. **Zhao L, Birdwell LD, Wu A, Elliott R, Rose KM, Phillips JM, Li Y, Grinspan J, Silverman RH, Weiss SR.** 2013. Cell-Type-Specific Activation of the Oligoadenylate Synthetase-RNase L Pathway by a Murine Coronavirus. *Journal of Virology* **87**:8408–8418.
17. **Gusho E, Zhang R, Jha BK, Thornbrough JM, Dong B, Gaughan C, Elliott R, Weiss SR, Silverman RH.** 2014. Murine AKAP7 Has a

2',5'-Phosphodiesterase Domain That Can Complement an Inactive Murine Coronavirus ns2 Gene. *mBio* **5**.

18. **Sperry SM, Kazi L, Graham RL, Baric RS, Weiss SR, Denison MR.** 2005. Single-amino-acid substitutions in open reading frame (ORF) 1b-nsP14 and ORF 2a proteins of the coronavirus mouse hepatitis virus are attenuating in mice. *Journal of Virology* **79**:3391–3400.
19. **Gombold JL, Hingley ST, Weiss SR.** 1993. Fusion-defective mutants of mouse hepatitis virus A59 contain a mutation in the spike protein cleavage signal. *Journal of Virology* **67**:4504–4512.
20. **Luytjes W, Bredenbeek PJ, Noten AF, Horzinek MC, Spaan WJ.** 1988. Sequence of mouse hepatitis virus A59 mRNA 2: indications for RNA recombination between coronaviruses and influenza C virus. *Virology* **166**:415–422.
21. **St-Jean JR, Jacomy H, Desforgues M, Vabret A, Freymuth F, Talbot PJ.** 2004. Human Respiratory Coronavirus OC43: Genetic Stability and Neuroinvasion. *Journal of Virology* **78**:8824–8834.
22. **Zhang J, Guy JS, Snijder EJ, Denniston DA, Timoney PJ, Balasuriya UBR.** 2007. Genomic characterization of equine coronavirus. *Virology* **369**:92–104.
23. **Vijgen L, Keyaerts E, Lemey P, Maes P, Van Reeth K, Nauwynck H, Pensaert M, Van Ranst M.** 2006. Evolutionary history of the closely related group 2 coronaviruses: porcine hemagglutinating encephalomyelitis virus, bovine coronavirus, and human coronavirus OC43. *Journal of Virology* **80**:7270–7274.
24. **Snijder EJ, Boon den JA, Bredenbeek PJ, Horzinek MC, Rijnbrand R, Spaan WJ.** 1990. The carboxyl-terminal part of the putative Berne virus polymerase is expressed by ribosomal frameshifting and contains sequence motifs which indicate that toro- and coronaviruses are evolutionarily related. *Nucleic Acids Research* **18**:4535–4542.
25. **Ogden KM, Hu L, Jha BK, Sankaran B, Weiss SR, Silverman RH, Patton JT, Prasad BVV.** 2015. Structural Basis for 2'-5'-Oligoadenylate Binding and Enzyme Activity of a Viral RNase L Antagonist. *Journal of Virology* **89**:6633–6645.

26. **Brandmann T, Jinek M.** 2015. Crystal structure of the C-terminal 2',5'- phosphodiesterase domain of group a rotavirus protein VP3. *Proteins* **83**:997–1002.
27. **Gold MG, Smith FD, Scott JD, Barford D.** 2008. AKAP18 Contains a Phosphoesterase Domain that Binds AMP. *Journal of Molecular Biology* **375**:1329–1343.
28. **Ontiveros E, Kuo L, Masters PS, Perlman S.** 2001. Inactivation of expression of gene 4 of mouse hepatitis virus strain JHM does not affect virulence in the murine CNS. *Virology* **289**:230–238.
29. **Huang C, Liu WJ, Xu W, Jin T, Zhao Y, Song J, Shi Y, Ji W, Jia H, Zhou Y, Wen H, Zhao H, Liu H, Li H, Wang Q, Wu Y, Wang L, Liu D, Liu G, Yu H, Holmes EC, Lu L, Gao GF.** 2016. A Bat-Derived Putative Cross-Family Recombinant Coronavirus with a Reovirus Gene. *PLOS Pathogens* **12**:e1005883.
30. **Kim HK, Yoon S-W, Kim D-J, Koo B-S, Noh JY, Kim JH, Choi YG, Na W, Chang K-T, Song D, Jeong DG.** 2016. Detection of Severe Acute Respiratory Syndrome-Like, Middle East Respiratory Syndrome-Like Bat Coronaviruses and Group H Rotavirus in Faeces of Korean Bats. *Transbound Emerg Dis* **63**:365–372.
31. **Navas-Martin S, Weiss SR.** 2003. SARS: lessons learned from other coronaviruses. *Viral Immunology* **16**:461–474.
32. **Navas-Martín SR, Weiss S.** 2004. Coronavirus replication and pathogenesis: Implications for the recent outbreak of severe acute respiratory syndrome (SARS), and the challenge for vaccine development. *J Neurovirol* **10**:75–85.
33. **Cruz JLG, Sola I, Becares M, Alberca B, Plana J, Enjuanes L, Zuniga S.** 2011. Coronavirus Gene 7 Counteracts Host Defenses and Modulates Virus Virulence. *PLOS Pathogens* **7**:1–25.
34. **Weiss SR, Zoltick PW, Leibowitz JL.** 1993. The ns4 gene of mouse hepatitis virus (MHV), strain A 59 contains two ORFs and thus differs from ns4 of the JHM and S strains. *Archives of Virology* **129**:301–309.

## Chapter 3

# ANTAGONISM OF dsRNA-INDUCED INNATE IMMUNE PATHWAYS BY NS4A AND NS4B ACCESSORY PROTEINS DURING MERS-COV INFECTION

This chapter is in production at *mBio* (as of March 4, 2019) as the published article “Antagonism of dsRNA-induced innate immune pathways by NS4a and NS4b accessory proteins during MERS-CoV infection by Courtney E. Comar<sup>\*</sup>, Stephen A. Goldstein<sup>\*</sup>, Yize Li, Boyd Yount, Ralphs S. Baric, and Susan R. Weiss.

<sup>\*</sup>These authors made equivalent contributions

## Abstract

Middle East respiratory syndrome coronavirus (MERS-CoV) was first identified in 2012 as a novel etiological agent of severe respiratory disease in humans. As during infection by other viruses, host sensing of viral dsRNA induces several antiviral pathways. These include interferon (IFN), OAS-RNase L, and Protein Kinase R (PKR). Coronaviruses, including MERS-CoV, potently suppress the activation of these pathways, inducing only modest host responses. Our study describes the functions of two accessory proteins unique to MERS-CoV and related viruses, NS4a and NS4b, during infection in human airway epithelium-derived A549 cells. NS4a has been previously characterized as a double stranded RNA (dsRNA) binding protein, while NS4b is a 2',5' phosphodiesterase with structural and enzymatic similarity to the NS2 protein encoded by mouse hepatitis virus (MHV). We found that deletion of NS4a results in increased interferon lambda (*IFNL1*) expression, as does mutation of either the catalytic site or nuclear localization sequence of NS4b. All of the mutant viruses we tested exhibited slight decreases in replication. We previously reported that, like MHV NS2, NS4b antagonizes OAS-RNase L, but suppression of IFN is a previously unidentified function for viral phosphodiesterases. Unexpectedly, deletion of NS4a does not result in robust activation of the PKR or OAS-RNase L pathways. Therefore, MERS-CoV likely encodes other proteins that contribute to suppression or evasion of these antiviral innate immune pathways that should be an important focus of future work. This study provides additional insight into the complex interactions between MERS-CoV and the host immune response.

## **Importance**

Middle East respiratory syndrome coronavirus (MERS-CoV) is the second novel zoonotic coronavirus to emerge in the 21<sup>st</sup> century and cause outbreaks of severe respiratory disease. More than 2,200 cases and 800 deaths have been reported to date, yet there are no licensed vaccines or treatments. Coronaviruses encode unique accessory proteins that are not required for replication but most likely play roles in immune antagonism and/or pathogenesis. Our study describes the functions of MERS-CoV accessory proteins NS4a and NS4b during infection of a human airway-derived cell line. Loss of these accessory protein during MERS-CoV infection leads to host antiviral activation and modestly attenuates replication. In the case of both NS4a and NS4b, we have identified roles during infection not previously described, yet the lack of robust activation suggests much remains to be learned about the interactions between MERS-CoV and the infected host.

## Introduction

Middle East respiratory syndrome-associated coronavirus (MERS-CoV), is a recently emerged, highly pathogenic coronavirus first identified in the Middle East in 2012 (1, 2). Following the 2002-2003 SARS-CoV pandemic, MERS-CoV is the second zoonotic coronavirus discovered in the 21<sup>st</sup> century. Though cases have been largely concentrated on the Arabian Peninsula, a large travel-associated outbreak in South Korea in 2015 highlights that MERS-CoV remains a global concern. MERS-CoV circulates in dromedary camels in Africa and the Middle East, having established a reservoir in camels, while closely related viruses are found in African bats, suggesting a bat origin for MERS-CoV or its direct ancestors (3-9).

Like all coronaviruses, MERS-CoV has a large positive-sense single-stranded RNA (ssRNA) genome of 30,119 nucleotides in length. The 5' two-thirds of the genome encode the functionally conserved replicase proteins, while a core set of structural proteins are encoded by all viruses of the *Betacoronavirus* genus in the 3' 10 kb. Additionally found in the 3' end of the genome are accessory genes specific to each *Betacoronavirus* subgenus, interspersed with structural genes. The MERS-CoV accessory genes are found only in other betacoronaviruses of the subgenus *Merbecovirus* (formerly lineage C) while betacoronaviruses of other subgenera such as mouse hepatitis virus (MHV) (*Embecovirus*/lineage A) and SARS-CoV (*Sarbecovirus*/lineage B) encode unique accessory genes.

Several accessory proteins encoded by MHV and SARS-CoV have been identified as antagonists of the innate immune response (10), as have some MERS-CoV accessory proteins (11-16). Several studies utilizing ectopically expressed protein and reporter systems have identified NS4a, NS4b, and NS5 as putative interferon (IFN) antagonists, but these studies may not faithfully recapitulate the complex interactions between viral and host factors present during infection (12, 13, 15, 17, 18). Recent studies utilizing recombinant MERS-CoV have more completely elucidated the functions of some of these proteins, but in some cases conflict with the earliest studies. NS4a, a double-stranded RNA (dsRNA) binding protein, prevents the generation of PKR-induced stress granules in some cell types (19). We reported previously that NS4b is a homolog of the NS2 protein of MHV and closely related betacoronaviruses of the subgenus *Embecovirus* (formerly lineage A), has 2',5' phosphodiesterases (PDE) activity, and acts as an antagonist of the oligoadenylate synthetase-ribonuclease L (OAS-RNase L) pathway (20). In contrast to the *Embecovirus* PDEs, NS4b has an N-terminal nuclear localization signal (NLS) and is localized primarily to the nucleus of infected cells (17, 20). NS4b has also been reported to antagonize NF $\kappa$ B nuclear translocation during MERS-CoV (14, 16, 19, 20), as has NS5 (11).

Building on our previous study characterizing NS4b as an OAS-RNase L antagonist (20), we have used recombinant MERS-CoV to further elucidate the roles of NS4a and NS4b during infection of human airway epithelium-derived

A549 cells (21). Consistent with earlier studies, NS4a prevents phosphorylation of PKR and the induction of IFN and interferon-stimulated gene (ISG) expression. However, PKR activation in the absence of NS4a does not result in phosphorylation of eIF2 $\alpha$  or translation arrest in A549 cells, in contrast to recent findings in a different cell type (19). Unlike other viral dsRNA binding proteins such as Vaccinia virus E3L (22) and influenza virus NS1 (23), NS4a does not play a significant role in OAS-RNase L antagonism during MERS-CoV infection, as deletion of NS4a does not result in RNase L activation or enhance RNase L activation in the context of MERS-CoV encoding catalytically inactive NS4b.

Our studies of NS4b reveal that in addition to antagonizing OAS-RNase L and preventing NF $\kappa$ B activation, NS4b antagonizes *IFNL1* expression, with this function dependent on both its catalytic activity and nuclear localization and independent of its interaction with the OAS-RNase L pathway. This is a unique role for virus-encoded phosphodiesterases, which otherwise lack an NLS and act solely as OAS-RNase L antagonists (14, 24-27). Together, the results demonstrate that NS4a and NS4b mediate both expected and unexpected functions during MERS-CoV infection, and further demonstrate the importance of studying the function of these proteins in the context of infection to uncover the full range of their interactions with the innate immune response.

## Materials and Methods

**Recombinant viruses.** Recombinant WT MERS-CoV and mutants were derived from the EMC/2012 strain cDNA clone all by introducing mutations into cDNA fragment F assembling the genome fragment and recovering infectious virus as described previously (28).

To ablate expression of MERS NS4a, PCR was performed with primers EMCmut4A (5'-NNNNNNTTAATTAACGAACTCTATTGATTACGTGTCTCTGCTTAATCAAATTTGACAGAAGTACCTTAACTC-3') and MERS:F3941 (5'-CACCGAAATGCATGCCAGCC-3'). The position of the F3941 within the MERS genome is 28,321 to 28,302. This product was digested with *PacI* and *NcoI*, gel purified, and then ligated into the MERS F plasmid which had been similarly digested.

To ablate MERS NS4a and NS4b expression, PCR was performed with primers delta4AB (5'-NNNNNNTTAATTAAGTTCATTCTTATCCCATTTTACATC-3') and MERS:F3415 (5'-GAGGGGGTTTACTATCCTGG-3'). This product was digested with *PacI* and *SalI*, gel purified and then ligated into the MERS F plasmid which had been similarly digested. The delta4AB primer uses the *PacI* site just upstream of NS4a, then the rest of this primer's sequence is from 26,795 to 26,819 in the MERS genome. The deletion removes nucleotides 25,844 to

26,794 in the MERS genome, and does not disrupt either the ~40 nucleotides upstream of or the transcription regulatory sequence (TRS) of NS5.

MERS-NS4b<sup>H182R</sup> was previously described (20). MERS-4b<sup>NLSmut</sup> was constructed by substituting residues 31, 33, 36, 37, 38 and 43 each with alanine. Briefly, one PCR product was generated using primers MERS:F1376 (5'-GTTTCTGTCGATCTTGAGTC-3') and MERS4bR (5'-NNNNNNCGTCTCGCAACGTAGGCCAGTGCCTTAGTTGGAGAATGGCTCCTC-3'). A second PCR reaction was performed with the primers MERS4bF (5'-NNNNNNCGTCTCCGTTGCGGCTGCATTTTCTCTTCTGGCCCATGAAGACCTTAGTGTTATTG-3') and MERS:F3415 (5'-GAGGGGGTTTACTATCCTGG-3'). The position of the F1376 primer in context of the MERS genome is 25,748-25,767, while the position for the reverse F3415 primer is 27,815-27,796. The products were gel isolated, digested with BsmBI (underlined in the above primers) and ligated with T4 DNA ligase. The resultant product was digested with PacI and SmaI, gel purified, and then used to replace the corresponding region in the MERS F plasmid which had been similarly digested. All recombinant viruses were isolated as previously described (28).

Sindbis virus Girdwood (GW100) (SINV) was obtained from Dr. Mark Heise, University of North Carolina, Chapel Hill, and prepared as previously described (29) and Sendai virus (SeV), Cantell strain was obtained from Dr. Carolina Lopez, University of Pennsylvania, Philadelphia and prepared as

previously described (30).

**Cell lines.** Vero CCL-81 cells were cultured in DMEM+10% FBS, penicillin-streptomycin, gentamicin, sodium pyruvate, and HEPES. Human A549 cells were cultured in RPMI 1640 supplemented with 10% FBS and penicillin-streptomycin.

A549<sup>DPP4</sup> and 293T<sup>DPP4</sup> cells were constructed by lentivirus transduction of *DPP4*. The plasmid encoding the cDNA of *DPP4* was purchased from Sino Biological. The cDNA was amplified using forward primer:

5'-GACTCTAGAATGAAGACACCGTGGAAGGTTCTTC-3' and reverse primer:

5'-

TCGAGACCGAGGAGAGGGTTAGGGATAGGCTTACCAGGTAAAGAGAAACAT

TGTTTTATG-3'. A V5 tag was introduced to the 3' end of the cDNA by PCR to

enable easy detection of DPP4. The amplicon was cloned into pCR4-TOPO TA

cloning vector (Invitrogen #K457502), to make pCR4-DPP4-V5. The fragment

containing DPP4-V5 was digested by XbaI/SalI restriction enzymes from the

pCR4-DPP4-V5 and was cloned into pLenti-GFP in place of GFP, generating

pLenti-DPP4-V5. The resulting plasmids were packaged in lentiviruses

pseudotyped with VSV-G to establish the gene knock in cells as previously

described (31). Forty-eight hours after transduction cells were subjected to

hygromycin (1mg/ml) selection for 3 days and single-cell cloned. Clones were

screened for DPP4 expression and susceptibility to MERS-CoV replication.

RNase L knockout A549<sup>DPP4</sup> cells were generated as previously described for

parental A549 (31) cells. A549<sup>mCEACAM-1</sup> cells were generated as described

above for A549<sup>DPP4</sup> cells, but by insertion of mouse *Ceacam-1* (Genbank accession #: NM\_001039185.1) into the lentivirus vector rather than human *DPP4*.

**NS4b expression from pCAGGs plasmid.** WT NS4b and the indicated mutant NS4b constructs were synthesized and purchased from Bio Basic in vector pUC57 flanked by restriction sites *Clal*/*XhoI*. pUC57 plasmids were digested and NS4b fragments gel purified for ligation into pCAGGS expression vector. Ectopic expression was conducted using lipofectamine 2000 transfection reagent (Thermo Fisher # 11668027) following the provided protocol. 24 hours post-transfection cells were fixed and stained as described below.

**MERS-CoV infections and titration.** Viruses were diluted in serum-free RPMI and added to cells for absorption for 45 minutes at 37°C. Cells were washed three times with PBS and fed with RPMI+2% FBS. 150 µl of supernatant was collected at the times indicated and stored at -80°C for titration by plaque assay on Vero CCL-81 cells as previously described (28). All infections and virus manipulations were conducted in a biosafety level 3 (BSL3) laboratory using appropriate personal protective equipment and protocols.

**Immunofluorescent staining.** At indicated times post-infection cells were fixed with 4% paraformaldehyde for 30 minutes at room temperature. Cells were then washed three times with PBS and permeabilized for 10 minutes with PBS+0.1%

Triton-X100. Cells were then blocked in PBS and 2% BSA for 45-60 minutes at room temperature. Primary antibodies were diluted in block buffer and incubated on a rocker at room temperature for one hour. Cells were washed three times with block buffer and then incubated rocking at room temperature for 30 minutes with secondary antibodies diluted in block buffer. Finally, cells were washed twice with block buffer and once with PBS, and nuclei stained with DAPI diluted in PBS. Coverslips were mounted onto slides for analysis by confocal microscopy. NS4b was detected using anti-NS4b rabbit serum at 1:500 and NS4a with anti-NS4a rabbit serum at 1:500 (both obtained from Dr. Luis Enjuanes, Spanish National Centre for Biotechnology) (14). DsRNA was detected using commercial antibody J2 at 1:1000 and nsp8 using anti-nsp8 guinea pig serum (obtained from Dr. Mark Denison, Vanderbilt University). Secondary antibodies were all highly cross-adsorbed IgG (H+L) from Invitrogen: Goat-anti rabbit AF594 (Cat #: AA11037), goat anti-mouse AF488 (Cat #: AA11029), goat anti-rabbit AF647 (Cat #: A32733), goat anti-guinea pig AF594 (Cat #: A11076), goat anti-guinea pig AF568 (Cat #: A11075).

**Western immunoblotting.** Cells were washed twice with ice-cold PBS and lysates harvested at indicated times post infection with lysis buffer (1% NP40, 2mM EDTA, 10% glycerol, 150mM NaCl, 50mM Tris HCl) supplemented with protease inhibitors (Roche – cOmplete mini EDTA-free protease inhibitor) and phosphatase inhibitors (Roche – PhosStop easy pack). After 5 minutes lysates were harvested, incubated on ice for 20 minutes, centrifuged for 20 minutes at

4°C and supernatants mixed 3:1 with 4x Laemmli sample buffer. Samples were heated at 95°C for 5 minutes, then separated on 4-15% SDS-PAGE, and transferred to polyvinylidene difluoride (PVDF) membranes. Blots were blocked with 5% nonfat milk and probed with the following antibodies diluted in the same block buffer: anti-PKR (phospho-T446) [E120] rabbit mAb at 1:1000 (Abcam 32036), anti-PKR (D7F7) rabbit mAb at 1:1000 (Cell Signaling Technology 12297), anti-GAPDH (14C10) rabbit mAb (Cell Signaling Technology 2118) at 1:1000, SinoBiological anti-MERS N mouse mAb at 1:1000, anti-NS4a rabbit serum at 1:500 (obtained from Dr. Luis Enjuanes, Spanish National Centre for Biotechnology) (14), and anti-NS4b rabbit serum at 1:500 (obtained from Dr. Robert Silverman, Cleveland Clinic) {Canton, 2018 #4007}. For detection of eIF2 $\alpha$  and phosphorylated eIF2 $\alpha$ , blots were blocked with 5% BSA and probed with the following antibodies diluted in the block buffer: phospho-eIF2 $\alpha$  (Ser51) antibody at 1:1000 (Cell Signaling Technology 9721). Secondary antibodies used were: Santa Cruz goat anti-mouse IgG-HRP secondary antibody (SC2005) at 1:5000 and Cell Signaling Technology anti-rabbit IgG, HRP-linked secondary antibody (CS7074) at 1:3000. Blots were visualized using Thermo Scientific SuperSignal west chemiluminescent substrates (Cat #: 34095 or 34080). Blots were probed sequentially with antibodies and in between antibody treatments stripped using Thermo scientific Restore western blot stripping buffer (Cat #: 21059).

Protein synthesis was assessed by treatment of cells with 10 $\mu$ g/ml puromycin for 10 minutes prior to protein harvest (32). Lysates were harvested and run on SDS-PAGE gels as described above. For detection of puromycin, anti-puromycin mouse mAb (Millipore clone 4G11 MABE342) was used at 1:6000, and the secondary antibody used was goat anti-mouse IgG-HRP Thermo Scientific (31430) at 1:3000. For detection of total protein by Coomassie staining, cell lysates (as prepared above) were separated by 4-15% SDS-PAGE. Gels were fixed and stained with 0.05% Coomassie Brilliant Blue R250 (Biorad 161-0400) in 50% methanol, 10% acetic acid solution for 2 hours at a gentle rock at room temperature. Gels were de-stained with 7% methanol and 5% acetic acid for several hours and then imaged.

**Quantitative real time PCR (qRT-PCR).** At indicated times post-infection cells were lysed with buffer RLT Plus (Qiagen RNeasy Plus #74136) and RNA extracted following the prescribed protocol. cDNA was synthesized according to the protocol for Thermo Scientific Superscript III reverse transcriptase (Thermo Scientific #18080044). RT-qPCR was performed under conditions validated for the indicated primer set. Primer sequences are as follows: *IFNL1* (F: 5'-CGCCTTGGAAGAGTCACTCA-3' R: 5'-GAAGCCTCAGGTCCCAATTC-3'), *OAS2* (F: 5'-TTCTGCCTGCACCACTCTTCACGAC-3' R: 5'-GCCAGTCTTCAGAGCTGTGCCTTTG-3'), *IFIT2* (F: 5'-CTGAGAATTGCACTGCAACCATG-3' R: 5'-TCCCTCCATCAAGTTCCAGGTGAA-3'), *IFNB* (F: 5'-

GTCAGAGTGGAAATCCTAAG-3' R: 5'-ACAGCATCTGCTGGTTGAAG-3'),  
*GAPDH* (F: 5'-GCAAATTCCATGGCACCGT-3' R: 5'-  
TCGCCCCACTTGATTTTGG

-3'). Fold changes in mRNA were calculated using the formula  $2^{-\Delta(\Delta Ct)}$  ( $\Delta Ct = Ct_{\text{gene of interest}} - Ct_{\text{GAPDH}}$ ) and expressed as fold infected/mock-infected.

**Analyses of RNase L-mediated rRNA degradation.** RNA was harvested with buffer RLT (Qiagen RNeasy #74106) and analyzed on an RNA chip with an Agilent Bioanalyzer using the Agilent RNA 6000 Nano Kit and its prescribed protocol as we have described previously (Cat #: 5067-1511).

**Statistical analysis.** Plotting of data and statistical analysis were performed using GraphPad Prism software (GraphPad Software, Inc., CA). Statistical significance for viral replication curves was determined by two-way ANOVA and for RT-qPCR by unpaired student's t-test.

## Results

**Construction and characterization of recombinant NS4a and NS4b MERS-CoV mutants.** In order to study the effects of NS4a and NS4b on MERS-CoV interactions with the host innate immune system we used a panel of recombinant MERS-CoV mutants. Deletion mutants MERS- $\Delta$ NS4a, MERS- $\Delta$ NS4ab were generated from the MERS-CoV infectious clone derived from the MERS-

EMC2012 strain (28) as follows and are described in detail in Materials and Methods and diagramed in Figure 3.1A-B. Briefly, MERS- $\Delta$ NS4a was generated

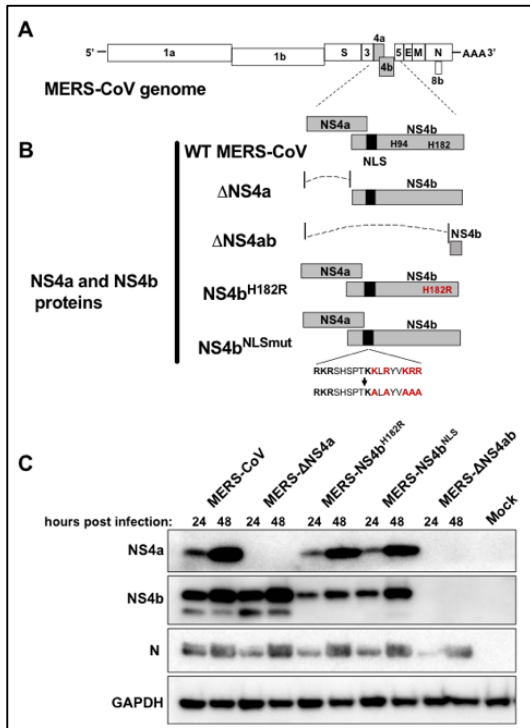


**Figure 3.1. MERS-CoV NS4a and NS4b recombinant mutants.** (A) MERS-CoV genome RNA with open reading frames shown. (B) NS4a and NS4b proteins expressed by wild type and mutant MERS-CoVs. The catalytic His residues of the PDE are shown and the vertical black bar indicates the NLS of NS4b; the red lettering indicates amino acid substitutions of the catalytic His residue and within the NLS (C) Expression of viral proteins from recombinant MERS-CoV viruses. A549<sup>DPP4</sup> cells were infected at an MOI of 10 with WT MERS-CoV, MERS-NS4a, MERS-NS4ab, MERS-NS4b<sup>H182R</sup>, MERS-NS4b<sup>NLSmut</sup> or mock infected. Cell lysates were prepared at 24 and 48 hours post-infection, analyzed by SDS-PAGE and probed by western blot with rabbit anti-serum against NS4a and NS4b, or mouse monoclonal antibodies against MERS nucleocapsid protein (N) and GAPDH. **Contributors:** SAG and CEC

by altering the start codon (ATG→ATT) and adding an in-frame stop codon ten codons downstream (TGG→TGA) to ablate synthesis of the NS4a protein. MERS- $\Delta$ NS4ab was generated by engineering a 951 nucleotide deletion of ORF4a and the majority of ORF4b without disrupting the transcription regulatory sequence (TRS) of NS5. To verify the loss of NS4b and/or NS4a expression by these mutants, human A549 cells stably expressing the MERS-CoV receptor DPP4 (A549<sup>DPP4</sup>) were infected with MERS-CoV mutants at an MOI of 10 and protein lysates harvested at 24 and 48 hours post-

infection to assess protein expression by western blot. As expected, NS4a is not synthesized during infection with MERS- $\Delta$ NS4a, and neither protein is detectable during MERS- $\Delta$ NS4ab infection (Fig 3.1C).

To further investigate the functional domains of NS4b, we utilized two mutant viruses with targeted mutations in either the phosphodiesterase domain or the NLS. MERS-NS4b<sup>H182R</sup> encodes NS4b with a catalytically inactive phosphodiesterase domain, which was generated from the MERS-CoV infectious clone as previously described (20, 28).

The NS4b NLS was previously described as bipartite (RKR<sub>11</sub>KRR), with the first basic motif more potently determining nuclear localization (14, 17). However, this first motif overlaps with the upstream ORF4a and so mutation of the RKR motif without causing amino acid changes in ORF4a is impossible. To determine how to construct NS4b<sup>NLSmut</sup> we mapped the nuclear localization sequence (NLS) by expressing WT and various NLS-mutant NS4b genes from a pCAGGS vector in A549 cells and detecting NS4b proteins by immunofluorescent staining (Fig 3.2A). These plasmids expressed NS4b proteins with mutations of the RKR motif, the downstream KRR motif, and a previously undescribed basic motif that lies between the two previously characterized motifs (RKR<sub>5</sub>KKLR<sub>2</sub>KRR). All mutant proteins exhibited primarily cytoplasmic localization, thus we engineered mutation of the central (KKLR) and downstream (KRR) motifs into the MERS-CoV infectious clone to generate MERS-NS4b<sup>NLSmut</sup> (Fig 3.1B), as described in detail in Materials and Methods (28).

While NS4b expressed during MERS-CoV infection is primarily expressed in the nucleus, during infection with MERS-NS4b<sup>NLSmut</sup>, NS4b exhibits

predominantly cytoplasmic localization, as expected (Fig 3.2B). During infection with MERS-NS4b<sup>H182R</sup> and MERS-NS4b<sup>NLSmut</sup>, slightly less NS4b was

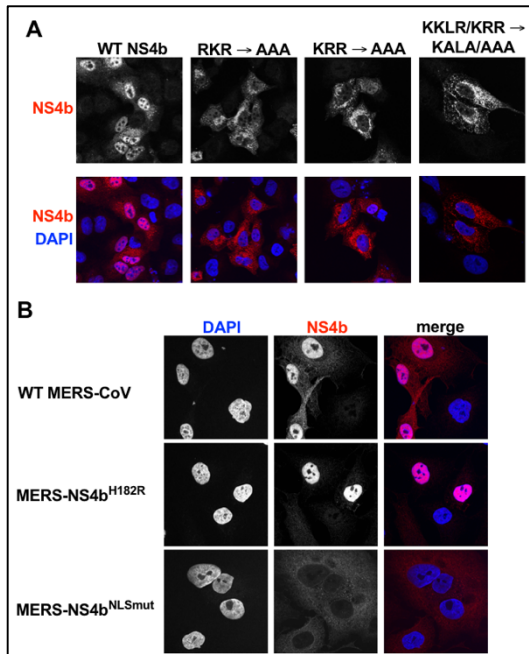


**Figure 3.2. Subcellular localization of MERS-CoV NS4b expression.** (A) The nuclear localization signal (NLS) was mapped by mutating basic residues in pCAGGS-NS4b and NS4b was ectopically expressed in A549 cells by DNA transfection. Twenty four hours post-transfection cells were fixed and stained for NS4b using anti-NS4b rabbit serum. (B) A549<sup>DPP4</sup> cells were infected with WT MERS-CoV, MERS-NS4b<sup>H182R</sup>, or MERS-NS4b<sup>NLSmut</sup> (MOI=5). Cells were fixed 24 hours post-infection and stained with anti-NS4b rabbit serum and goat anti-rabbit AF594 secondary antibody. **Contributor:** SAG

synthesized than during wild-type (WT) MERS-CoV infection (Fig 3.1C), consistent with previous studies of viral PDEs in which mutant protein expression was less robust than expression of wild-type protein (20). We consistently detected an extra lower band when probing for NS4b. This will be addressed in the Discussion.

**NS4a colocalizes with dsRNA around replication/transcription complexes (RTC).** Previous studies

have shown that overexpressed NS4a binds to dsRNA (15, 18). Additionally, NS4a is broadly cytoplasmic when overexpressed in uninfected cells, but colocalizes with dsRNA during infection (12, 14, 15). We infected A549<sup>DPP4</sup> cells with MERS-CoV and used immunofluorescent microscopy to determine NS4a localization. NS4a exhibits primarily punctate, perinuclear distribution with some diffuse distribution in the cytoplasm (Fig 3.3). Cells were co-stained for NS4a with J2 antibody to detect dsRNA and antiserum against the viral primase, nsp8, a

component of the viral polymerase complex and therefore a marker for virus RTCs (33). NS4a co-localizes with dsRNA and both are largely co-localized with nsp8, though dsRNA/NS4a appear more broadly distributed (Fig 3.3). This may indicate either that some dsRNA and NS4a localized outside the RTC, or that sensitivity of the assay is insufficient to detect all of the nsp8.

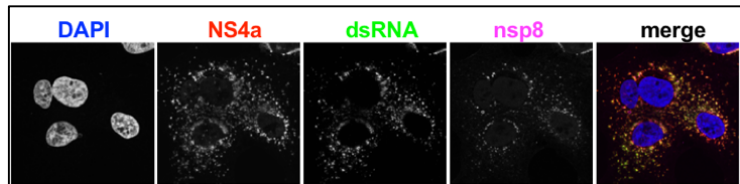


**Figure 3.3. NS4a colocalizes with dsRNA around replication/transcription complexes (RTC) during MERS-CoV infection.** A549<sup>DPP4</sup> cells were infected with WT MERS-CoV (MOI=5), fixed 24 hours post-infection, and stained with rabbit anti-NS4a serum, mouse anti-dsRNA J2, and guinea pig anti-nsp8 serum and then with secondary antibodies goat anti-rabbit AF647, goat anti-mouse AF488, and goat anti-guinea pig AF568. **Contributor:** SAG and CEC

### **NS4a and NS4b deletion mutants are modestly attenuated in A549<sup>DPP4</sup> cells.**

To assess the impact of NS4a and NS4b mutation on viral replication, we carried out growth curves in Vero and A549<sup>DPP4</sup> cells with MERS- $\Delta$ NS4a and MERS- $\Delta$ NS4ab. Vero cells lack a type I IFN response and were used to ensure recombinant viruses are not inherently replication-deficient. We infected both cell types with WT or mutant MERS-CoV at MOI=1 and harvested supernatant at pre-determined times post-infection for titration by plaque assay. All viruses replicated with equivalent kinetics to WT MERS-CoV and to equal titers in Vero cells, indicating that deletion of NS4a and NS4b does not disrupt critical aspects of the viral life-cycle (Fig 3.4A). In contrast, deletion of NS4a and/or NS4b modestly attenuated MERS-CoV replication in A549<sup>DPP4</sup> cells at an MOI of 1, with the reductions in titer significant at most time points (Fig 3.4B-C). Deletion of both NS4a and NS4b resulted in a slightly greater attenuation than deletion of NS4a

alone, though this difference was not statistically significant. That replication of these mutant viruses is attenuated in A549<sup>DPP4</sup> cells and not in permissive Vero cells strongly suggests that the deficiency is linked to the intact antiviral responses in A549 cells.

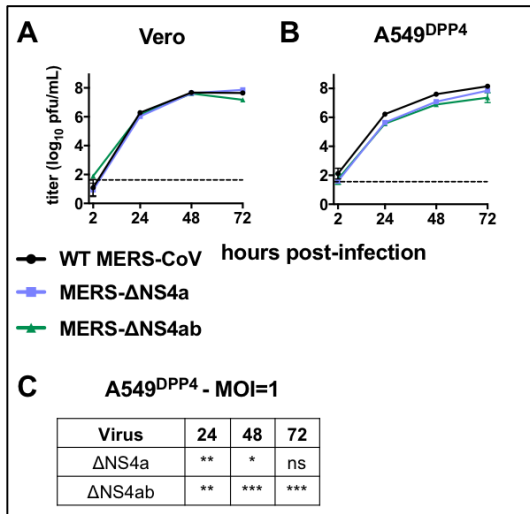


**Figure 3.4. MERS-CoV NS4a and NS4b mutants are attenuated in IFN-competent cells.** (A) Vero cells were infected in triplicate at MOI=1 with WT MERS-CoV, MERS-NS4a, and MERS-NS4ab. Supernatants were collected at indicated times post-infection and infectious virus quantified by plaque assay. (B) A549<sup>DPP4</sup> cells were infected in triplicate at MOI=1 with WT MERS-CoV, MERS-NS4a, and MERS-NS4ab and replication quantified as in (A). (C) Statistical significance for mutant virus replication vs WT was calculated by two-way ANOVA. Data are from one representative of three independent experiments. In (A) the 72 hours post-infection data point was only assessed in one out of three experiments. Data are displayed as means ± standard deviation (SD); \* p ≤ 0.05, \*\* p ≤ 0.01, \*\*\* p ≤ 0.001, \*\*\*\* p ≤ 0.0001. **Contributors:** CEC and SAG

### NS4a and NS4b modestly suppress

### IFN expression.

Previous studies of NS4a and NS4b have conflicted on the role of these proteins in suppressing the IFN response (12-16, 19). We aimed to systematically characterize the role of

NS4a and NS4b in antagonism of

IFN induction during MERS-CoV

infection. To ensure that our

newly generated A549<sup>DPP4</sup> cells

were a suitable platform for

investigating MERS-CoV

suppression of the IFN response, we infected them with Sendai virus (SeV),

Sindbis virus (SINV), and WT MERS-CoV. In contrast to SeV and SINV, which

robustly induced IFN and ISG expression by 12 hpi, MERS-CoV induced little

*IFNL1* or *IFNB* expression throughout a 36-hour course of infection (3.5A-B).

To determine if NS4a and/or NS4b contribute to suppressing IFN expression, we infected A549<sup>DPP4</sup> cells with WT MERS-CoV, MERS-ΔNS4a, and MERS-ΔNS4ab and at 24 and 36 hours post-infection compared gene expression of IFN and selected ISGs by qRT-PCR. In contrast to the minimal increases observed during WT MERS-CoV infection over mock-infected cells,

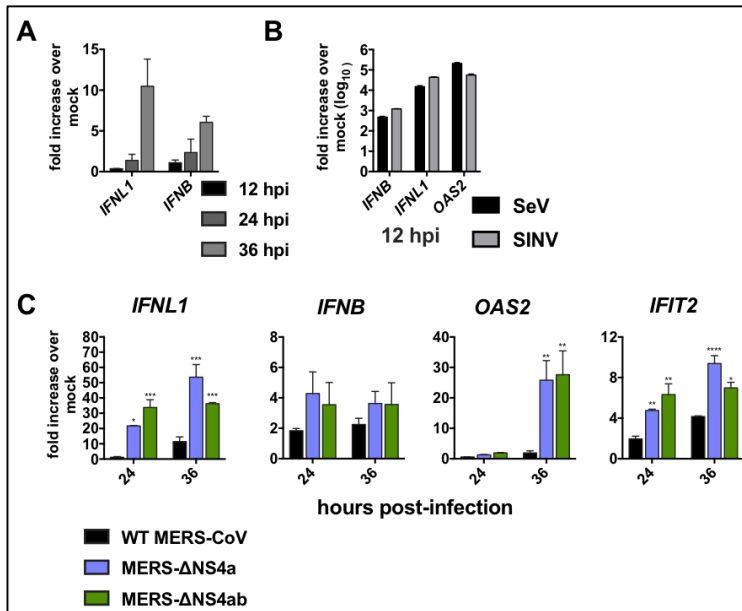


**Figure 3.5. NS4a and NS4b antagonize IFN expression.** (A) A549<sup>DPP4</sup> cells were mock-infected or infected in triplicate with WT MERS-CoV at MOI=5. RNA was harvested and gene expression was quantified by qRT-PCR and expressed as fold over mock-infected using the  $2^{-\Delta(\Delta Ct)}$  formula. (B) A549<sup>DPP4</sup> cells were infected in triplicate with SeV or SINV at MOI=5 and at 12 hours post-infection expression of the indicated genes in infected/mock-infected cells calculated as in (A). (C) A549<sup>DPP4</sup> cells were mock-infected or infected in triplicate with WT MERS-CoV, MERS-NS4a, and MERS-NS4ab at MOI=5 and RNA harvested at the indicated times post-infection. *IFNL1*, *IFNB*, *OAS2*, and *IFIT2* mRNA levels were quantified by qRT-PCR and calculated over mock-infected cells calculated as in (A). Data are from one representative of three independent experiments and displayed as means  $\pm$  standard errors of the mean (SEM). Statistical significance was calculated by unpaired student's t-test; \*  $p \leq 0.05$ , \*\*  $p \leq 0.01$ , \*\*\*  $p \leq 0.001$ , \*\*\*\*  $p \leq 0.0001$ . **Contributor:** SAG

additional deletion of NS4b. However, deletion of ORFs 4a and/or 4b did not result in IFN induced approaching the levels we observed in response to SeV and SINV infection (Fig 3.5B), suggesting MERS-CoV encodes additional, potent

MERS-ΔNS4a or MERS-ΔNS4ab infection resulted in significantly elevated levels of *IFNL1* mRNA and representative ISGs *OAS2* and *IFIT2* mRNAs. Interestingly there was no significant induction of type I IFN (Fig 3.5C). We did not observe any significant additive effect on antiviral gene expression from the

IFN antagonists and/or utilizes other mechanisms such as sequestration of

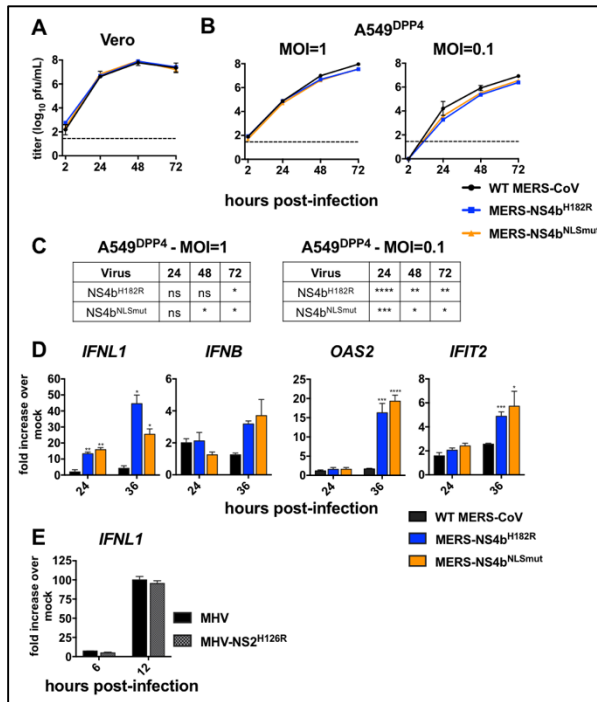


**Figure 3.6. MERS-CoV NS4b NLS and PDE catalytic mutants are attenuated in A549 cells and exhibit increased type III IFN expression.** (A) Vero cells were infected in triplicate at MOI=1 with WT MERS-CoV, MERS-NS4a, and MERS-NS4b. Supernatants were collected at indicated times post-infection and infectious virus quantified by plaque assay. (B) A549<sup>DPP4</sup> cells were infected in triplicate at MOI=1 or 0.1 with WT MERS-CoV, MERS-NS4a, and MERS-NS4b and replication quantified as in (A). Data are from one representative of three independent experiments and displayed as means  $\pm$  standard deviation (SD). (C) Statistical significance for mutant virus replication vs WT was determined by two-way ANOVA; \*  $p \leq 0.05$ , \*\*  $p \leq 0.01$ , \*\*\*  $p \leq 0.001$ , \*\*\*\*  $p \leq 0.0001$ . (D) A549<sup>DPP4</sup> cells were mock infected or infected in triplicate at MOI=5 with WT MERS-CoV, MERS-NS4b<sup>NLS</sup>, and MERS-NS4b<sup>H182R</sup> and RNA harvested at the indicated times post-infection. Gene expression over mock-infected cells was measured by RT-qPCR and calculated over mock-infected cells using the  $2^{-\Delta(\Delta CT)}$  formula. Data are from one representative of three independent experiments and expressed as mean  $\pm$  SEM. Statistical significance was determined by unpaired student's t-test; \*  $p \leq 0.05$ , \*\*  $p \leq 0.01$ , \*\*\*  $p \leq 0.001$ , \*\*\*\*  $p \leq 0.0001$ . (E) A549<sup>mCEACAM-1</sup> cells were mock treated or infected with WT MHV or MHV-NS2<sup>H126R</sup> at MOI=5 and RNA harvested at 6 and 12 hours post-infection. *IFNL1* expression was determined as in (D). Data are from one representative experiment of three. **Contributor:** SAG

dsRNA in membrane-bound RTCs to evade sensing by antiviral receptors.

**NS4b is a novel IFN antagonist.** We

previously reported that MERS-CoV

NS4b is a member of the 2H-

phosphoesterase superfamily of

proteins and antagonizes OAS-

RNase L activation during MERS-

CoV infection through its 2',5' PDE

activity (20, 34).

Unlike previously

studied viral

PDEs such as

mouse hepatitis

virus (MHV) NS2,

the torovirus

pp1a C-terminal

domain and the rotavirus VP3 C-terminal domain which exhibit primarily

cytoplasmic localization (24, 25), NS4b localizes primarily to the nucleus (Fig

3.2B), suggesting additional functions. Earlier studies suggested that NS4b

nuclear localization might be important for suppressing IFN expression (13), but

no previous studies have specifically addressed the role of its catalytic activity in IFN antagonism (35).

To characterize the function of the NS4b PDE domain and NLS we used recombinant MERS-NS4b<sup>H182R</sup> and MERS-NS4b<sup>NLSmut</sup>. In Vero cells both mutant

viruses replicated with equivalent kinetics to WT MERS-CoV and to equal titers (Fig 3.6A). In A549<sup>DPP4</sup>

cells both viruses are modestly and similarly attenuated at late

time points at an MOI of 1, and

throughout the course of infection at an MOI of 0.1, where two out of

three independent experiments yielded significant differences (Fig

3.6B-C). qRT-PCR analysis demonstrated that mutation of either the catalytic site or NLS results in significantly increased IFN and ISG expression during MERS-CoV infection (Fig 3.6D).

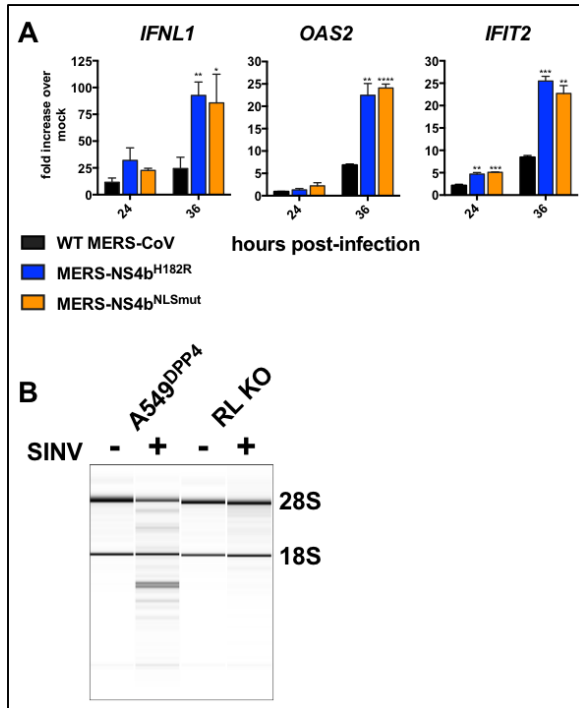


**Figure 3.7. NS4b antagonizes IFN expression independently of RNase L activation.** (A) RNase L KO A549<sup>DPP4</sup> cells were mock infected or infected in triplicate at MOI=5 with MERS-CoV, MERS-NS4b<sup>NLS</sup>, and MERS-NS4b<sup>H182R</sup>. RNA was harvested at the indicated times post-infection, mRNA levels expression was quantified by qRT-PCR in and expression in infected/mock-infected cells calculated using the  $2^{-\Delta(\Delta Ct)}$  formula. Data are from one representative experiment of three, expressed as mean  $\pm$  SEM and statistical significance determined by unpaired student's t-test; p  $\leq$  0.05, \*\* p  $\leq$  0.01, \*\*\* p  $\leq$  0.001 \*\*\*\* p  $\leq$  0.0001. (B) A549<sup>DPP4</sup> and RNase L KO A549<sup>DPP4</sup> cells were mock treated or infected with SINV at MOI=1 with SINV and RNA was harvested at 24 hours post-infection. RNA was assessed for ribosomal RNA degradation using an Agilent Bioanalyzer. 28S and 18S rRNA positions are indicated. **Contributor:** SAG

To further investigate whether PDE-dependent IFN antagonism is unique to MERS-CoV NS4b, we infected A549 cells stably expressing the MHV receptor CEACAM-1 (A549<sup>mCEACAM-1</sup>) with WT MHV or MHV encoding catalytically inactive NS2 (MHV-NS2<sup>H126R</sup>), its native PDE. Both viruses induced slightly more *IFNL1* expression than we observed for MERS-CoV, but MHV-NS2<sup>H126R</sup> did so to an identical degree as WT MHV (Fig 3.6E) demonstrating that the MHV PDE does not antagonize IFN induction in this cell type, consistent with our previous observation in murine cells (36).

Finally, to confirm that NS4b antagonism of IFN expression is a novel viral PDE function and uncoupled from its interaction with the OAS-RNase L pathway we assessed immune activation by MERS-CoV and NS4b mutants in A549<sup>DPP4</sup> cells ablated of RNase L expression by CRISPR-Cas9 as previously described (31). Both MERS-NS4b<sup>H182R</sup> and MERS-NS4b<sup>NLSmut</sup> induced greater *IFNL1*, *OAS2*, and *IFIT2* expression than WT MERS-CoV (Fig 3.7A) in RNase L KO cells, recapitulating the results we observed in wild-type A549<sup>DPP4</sup> cells. To confirm that these cells were indeed unable to activate RNase L, cells were infected with SINV, a known potent activator of OAS-RNase L (31), and rRNA integrity was analyzed by Bioanalyzer as previously described (20, 24).

**NS4a does not contribute to OAS-RNase L antagonism during MERS-CoV infection.** DsRNA binding proteins encoded by viruses such as Vaccinia virus (E3L) and Influenza A virus (NS1) antagonize activation of the antiviral OAS-

RNase L pathway, presumably by sequestration of viral RNA (22, 23, 37). Since RNase L activation by MERS-NS4b<sup>H182R</sup> is less robust than by other viruses such as SINV in A549<sup>DPP4</sup> cells (Fig 3.7) we hypothesized that NS4a may contribute to

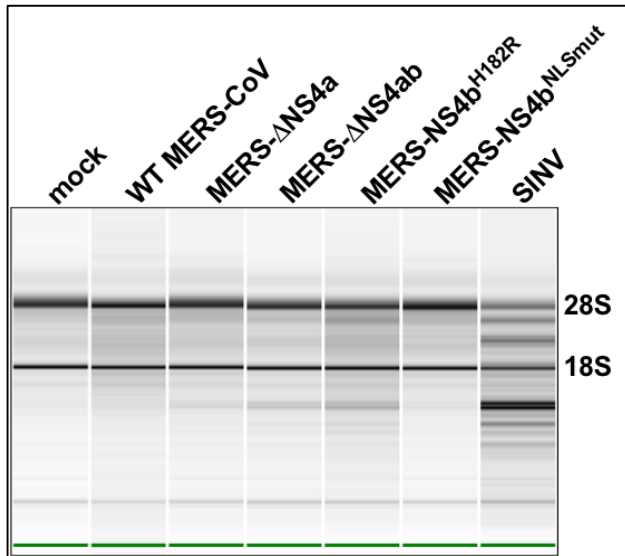


**Figure 3.8. Loss of NS4a does not activate RNase L during MERS-CoV infection.** A549<sup>DPP4</sup> cells were mock infected or infected with WT MERS-CoV, MERS-NS4a, MERS-NS4ab, MERS-NS4b<sup>H182R</sup>, MERS-NS4b<sup>NL.Smut</sup> (MOI=5) or SINV (MOI = 1). RNA was harvested at 48 hours post-infection for MERS-CoV infection and at 24 hours post-infection for SINV infection and assessed for ribosomal RNA degradation by Agilent Bioanalyzer. 28S and 18S rRNA positions are indicated. RINs and 28S/18S rRNA ratios are shown for each sample. Data are from one representative of three independent experiments. **Contributor:** CEC

antagonism of this pathway during MERS-CoV infection. To test this hypothesis, we infected A549<sup>DPP4</sup> cells at an MOI of 5 and harvested RNA 48 hours-post infection and assessed rRNA degradation using a Bioanalyzer (20, 24). We included SINV as a control for robust RNase L activation (31). RNase L activation is inferred from RNA degradation depicted by the banding pattern in the pseudogel

image. MERS-NS4b<sup>H182R</sup> and MERS-ΔNS4ab induced more rRNA degradation than WT MERS-CoV indicating activation of RNase L (Fig 4.8). Infection with MERS-NS4b<sup>NL.Smut</sup> also did not result in increased rRNA degradation, as expected given previous work demonstrating cytoplasmic PDE localization mediates RNase L antagonism (38). However, infection with MERS-ΔNS4a also did not induce increased rRNA degradation relative to WT MERS-CoV indicating that the absence of NS4a alone is not enough to activate RNase L in this cell

type (Fig 3.8). Infection with MERS-ΔNS4a did not induce more robust rRNA degradation than MERS-NS4b<sup>H182R</sup>, suggesting that NS4a does not play a significant role in antagonism of RNase L during MERS-CoV infection. This result demonstrates that NS4a has both functional similarities and differences to other viral dsRNA binding proteins.

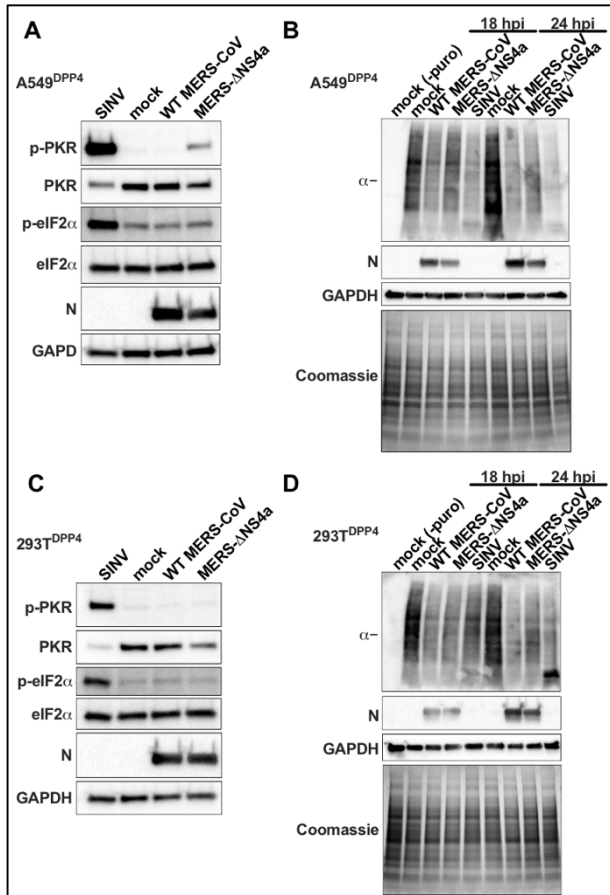


**Figure 3.9. Loss of NS4a activates PKR but does not lead to eIF2α phosphorylation or translation arrest in A549<sup>DPP4</sup>.** A549<sup>DPP4</sup> cells were mock infected or infected with WT MERS-CoV and MERS-NS4a (MOI=3) or SINV (MOI=1). (A) Cell lysates were harvested at 24 hours-post infection and proteins separated by SDS-PAGE and immunoblotted with antibodies against phosphorylated PKR (p-PKR), PKR, phosphorylated eIF2α (p-eIF2α), eIF2α, MERS-CoV N, and GAPDH. (B) Prior to cell lysate harvest, at 18 and 24 hours post-infection cell were treated with puromycin (10μg/ml) for 10 minutes. Proteins were separated by SDS-PAGE and analyzed either by immunoblotting with antibodies against puromycin, MERS N, or GAPDH or Coomassie stain for labeling of total proteins. (C) 293T<sup>DPP4</sup> cells were infected and cell lysates harvested same as in (A). (D) 293T<sup>DPP4</sup> cells were infected and cell lysates harvested as in (B). Data are from one representative of four (A), three (B), or two (C,D) independent experiments. **Contributor:** CEC

**NS4a antagonizes PKR activation, but not protein synthesis, during MERS-CoV infection.** A recent study showed that loss of NS4a during infection led to PKR activation, translational arrest, and stress granule formation, but only in certain cell types (19). We investigated whether NS4a antagonizes the dsRNA binding antiviral effector

Protein Kinase R (PKR) during MERS-CoV infection in A549<sup>DPP4</sup> cells. A549<sup>DPP4</sup> cells

were infected with WT MERS-CoV and MERS- $\Delta$ NS4a at an MOI of 3, lysed at 24 hours post-infection and analyzed for PKR activation by western blot. MERS- $\Delta$ NS4a, but not WT MERS-CoV induced PKR phosphorylation (Fig 3.9A). PKR phosphorylation during MERS- $\Delta$ NS4a infection was also observed at 16 and 48 hours post-infection (data not shown). However, despite the activation of PKR, we did not detect phosphorylation of eIF2 $\alpha$  above background levels, suggesting that activation of PKR by MERS- $\Delta$ NS4a in A549<sup>DPP4</sup> cells is not sufficient to engage downstream elements of this pathway or that MERS-CoV encodes an additional antagonist that blocks steps downstream of PKR phosphorylation. In contrast, SINV infection promotes robust phosphorylation of PKR and eIF2 $\alpha$  in the same cells, indicating the lack of eIF2 $\alpha$  phosphorylation during MERS- $\Delta$ NS4a is not due to a deficiency of this pathway in A549<sup>DPP4</sup> cells (Fig 3.9A).

Although we did not detect eIF2 $\alpha$  phosphorylation by immunoblotting, we wanted to confirm that PKR activation during MERS- $\Delta$ NS4a infection does not mediate translation arrest in A549<sup>DPP4</sup> cells. Thus, we compared protein synthesis during infection with MERS- $\Delta$ NS4a and WT MERS-CoV. We either mock infected or infected A549<sup>DPP4</sup> cells with WT MERS-CoV or MERS- $\Delta$ NS4a. We treated cells 18 and 24 hours post-infection with puromycin for 10 minutes to label nascent proteins prior to protein harvest. We used immunoblotting with an anti-puromycin antibody to specifically detect newly synthesized proteins and used Coomassie staining to assess total protein levels (32). Decrease in puromycin signal indicates translation arrest. Puromycin signal was not lower in MERS-

$\Delta$ NS4a infected A549<sup>DPP4</sup> cells compared to WT MERS-CoV, indicating PKR phosphorylation did not induce downstream translation arrest (Fig 3.9B).

In contrast to A549<sup>DPP4</sup> cells, we observed no phosphorylation of PKR during MERS- $\Delta$ NS4a infection in 293T<sup>DPP4</sup> cells (Fig 3.9C). Furthermore, MERS-CoV shut down protein synthesis during infection of these cells as previously reported with no enhancement of translation arrest from deletion of NS4a (Fig 3.9D) (39). This confirms the observed loss of protein synthesis occurs by an NS4a-independent mechanism and highlights that differences in cell type may affect levels of activation of the dsRNA-induced innate immune pathways.

## **Discussion**

Studies from other labs as well as data presented herein have demonstrated that MERS-CoV only modestly induces three major antiviral pathways, IFN production and signaling, OAS-RNase L and PKR. This is likely due largely to viral antagonists of dsRNA-induced host responses. Our study as well as recent reports from other labs have shown that deletion of MERS-CoV accessory proteins from recombinant viruses leads to enhanced activation of antiviral pathways. However, these effects are relatively small compared to other RNA viruses, and deletion of these accessory proteins only mildly attenuates replication. This is in contrast to early studies utilizing overexpression and reporter plasmids or ectopic expression from heterologous virus studies showing robust suppression of *IFNB* induction by NS4a and NS4b (12, 13, 15, 17, 40).

Thus, caution is warranted in extrapolating from studies that rely only on ectopic expression.

We have used recombinant MERS-CoV mutants to study interactions between the accessory proteins NS4a and NS4b and the host immune response. All of the viruses with mutations or deletions in NS4a and NS4b were modestly attenuated compared to WT MERS-CoV in A549<sup>DPP4</sup> cells. These modest differences are consistent with previous studies of MERS-CoV accessory proteins (11, 14, 19, 35, 40). Furthermore, there is a clinical report of human isolates with a 16 amino acid deletion in NS4a (41) and West African camel MERS-CoV isolates with ORF3 and ORF4b deletions, likely due to founder effects upon introduction into these populations (35). The isolation of these viruses supports findings that MERS-CoV accessory proteins are not definitive determinants of viral replication. However, all other known circulating MERS-CoV isolates and MERS-CoV-like viruses encode intact accessory ORFs, strongly suggesting that these proteins do play important roles in promoting viral fitness.

We found roles for both NS4a and NS4b in suppressing *IFNL1* expression in response to MERS-CoV infection, which is notably muted compared to other RNA viruses (Fig 3.5, 3.6). The lack of a similar increase in *IFNB* expression in response to mutant MERS-CoV infection is likely due to generally less robust expression of *IFNB* in A549 cells, which preferentially express *IFNL1* like other epithelial cells derived from barrier surfaces (42). We found that NS4b IFN

antagonism was dependent on nuclear localization, confirming an earlier report characterizing ectopically expressed NS4b (13), and its catalytic activity.

NS4b is the first viral phosphodiesterase known to suppress antiviral pathways in addition to RNase L, distinguishing it from phosphodiesterases found in the genomes of other coronavirus subgenera (Fig 3.6). While the exact mechanism of NS4b IFN antagonism remains unclear, several host-encoded PDEs within the same protein family are known or believed to participate in various steps of RNA processing (34, 43-49). Whether, like some cellular PDEs (43, 45), NS4b can cleave 3'-5' linked phosphodiester bonds in addition to 2'-5' oligoadenylates and whether it mediates any of its immune antagonist functions through directly or indirectly acting on host RNAs is an ongoing area of study. Finally, our data demonstrate that NS4b antagonism of IFN is distinct from its RNase L antagonist activity (Fig 3.7) demonstrating that NS4b has at least two independent functions.

We observed reduced expression of mutant NS4b compared to WT protein, as we reported previously (20). It is not known whether this reduced expression is due to reduced protein stability or to the antibody not recognizing the mutant protein form as readily. However, the abundance of NS4b during infection with MERS-NS4b<sup>NLSmut</sup>, though lower than WT protein, is sufficient to fully prevent RNase L activation, indicating mutation does not reduce NS4b levels below an effective concentration (Fig 3.7) (24, 38, 50). Thus, it is unlikely

that decreased mutant protein abundance is responsible for the observed IFN phenotype (25). We consistently observed a faster migrating band staining with antiserum directed against NS4b (Fig 3.1C). We presume that this band is less easily detected in the NS4b mutants due to the lower expression level and because this faster band is already faint in the WT MERS-CoV NS4b. We do not know the identity of this band. However, we speculate it could be a breakdown product of full length NS4b or more interestingly a protein initiated at one of several ATGs located downstream and in frame with the NS4b initiation site.

Activation of RNase L during MERS-NS4b<sup>H182R</sup> infection is less robust than during infection with MHV-NS2<sup>H126R</sup> in macrophages (24) or SINV infection of A549 cells (Fig 3.7) (31), suggesting MERS-CoV may have redundant mechanisms for inhibiting this pathway. Based on the role of the viral dsRNA binding proteins NS1 of Influenza and E3L of Vaccinia virus (22, 23, 37) in blocking RNase L activation as well as IFN and PKR, we hypothesized that NS4a contributes to antagonism of OAS-RNase L. Surprisingly, infection with MERS- $\Delta$ NS4a did not induce increased rRNA degradation compared to wild-type virus, nor did NS4a deletion produce any additive effect on RNase L activation in combination with deletion of NS4b. Nevertheless, the lack of robust RNase L activation even when NS4b is catalytically inactive suggests the possibility MERS-CoV does encode additional antagonists. One intriguing possibility is nsp15; its MHV ortholog has recently been described as contributing to evasion of multiple dsRNA-sensing pathways (51, 52). Alternatively, as has been

speculated for MHV, MERS-CoV dsRNA may, even in the absence of NS4a, be contained in viral replication/transcription complexes (RTCs) and therefore hidden from antiviral sensors (53, 54).

Due to its dsRNA-binding activity, we also hypothesized that NS4a inhibits PKR activation. One previous study showed that ectopically expressed NS4a inhibits PKR activation and can functionally replace the native PKR antagonist of encephalomyocarditis virus (40). Deletion of NS4a within recombinant MERS-CoV has previously been shown to result in enhanced translation arrest compared to WT MERS-CoV in HeLa cells (19). Consistent with this, we found that deletion of NS4a results in PKR phosphorylation, but in A549<sup>DPP4</sup> cells this did not lead to phosphorylation of eIF2 $\alpha$  above background levels, and MERS- $\Delta$ NS4a did not induce more translation arrest than WT MERS-CoV. In 293T<sup>DPP4</sup> cells, MERS-CoV induced translation arrest as previously reported (39), but we did not observe a more robust effect during MERS- $\Delta$ NS4a infection. Furthermore, PKR was not phosphorylated in 293T<sup>DPP4</sup> cells during MERS- $\Delta$ NS4a infection, confirming the PKR-independent mechanism of translational arrest and highlighting differences between cell types in antiviral pathway activation. These differences demonstrate the importance of using multiple model systems to fully elucidate interactions between viral proteins and host immune pathways.

Despite the lack of robust replication phenotypes, studies of MERS-CoV accessory proteins from other labs as well as our own have identified novel and important virus-host interactions that likely contribute in important ways to maintenance of MERS-CoV in its ecological niche and possibly during infection of the human respiratory tract. Future work on MERS-CoV accessory proteins in animal models and *in vitro* systems that more faithfully recapitulate the human airway should more fully answer the question of how these proteins contribute to replication under immune pressure and to pathogenesis.

### **Author Contributions**

**Manuscript and figure preparation:** SAG, CEC, and SRW

**Fig 3.1:** SAG and CEC

**Fig 3.2:** SAG

**Fig 3.3:** SAG and CEC

**Fig 3.4:** CEC and SAG

**Fig 3.5:** SAG

**Fig 3.6:** SAG

**Fig 3.7:** SAG

**Fig 3.8:** CEC

**Fig 3.9:** CEC

**Acknowledgements.** Research reported in this publication was supported by the National Institute of Allergy and Infectious Disease of the National Institutes of Health (NIH) under award F31 AI126673 to S.A.G., R21 AI114920 and R01 AI140442 to S.R.W., and R01 AI110700 and U19 AI109761 to R.S.B. Confocal microscopy was conducted in the Cell and Developmental Biology Microscopy Core at the University of Pennsylvania Perelman School of Medicine with support from Dr. Andrea Stout and Jasmine Zhao.

### **References**

1. **van Boheemen S, de Graaf M, Lauber C, Bestebroer TM, Raj VS, Zaki AM, Osterhaus ADME, Haagmans BL, Gorbalenya AE, Snijder EJ,**

- Fouchier RAM.** 2012. Genomic Characterization of a Newly Discovered Coronavirus Associated with Acute Respiratory Distress Syndrome in Humans. *mBio* **3**:e00473–12–e00473–12.
2. **Zaki AM, van Boheemen S, Bestebroer TM, Osterhaus ADME, Fouchier RAM.** 2012. Isolation of a Novel Coronavirus from a Man with Pneumonia in Saudi Arabia. *The New England Journal of Medicine* **367**:1814–1820.
  3. **Khalafalla AI, Lu X, Al-Mubarak AIA, Dalab AHS, Al-Busadah KAS, Erdman DD.** 2015. MERS-CoV in Upper Respiratory Tract and Lungs of Dromedary Camels, Saudi Arabia, 2013–2014. *Emerging Infectious Diseases* **21**:1153–1158.
  4. **Reusken CBEM, Messadi L, Feyisa A, Ularamu H, Godeke G-J, Danmarwa A, Dawo F, Jemli M, Melaku S, Shamaki D, Woma Y, Wungak Y, Gebremedhin EZ, Zutt I, Bosch B-J, Haagmans BL, Koopmans MPG.** 2014. Geographic Distribution of MERS Coronavirus among Dromedary Camels, Africa. *Emerging Infectious Diseases* **20**:1370–1374.
  5. **Wernery U, Rasoul IE, Wong EY, Joseph M, Chen Y, Jose S, Tsang AK, Patteril NAG, Chen H, Elizabeth SK, Yuen K-Y, Joseph S, Xia N, Wernery R, Lau SK, Woo PC.** 2015. A phylogenetically distinct Middle East respiratory syndrome coronavirus detected in a dromedary calf from a closed dairy herd in Dubai with rising seroprevalence with age. *Emerg Microbes Infect* **4**:e74 EP –.
  6. **Wernery U, Corman VM, Wong EYM, Tsang AKL, Muth D, Lau SKP, Khazanehdari K, Zirkel F, Ali M, Nagy P, Juhasz J, Wernery R, Joseph S, Syriac G, Elizabeth SK, Patteril NAG, Drosten C.** 2015. Acute Middle East Respiratory Syndrome Coronavirus Infection in Livestock Dromedaries, Dubai, 2014. *Emerging Infectious Diseases* **21**:1019–1022.
  7. **Geldenhuis M, Mortlock M, Weyer J, Bezuidt O, Seamark ECJ, Kearney T, Gleasner C, Erkkila TH, Cui H, Markotter W.** 2018. A metagenomic viral discovery approach identifies potential zoonotic and novel mammalian viruses in *Neoromicia* bats within South Africa. *PLoS ONE* **13**:e0194527.
  8. **Corman VM, Ithete NL, Richards LR, Schoeman MC, Preiser W, Drosten C, Drexler JF.** 2014. Rooting the Phylogenetic Tree of Middle

East Respiratory Syndrome Coronavirus by Characterization of a Conspecific Virus from an African Bat. *Journal of Virology* **88**:11297–11303.

9. **Anthony SJ, Gilardi K, Menachery VD, Goldstein T, Ssebide B, Mbabazi R, Navarrete-Macias I, Liang E, Wells H, Hicks A, Petrosov A, Byarugaba DK, Debbink K, Dinnon KH, Scobey T, Randell SH, Yount BL, Cranfield M, Johnson CK, Baric RS, Lipkin WI, Mazet JAK.** 2017. Further Evidence for Bats as the Evolutionary Source of Middle East Respiratory Syndrome Coronavirus. *mBio* **8**:e00373–17.
10. **Liu DX, Fung TS, Chong KK-L, Shukla A, Hilgenfeld R.** 2014. Accessory proteins of SARS-CoV and other coronaviruses. *Antiviral Research* **109**:97–109.
11. **Menachery VD, Mitchell HD, Cockrell AS, Gralinski LE, Boyd L Yount J, Graham RL, McAnarney ET, Douglas MG, Scobey T, Beall A, Dinnon K III, Kocher JF, Hale AE, Stratton KG, Waters KM, Baric RS.** 2017. MERS-CoV Accessory ORFs Play Key Role for Infection and Pathogenesis. *mBio* **8**:e00665–17.
12. **Yang Y, Zhang L, Geng H, Deng Y, Huang B, Guo Y, Zhao Z, Tan W.** 2013. The structural and accessory proteins M, ORF 4a, ORF 4b, and ORF 5 of Middle East respiratory syndrome coronavirus (MERS-CoV) are potent interferon antagonists. *Protein & Cell* **4**:951–961.
13. **Yang Y, Ye F, Zhu N, Wang W, Deng Y, Zhao Z, Tan W.** 2015. Middle East respiratory syndrome coronavirus ORF4b protein inhibits type I interferon production through both cytoplasmic and nuclear targets. *Sci Rep* **5**.
14. **Canton J, Fehr AR, Fernandez-Delgado R, Gutierrez-Alvarez FJ, Sanchez-Aparicio MT, Garcia-Sastre A, Perlman S, Enjuanes L, Sola I.** 2018. MERS-CoV 4b protein interferes with the NF- $\kappa$ B-dependent innate immune response during infection. *PLOS Pathogens* **14**:e1006838.
15. **Niemeyer D, Zillinger T, Muth D, Zielecki F, Horvath G, Suliman T, Barchet W, Weber F, Drosten C, Müller MA.** 2013. Middle East Respiratory Syndrome Coronavirus Accessory Protein 4a Is a Type I Interferon Antagonist. *Journal of Virology* **87**:12489–12495.
16. **Rabouw HH, Langereis MA, Knaap RCM, Dalebout TJ, Canton J, Sola**

- I, Enjuanes L, Bredenbeek PJ, Kikkert M, de Groot RJ, van Kuppeveld FJM.** 2016. Middle East Respiratory Coronavirus Accessory Protein 4a Inhibits PKR-Mediated Antiviral Stress Responses. *PLOS Pathogens* **12**:e1005982.
17. **Matthews KL, Coleman CM, van der Meer Y, Snijder EJ, Frieman MB.** 2014. The ORF4b-encoded accessory proteins of Middle East respiratory syndrome coronavirus and two related bat coronaviruses localize to the nucleus and inhibit innate immune signalling. *Journal of General Virology* **95**:874–882.
18. **Siu K-L, Yeung ML, Kok K-H, Yuen K-S, Kew C, Lui P-Y, Chan C-P, Tse H, Yuen K-Y, Jin D-Y.** 2014. Middle East Respiratory Syndrome Coronavirus 4a Protein Is a Double-Stranded RNA-Binding Protein That Suppresses PACT-Induced Activation of RIG-I and MDA5 in the Innate Antiviral Response. *Journal of Virology* **88**:4866–4876.
19. **Nakagawa K, Narayanan K, Wada M, Makino S.** 2018. Inhibition of stress granule formation by Middle East respiratory syndrome coronavirus 4a accessory protein facilitates viral translation, leading to efficient virus replication. *Journal of Virology* JVI.00902–18.
20. **Thornbrough JM, Jha BK, Yount B, Goldstein SA, Li Y, Elliott R, Sims AC, Baric RS, Silverman RH, Weiss SR.** 2016. Middle East Respiratory Syndrome Coronavirus NS4b Protein Inhibits Host RNase L Activation. *mBio* **7**:e00258–16.
21. **Giard DJ, Aaronson SA, Todaro GJ, Arnstein P, Kersey JH, Dosik H, Parks WP.** 1973. In vitro cultivation of human tumors: establishment of cell lines derived from a series of solid tumors. *J Natl Cancer Inst* **51**:1417–1423.
22. **Liu R, Moss B.** 2016. Opposing Roles of Double-Stranded RNA Effector Pathways and Viral Defense Proteins Revealed with CRISPR-Cas9 Knockout Cell Lines and Vaccinia Virus Mutants. *Journal of Virology* **90**:7864–7879.
23. **Min JY, Krug RM.** 2006. The primary function of RNA binding by the influenza A virus NS1 protein in infected cells: Inhibiting the 2<sup>′</sup>-5<sup>′</sup> oligo (A) synthetase/RNase L pathway. *Proc Natl Acad Sci USA* **103**:7100–7105.
24. **Zhao L, Jha BK, Wu A, Elliott R, Ziebuhr J, Gorbalenya AE, Silverman**

- RH, Weiss SR.** 2012. Antagonism of the Interferon-Induced OAS-RNase L Pathway by Murine Coronavirus ns2 Protein Is Required for Virus Replication and Liver Pathology. *Cell Host and Microbe* **11**:607–616.
25. **Goldstein SA, Thornbrough JM, Zhang R, Jha BK, Li Y, Elliott R, Quiroz-Figueroa K, Chen AI, Silverman RH, Weiss SR.** 2016. Lineage A Betacoronavirus NS2 proteins and homologous Torovirus Berne pp1a-carboxyterminal domain are phosphodiesterases that antagonize activation of RNase L. *Journal of Virology* JVI.02201–16.
26. **Roth-Cross JK, Stokes H, Chang G, Chua MM, Thiel V, Weiss SR, Gorbalenya AE, Siddell SG.** 2009. Organ-Specific Attenuation of Murine Hepatitis Virus Strain A59 by Replacement of Catalytic Residues in the Putative Viral Cyclic Phosphodiesterase ns2. *Journal of Virology* **83**:3743–3753.
27. **Zhao L, Birdwell LD, Wu A, Elliott R, Rose KM, Phillips JM, Li Y, Grinspan J, Silverman RH, Weiss SR.** 2013. Cell-Type-Specific Activation of the Oligoadenylate Synthetase-RNase L Pathway by a Murine Coronavirus. *Journal of Virology* **87**:8408–8418.
28. **Scobey T, Yount BL, Sims AC, Donaldson EF, Agnihothram SS, Menachery VD, Graham RL, Swanstrom J, Bove PF, Kim JD, Grego S, Randell SH, Baric RS.** 2013. Reverse genetics with a full-length infectious cDNA of the Middle East respiratory syndrome coronavirus. *Proceedings of the National Academy of Sciences* **110**:16157–16162.
29. **Suthar MS, Shabman R, Madric K, Lambeth C, Heise MT.** 2005. Identification of adult mouse neurovirulence determinants of the Sindbis virus strain AR86. *Journal of Virology* **79**:4219–4228.
30. **Basler CF, Mikulasova A, Martinez-Sobrido L, Paragas J, Mühlberger E, Bray M, Klenk H-D, Palese P, Garcia-Sastre A.** 2003. The Ebola virus VP35 protein inhibits activation of interferon regulatory factor 3. *Journal of Virology* **77**:7945–7956.
31. **Li Y, Banerjee S, Wang Y, Goldstein SA, Dong B, Gaughan C, Silverman RH, Weiss SR.** 2016. Activation of RNase L is dependent on OAS3 expression during infection with diverse human viruses. *Proc Natl Acad Sci USA* 201519657.
32. **Schmidt EK, Clavarino G, Ceppi M, Pierre P.** SUnSET, a nonradioactive

method to monitor protein synthesis. *Nat Meth* **6**:275 EP –.

33. **Velthuis te AJ, van den Worm SHE, Snijder EJ.** 2012. The SARS-coronavirus nsp7+nsp8 complex is a unique multimeric RNA polymerase capable of both de novo initiation and primer extension. *Nucleic Acids Research* **40**:1737–1747.
34. **Mazumder R, Iyer LM, Vasudevan S, Aravind L.** 2002. Detection of novel members, structure–function analysis and evolutionary classification of the 2H phosphoesterase superfamily. *Nucleic Acids Research* **30**:5229–5243.
35. **Chu DKW, Hui KPY, Perera RAPM, Miguel E, Niemeyer D, Zhao J, Channappanavar R, Dudas G, Oladipo JO, Traore A, Fassi-Fihri O, Ali A, Demissié GF, Muth D, Chan MCW, Nicholls JM, Meyerholz DK, Kurunga SA, Mamo G, Zhou Z, So RTY, Hemida MG, Webby RJ, Roger F, Rambaut A, Poon LLM, Perlman S, Drosten C, Chevalier V, Peiris M.** 2018. MERS coronaviruses from camels in Africa exhibit region-dependent genetic diversity. *Proceedings of the National Academy of Sciences* **115**:3144–3149.
36. **Zhao L, Rose KM, Elliott R, Van Rooijen N, Weiss SR.** 2011. Cell-Type-Specific Type I Interferon Antagonism Influences Organ Tropism of Murine Coronavirus. *Journal of Virology* **85**:10058–10068.
37. **Rivas C, Gil J, Mělková Z, Esteban M, Díaz-Guerra M.** 1998. Vaccinia Virus E3L Protein Is an Inhibitor of the Interferon (IFN)-Induced 2-5A Synthetase Enzyme. *Virology* **243**:406–414.
38. **Gusho E, Zhang R, Jha BK, Thornbrough JM, Dong B, Gaughan C, Elliott R, Weiss SR, Silverman RH.** 2014. Murine AKAP7 Has a 2',5'-Phosphodiesterase Domain That Can Complement an Inactive Murine Coronavirus ns2 Gene. *mBio* **5**.
39. **Lokugamage KG, Narayanan K, Nakagawa K, Terasaki K, Ramirez SI, Tseng C-TK, Makino S.** 2015. Middle East Respiratory Syndrome Coronavirus nsp1 Inhibits Host Gene Expression by Selectively Targeting mRNAs Transcribed in the Nucleus while Sparing mRNAs of Cytoplasmic Origin. *Journal of Virology* **89**:10970–10981.
40. **Rabouw HH, Langereis MA, Knaap RCM, Dalebout TJ, Canton J, Sola I, Enjuanes L, Bredenbeek PJ, Kikkert M, de Groot RJ, van Kuppeveld FJM.** 2016. Middle East Respiratory Coronavirus Accessory Protein 4a

Inhibits PKR-Mediated Antiviral Stress Responses. *PLOS Pathogens* **12**:e1005982.

41. **Lamers MM, Raj VS, Shafei M, Ali SS, Abdalh SM, Gazo M, Nofal S, Lu X, Erdman DD, Koopmans MP, Abdallat M, Haddadin A, Haagmans BL.** 2016. Deletion Variants of Middle East Respiratory Syndrome Coronavirus from Humans, Jordan, 2015. *Emerging Infectious Diseases* **22**:716–719.
42. **Wells AI, Coyne CB.** 2018. Type III Interferons in Antiviral Defenses at Barrier Surfaces. *Trends in Immunology*.
43. **Hilcenko C, Simpson PJ, Finch AJ, Bowler FR, Churcher MJ, Jin L, Packman LC, Shlien A, Campbell P, Kirwan M, Dokal I, Warren AJ.** 2013. Aberrant 3' oligoadenylation of spliceosomal U6 small nuclear RNA in poikiloderma with neutropenia. *Blood* **121**:1028–1038.
44. **Didychuk AL, Montemayor EJ, Carrocci TJ, DeLaitsch AT, Lucarelli SE, Westler WM, Brow DA, Hoskins AA, Butcher SE.** 2017. Usb1 controls U6 snRNP assembly through evolutionarily divergent cyclic phosphodiesterase activities. *Nat Commun* **8**:497.
45. **Nomura Y, Roston D, Montemayor EJ, Cui Q, Butcher SE.** 2018. Structural and mechanistic basis for preferential deadenylation of U6 snRNA by Usb1. *Nucleic Acids Research* **24**:791–gky812 VL – IS –.
46. **Shchepachev V, Wischnewski H, Missiaglia E, Soneson C, Azzalin CM.** 2012. Mpn1, Mutated in Poikiloderma with Neutropenia Protein 1, Is a Conserved 3'-to-5' RNA Exonuclease Processing U6 Small Nuclear RNA. *Cell Reports* **2**:855–865.
47. **Shchepachev V, Azzalin CM.** 2013. The Mpn1 RNA exonuclease: Cellular functions and implication in disease. *FEBS Lett* **587**:1858–1862.
48. **Shchepachev V, Wischnewski H, Soneson C, Arnold AW, Azzalin CM.** 2015. Human Mpn1 promotes post-transcriptional processing and stability of U6atac. *FEBS Lett* **589**:2417–2423.
49. **Mroczek S, Krwawicz J, Kutner J, Lazniewski M, Kuciński I, Ginalski K, Dziembowski A.** 2012. C16orf57, a gene mutated in poikiloderma with neutropenia, encodes a putative phosphodiesterase responsible for the U6 snRNA 3' end modification. *Genes & Development* **26**:1911–1925.

50. **Zhang R, Jha BK, Ogden KM, Dong B, Zhao L, Elliott R, Patton JT, Silverman RH, Weiss SR.** 2013. Homologous 2',5'-phosphodiesterases from disparate RNA viruses antagonize antiviral innate immunity. *Proceedings of the National Academy of Sciences* **110**:13114–13119.
51. **Deng X, Baker SC.** 2018. An “Old” protein with a new story: Coronavirus endoribonuclease is important for evading host antiviral defenses. *Virology* **517**:157–163.
52. **Kindler E, Gil-Cruz C, Spanier J, Li Y, Wilhelm J, Rabouw HH, Züst R, Hwang M, Vkovski P, Stalder H, Marti S, Habjan M, Cervantes-Barragan L, Elliot R, Karl N, Gaughan C, van Kuppeveld FJM, Silverman RH, Keller M, Ludewig B, Bergmann CC, Ziebuhr J, Weiss SR, Kalinke U, Thiel V.** 2017. Early endonuclease-mediated evasion of RNA sensing ensures efficient coronavirus replication. *PLOS Pathogens* **13**:e1006195.
53. **Zhou H, Perlman S.** 2007. Mouse hepatitis virus does not induce Beta interferon synthesis and does not inhibit its induction by double-stranded RNA. *Journal of Virology* **81**:568–574.
54. **Versteeg GA, Bredenbeek PJ, van den Worm SHE, Spaan WJM.** 2007. Group 2 coronaviruses prevent immediate early interferon induction by protection of viral RNA from host cell recognition. *Virology* **361**:18–26.

## **Chapter 4**

# **PRELIMINARY NS4B MECHANISTIC INSIGHTS**

## Introduction

My published work on the MERS-CoV NS4b accessory protein, described in Chapter 4 and Thornbrough *et. al.* (1) has identified it as a phosphodiesterase with both conserved and unique interactions with host innate immunity. As with other viral phosphodiesterases (2-4), NS4b antagonizes the OAS-RNase L antiviral pathway through cleavage of the RNase L-activating second messenger 2-5A (5, 6). Additionally, we demonstrated as described in Chapter 4 that mutation of either the catalytic site or nuclear localization sequence (NLS) of NS4b results in elevated interferon (IFN) and interferon-stimulated gene (ISG) expression. However, we have so far not determined the mechanism by which NS4b modulates the abundance of IFN and ISG transcripts, whether through the inhibition of transcription or some interference at the co-transcriptional or post-transcriptional level. Earlier studies of NS4b have suggested it may be able to prevent IFN gene expression (7, 8), but the mechanism of doing so and particularly the involvement of its catalytic activity has not been well studied.

We have determined that while some reports describe ectopically expressed NS4b as blocking nuclear translocation of interferon regulatory factor-3 (IRF3) (7, 8), a critical transcription factor for IFN gene expression, mutation of the NS4b catalytic site or NLS does not result in increased IRF3 phosphorylation and we likewise did not detect any increase in IRF3 nuclear accumulation during MERS-CoV infection (Fig 4.1). Having excluded this possibility, we sought to draw on the literature describing other members of the 2H-phosphoesterase (2H-

PE) superfamily of phosphodiesterases (PDEs), the superfamily that includes the coronavirus PDEs, in order to generate hypotheses regarding the mechanistic interactions between NS4b and the host. This literature, reviewed briefly below, clearly indicates that the characterized functions of 2H-PE almost uniformly involve some element of RNA processing though the function is not known for every member of the superfamily.

### ***Known functions of cellular 2H-phosphoesterases***

2H-phosphoesterases are nearly ubiquitous among cellular life forms and are believed to have been present in the last universal common ancestor of all modern life, though they have been lost in some bacterial lineages (9). Within the 2H-phosphoesterase superfamily are several families. These include the prototypical archaeo-bacterial LigT group, the eukaryotic-viral LigT-like group (including MHV NS2 and MERS-CoV NS4b), the bacterial Yjcg-like group, and the mlr3352-like group from bacteria but which also appears in the genomes of some large eukaryotic DNA viruses, likely as a result of horizontal gene transfer (9). In addition, several 2H-phosphoesterases do not fit neatly within any of these groups, such as the 2',3' cyclic nucleotide phosphodiesterases found in the nervous system of vertebrates and a group of enzymes encoded by retroviruses of fish (9-11).

The prototypical member of the LigT-like family of 2H-phosphoesterases is the *E. coli* LigT protein, evidence of which was first identified through the

observation of 2',5' RNA ligase activity in an *E. coli* extract, then purified and cloned (9, 12-14). LigT can both catalyze and break 2',5' linkages between tRNA halves. Proteins with similar activity have also been identified in hyperthermophilic archaea of the genus *Pyrococcus* (15), as well as in fungi and the bacteriophage T4 (9). The presence of genes encoding archaeo-bacterial LigT-like proteins in fungal genomes likely is explained by virus-mediated cross-kingdom horizontal gene transfer (HGT) between prokaryotes and fungi (9). Although such cross-kingdom HGT has historically been considered unlikely or rare, recent evidence suggests otherwise (16, 17).

Among eukaryotes, LigT-like 2H-PEs are also ubiquitous and may best inform predictions about the function of the viral 2H-PEs they are presumably ancestral to. Prior to the discovery of LigT-like 2H-PEs in eukaryotes, 2',3' cyclic nucleotide phosphodiesterases (CPDases), a divergent family of 2H-phosphoesterases, were identified as active in tRNA ligation in yeast and in the nervous system of complex eukaryotes, including humans (10, 18-20). Although the RNA ligase domain of these proteins is similar to that of archaeo-bacterial LigT-like proteins, they belong to a distinct family. In contrast, eukaryotes and some of their viruses encode LigT-like 2H-PEs that have distinct functions unrelated to tRNA ligation.

The eukaryotic-viral LigT-like 2H-PEs are typified by the human CGI-18 gene, also known as the ASCC1 subunit of activating signal co-integrator

complex 1 (ASC-1) (9, 21, 22). Although CGI-18 is the family prototype, relatively little is known about its function within ASC1, though interest has grown recently as truncating mutations of CGI-18 have been associated with a range of genetic diseases (23, 24). One report has demonstrated a critical role for the catalytic histidines of CGI-18 in regulating its localization within the nucleus (25), but an enzymatic substrate or function for CGI-18 remains unidentified. Another of the cellular LigT-like 2H-PEs,  $\alpha$ -kinase anchoring protein-18 (AKAP18), has been more extensively studied than CGI-18 although the physiological significance of its enzymatic activity is likewise not known. AKAP18 in fact refers to several isoforms of the same protein expressed from a single AKAP7 gene, and only two of the 4 isoforms ( $\gamma$  and  $\delta$ ) contain a central PDE domain (26, 27). The AKAP18 PDE, like MHV NS2 and MERS-CoV NS4b, has 2',5' PDE activity and it or a similar gene may be ancestral to the viral PDEs, though the degree of sequence divergence aside from the conserved catalytic motifs makes this currently impossible to determine. Bolstering this possibility, however, is that the known MHV NS2 and rotavirus VP3 CTD structures and predicted MERS-CoV NS4b structure are most similar to that of the AKAP18 central domain, more so than to other eukaryotic 2H-PE known structures or of bacterial LigT (1, 28). AKAP18 anchors protein kinase A to cellular membranes and binds to cAMP and experimental evidence demonstrates that AKAP18 $\gamma$  and  $\delta$  isoforms regulate PKA activity, however whether it has a catalytic substrate and what that may be is unknown (26, 29, 30).

Unlike AKAP18 and CGI-18, the physiological role of the eukaryotic 2H-PE USB1 is well understood. As is true for the prokaryotic LigT-like 2H-PEs, USB1 participates in RNA processing. Specifically, USB1 of both yeast and humans associates with the spliceosome and is essential for processing of the U6 snRNA. USB1 is a 3'-5' exonuclease that removes Us and As from the 3' prime end of U6 and catalyzes the formation of a 2',3' cyclic phosphate that protects U6 from exosomal degradation (31-33). Although USB1 was first recognized as removing uridines from the 3' end of U6, it actually has a higher level of activity against *in vitro* oligoA substrates, which is consistent with observations that a lack of USB1 leads to aberrantly 3' polyadenylated U6, decreased stability of the snRNA, and consequent defects in splicing (31, 33-35). It is not known whether USB1, like AKAP18 and viral 2H-PEs, has 2',5' PDE activity in addition to the 3',5' activity necessary for its post-transcriptional processing of U6, though this is an active area of investigation in collaboration with Dr. Robert Silverman of the Cleveland Clinic.

Given the extensive demonstrated involvement of cellular 2H-PEs in RNA metabolism, and after determining that NS4b does not participate in IRF3 inhibition during infection through its catalytic domain or NLS (Fig 4.1), we hypothesized that it may modulate antiviral responses through participation in RNA processing. Our initial hypothesis was that NS4b might, like USB1, have 3'-5' exonuclease activity that would allow it to shorten mRNA poly(A) tails, resulting in accelerated turnover. However, mutation of neither the NS4b catalytic site nor

nuclear localization sequence resulted in reproducible changes in the decay rates of several antiviral mRNAs, as measurable by the RT-qPCR assay we used (Fig 4.2). In collaboration with Dr. Robert Silverman, we are continuing to investigate the substrate range of MERS-CoV NS4b and other 2H-PEs. We previously demonstrated that it has 2',5' PDE activity (1), but do not yet know if it can act on other types of phosphodiester linkages as well. Most recently, we have developed preliminary evidence that NS4b may participate in the splicing process. Infection with MERS-NS4b<sup>H182R</sup> or MERS-NS4b<sup>NLSmut</sup> results in elevated abundance of *IFNL1* and ISG mRNAs (Fig 3.6). In addition, during infection with MERS-NS4b<sup>H182R</sup> but not MERS-NS4b<sup>NLSmut</sup> the abundance of some intronic RNA is increased relative to during WT MERS-CoV infection. Post-splicing, branched intron lariats contain a 2',5' phosphodiester linkage that must be cleaved so that the intron can be degraded and the nucleotide pool replenished. The cellular enzyme DBR1 is responsible for lariat debranching (36), and we hypothesized that NS4b may accelerate this process during infection to prevent accumulation of circular intron-derived RNAs due to virus-induced transcriptional increases (37), though the possible impact of such accumulation remains unknown. Future studies will more extensively investigate this observation and seek to uncover the underlying mechanism. Nevertheless, though preliminary, these data suggest that, like cellular 2H-PEs but unique among viral PDEs, MERS-CoV may participate in cellular RNA metabolism.

## Materials and Methods

**Recombinant viruses.** Recombinant WT MERS-CoV and mutants were derived from the EMC/2012 strain cDNA clone by Dr. Ralph Baric, all by introducing mutations into cDNA fragment F assembling the genome fragment and recovering infectious virus as described previously (38).

MERS-NS4b<sup>H182R</sup> was previously described (20). MERS-4b<sup>NLSmut</sup> was constructed by substituting residues 31, 33, 36, 37, 38 and 43 each with alanine. Briefly, one PCR product was generated using primers MERS:F1376 (5'-GTTTCTGTTCGATCTTGAGTC-3') and MERS4bR (5'-NNNNNNCGTCTCGCAACGTAGGCCAGTGCCTTAGTTGGAGAATGGCTCCTC-3'). A second PCR reaction was performed with the primers MERS4bF (5'-NNNNNNCGTCTCCGTTGCGGCTGCATTTTCTTCTTGCCCATGAAGACCTTAGTGTTATTG-3') and MERS:F3415 (5'-GAGGGGGTTTACTATCCTGG-3'). The position of the F1376 primer in context of the MERS genome is 25,748-25,767, while the position for the reverse F3415 primer is 27,815-27,796. The products were gel isolated, digested with BsmBI (underlined in the above primers) and ligated with T4 DNA ligase. The resultant product was digested with PacI and SanDI, gel purified, and then used to replace the corresponding region in the MERS F plasmid which had been similarly digested. All recombinant viruses were isolated as previously described (38).

**Cell lines.** A549<sup>DPP4</sup> cells were constructed by lentivirus transduction of *DPP4*.

The plasmid encoding the cDNA of *DPP4* was purchased from Sino Biological.

The cDNA was amplified using forward primer:

5'-GACTCTAGAATGAAGACACCGTGGAAGGTTCTTC-3' and reverse primer:

5'-

TCGAGACCGAGGAGAGGGTTAGGGATAGGCTTACCAGGTAAAGAGAAACAT

TGTTTTATG-3'. A V5 tag was introduced to the 3' end of the cDNA by PCR to

enable easy detection of DPP4. The amplicon was cloned into pCR4-TOPO TA

cloning vector (Invitrogen #K457502), to make pCR4-DDP4-V5. The fragment

containing DPP4-V5 was digested by XbaI/SalI restriction enzymes from the

pCR4-DPP4-V5 and was cloned into pLenti-GFP in place of GFP, generating

pLenti-DPP4-V5. The resulting plasmids were packaged in lentiviruses

pseudotyped with VSV-G to establish the gene knock in cells as previously

described (39). Forty-eight hours after transduction cells were subjected to

hygromycin (1mg/ml) selection for 3 days and single-cell cloned. Clones were

screened for DPP4 expression and susceptibility to MERS-CoV replication.

**MERS-CoV infections.** Viruses were diluted in serum-free RPMI and added to

cells for absorption for 45 minutes at 37°C. Cells were washed three times with

PBS and fed with RPMI+2% FBS. RNA was harvested at indicated hours post-

infection by lysing cells with Qiagen buffer RLT Plus and isolating RNA using the

RNeasy Plus kit (Cat #: 74136) and provided protocol. All infections and virus

manipulations were conducted in a biosafety level 3 (BSL3) laboratory using appropriate personal protective equipment and protocols.

**Western immunoblotting.** Cells were washed twice with ice-cold PBS and lysed with lysis buffer (1% NP40, 2mM EDTA, 10% glycerol, 150mM NaCl, 50mM Tris HCl) supplemented with protease inhibitors (Roche – cOmplete mini EDTA-free protease inhibitor) and phosphatase inhibitors (Roche – PhosStop easy pack). Lysates were incubated on ice for 20 minutes, centrifuged for 20 minutes at 4°C and supernatants mixed 3:1 with 4x Laemmli sample buffer. Samples were heated at 95°C for 5 minutes, then separated on 4-15% SDS-PAGE, and transferred to polyvinylidene difluoride (PVDF) membranes. Blots were blocked with 5% BSA and probed with the following antibodies diluted in 5% BSA at 1:1000 dilution: rabbit anti-IRF3 mAb D83B9 (Cell Signaling Technologies Cat #: 4302), rabbit anti-phospho-IRF3 mAb (Abcam Cat #: 76493), anti-MERS N mouse mAb (SinoBiological Cat #: 40068-MM10), anti-GAPDH rabbit mAb 14C10 (Cell Signaling Technology Cat #: 2118). Secondary antibodies used were: Santa Cruz goat anti-mouse IgG-HRP secondary antibody (Cat #: SC2005) at 1:5000 and Cell Signaling Technology anti-rabbit IgG, HRP-linked secondary antibody (Cat #: CS7074) at 1:3000. Blots were visualized using Thermo Scientific SuperSignal west chemiluminescent substrates (Cat #: 34095 or 34080). Blots were probed sequentially with antibodies and in between antibody treatments stripped using Thermo scientific Restore western blot stripping buffer (Cat #: 21059).

**Immunofluorescent staining.** At indicated times post-infection cells were fixed with 4% paraformaldehyde for 30 minutes at room temperature. Cells were then washed three times with PBS and permeabilized for 10 minutes with PBS+0.1% Triton-X100. Cells were then blocked in PBS and 2% BSA for 45-60 minutes at room temperature. Primary antibodies were diluted in block buffer and incubated on a rocker at room temperature for one hour. Cells were washed three times with block buffer and then incubated rocking at room temperature for 30 minutes with secondary antibodies diluted in block buffer. Finally, cells were washed twice with block buffer and once with PBS, and nuclei stained with DAPI diluted in PBS. Coverslips were mounted onto slides for analysis by widefield microscopy. Proteins of interest were detected using primary antibodies (1:1000 dilution) rabbit anti-IRF3 mAb D83B9 (Cell Signaling Technologies Cat #: 4302), anti-MERS N mouse mAb (SinoBiological Cat #: 40068-MM10). Secondary antibodies were all highly cross-adsorbed IgG (H+L) from Invitrogen: Goat-anti rabbit AF594 (Cat #: AA11037), goat anti-mouse AF488 (Cat #: AA11029).

**Quantitative real time PCR (qRT-PCR).** At indicated times post-infection cells were lysed with Qiagen Buffer RLT Plus (Cat #: 74136) and RNA extracted following the prescribed protocol. cDNA was synthesized according to the protocol for Thermo Scientific Superscript III reverse transcriptase (Thermo Scientific #18080044). RT-qPCR was performed under conditions validated for the indicated primer set. Primer sequences are as follows: *IFIT2*-exonic (F: 5' -

CTGAGAATTGCACTGCAACCATG - 3', R: 5'-  
TCCCTCCATCAAGTTCCAGGTGAA-3'), *IFIT2*-intronic (F: 5'-  
TGTCCAATGCAAATCCTGAGAAGC  
-3', R: 5'- AAATGGAGCTGGCCCTCTTTGG-3') *GAPDH*-exonic (F: 5'-  
GCAAATTCCATGGCACCGT-3', R: 5'-TCGCCCCACTTGATTTTGG-3'),  
*GAPDH*-intronic (F: GACCTTTACTCCTGCCCTTTGA-3', R: 5'-  
TGGTATTCACCACCCCACTATG-3'), *DDX58*-exonic (F: 5'-  
TAGCTCAGCTGATGAGGGACAC-3', R: 5'-CTTTGTCTGGCATCTGGAACAC-  
3'), *DDX58*-intronic (F: 5'-AAAGTCCGGCTCCTCTCCAGCTT-3', R: 5'-  
GTCCAAGGGATGGGACACAAAGG-3'), 18S rRNA (F: 5'-  
TTCGATGGTAGTCGCTGTGC-3', R: 5'- CTGCTGCCTTCCTTGAATGTGGTA  
-3'. Fold changes in mRNA over mock-infected cells were calculated using the  
formula  $2^{-\Delta(\Delta Ct)}$  ( $\Delta Ct = Ct_{\text{gene of interest}} - Ct_{\text{GAPDH}}$ ) and expressed as fold  
infected/mock-infected. To calculate RNA abundance for experiments measuring  
mRNA decay, I first calculated the amount of RNA relative to the highly stable  
18S mRNA using the formula  $2^{-\Delta Ct}$ , with the 0 hour time point set as 1. I then  
calculated mRNA remaining by dividing the relative mRNA level (to 18S) at later  
time points by the relative RNA level at the 0 hour time point.

**Statistical analysis.** Plotting of data and statistical analysis were performed  
using GraphPad Prism software (GraphPad Software, Inc., CA). Statistical  
significance for RT-qPCR was determined by application of an unpaired student's  
t-test, with a significance threshold of  $p > 0.05$ .

## Results

**Mutation of NS4b does not alter IRF3 activation.** Previous studies have demonstrated that ectopically expressed NS4b inhibits nuclear accumulation of IRF3, a critical antiviral transcription factor, contributing to its IFN antagonism (7, 8, 40). To determine whether the elevated IFN and ISG mRNA levels induced by MERS-NS4b<sup>H182R</sup> and MERS-NS4b<sup>NLSmut</sup> are linked to increased activation of

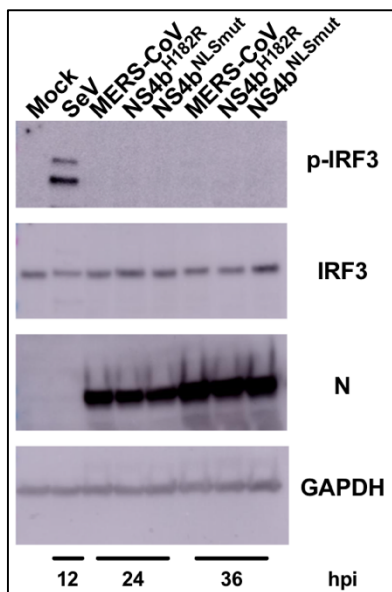


**Figure 4.1. WT and NS4b mutant MERS-CoV do not induce IRF3 phosphorylation.** A549<sup>DPP4</sup> cells were mock infected or infected at MOI=5 with Sendai virus (SeV), WT MERS-CoV, MERS-NS4b<sup>H182R</sup>, or MERS-NS4b<sup>NLSmut</sup>. Cells were lysed for protein harvesting at the indicated times post-infection and proteins separated by SDS-PAGE and immunoblotted with antibodies against phospho-IRF3, IRF3, MERS-CoV nucleocapsid, or GAPDH. Data are representative of two independent experiments.

MERS-NS4b<sup>H182R</sup> and MERS-NS4b<sup>NLSmut</sup> that presumably require some low

IRF3, I infected A549<sup>DPP4</sup> cells with these viruses and WT MERS-CoV at MOI=5 and assayed for IRF3 phosphorylation by western blot and nuclear localization by immunofluorescent microscopy. I used Sendai virus (SeV) as a positive control for IRF3 phosphorylation and nuclear translocation, as it is a known potent inducer of IFN (Fig 3.5). SeV-infected A549<sup>DPP4</sup> cells were lysed for protein

extraction 12 hours post-infection (hpi), while MERS-CoV infected cells were lysed 24 and 36 hpi. Only SeV induced the appearance of detectable phospho-IRF3 (Fig 4.1), despite modest IFN induction by

amount of IRF3 activation, though IFN activation through another transcription factor may be possible.

To confirm that mutation of the NS4b catalytic site or NLS does not affect IRF3 activation, I quantified IRF3 nuclear localization during SeV, WT MERS-CoV, and mutant NS4b MERS-CoV infection. SeV-infected A549<sup>DPP4</sup> cells were fixed with 4% PFA 12 hpi, while MERS-CoV infected cells were fixed 24 hpi. I then stained the fixed cells with an anti-IRF3 monoclonal antibody and quantified the fluorescent intensity of

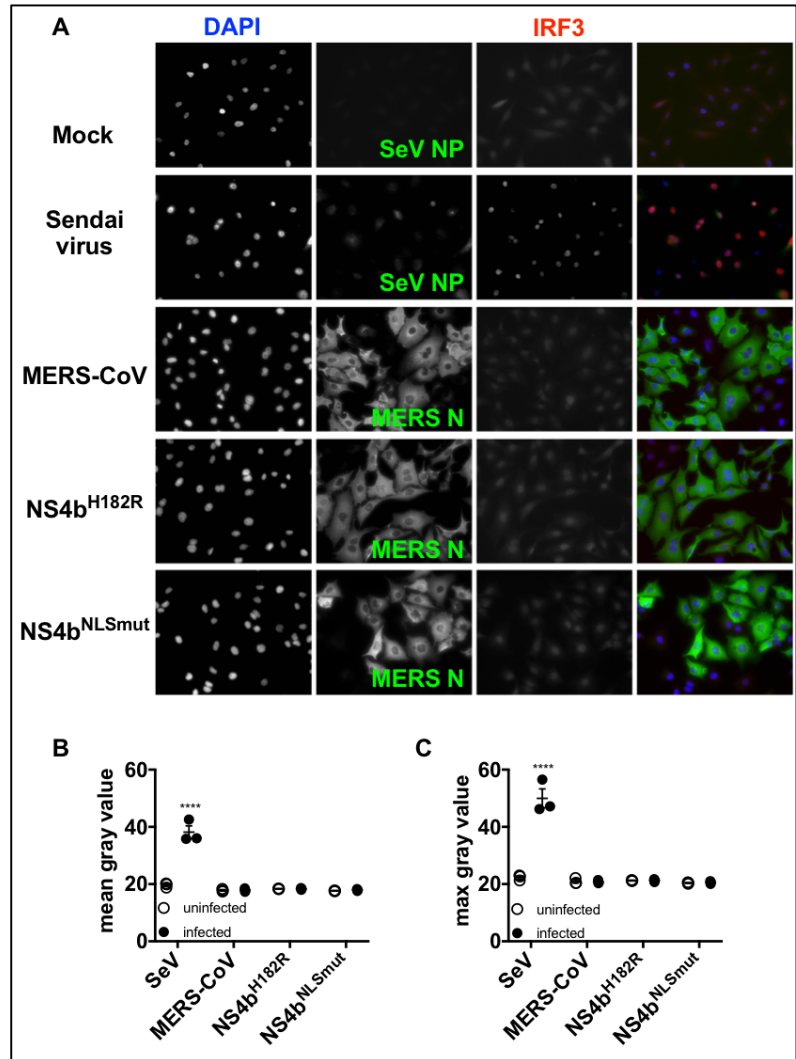


**Figure 4.2. WT and NS4b mutant MERS-CoV do not induce nuclear localization of IRF3.** A549<sup>DPP4</sup> cells were mock infected or infected at MOI=5 with Sendai virus (SeV), WT MERS-CoV, MERS-NS4b<sup>H182R</sup>, or MERS-NS4b<sup>NLSmut</sup>. At either 12 (SeV), or 24 hours post-infection cells were fixed and stained with DAPI and antibodies against IRF3, and either SeV nucleoprotein or MERS-CoV nucleocapsid and secondary antibody goat anti-rabbit AF594 or goat anti-mouse AF488. A) Cells were analyzed by widefield microscopy and images processed in ImageJ. B) and C) In ImageJ, nuclei were defined and cells classified as uninfected or infected based on the presence of viral antigen signal above background. In each nucleus, the mean or maximum gray value of IRF3 fluorescent signal was measured. Quantification was based on at least 50 cells for each condition, and statistical significance calculated by unpaired student's t-test. \* p ≤ 0.05, \*\* p ≤ 0.01, \*\*\* p ≤ 0.001, \*\*\*\* p ≤ 0.0001.

IRF3 in the nuclei of infected and uninfected cells. Antibodies against Sendai virus nucleoprotein (NP), and MERS-CoV nucleocapsid (N) were used in conjunction with the anti-IRF3 antibody to identify infected cells. Only Sendai virus induced a statistically significant increase in average or maximum IRF3 fluorescent intensity in the nucleus (Fig 4.1B-D).

**Mutation of MERS-CoV NS4b does not alter antiviral mRNA stability.** Based on the extensive involvement of 2H-PEs in RNA processing (9) and the 3'-5'

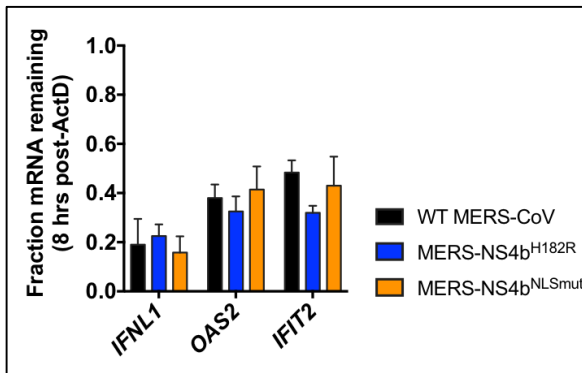


**Figure 4.3. Mutation of MERS-CoV NS4b does not alter antiviral mRNA stability.** A549<sup>DPP4</sup> cells were infected at MOI=5 with WT MERS-CoV, MERS-NS4b<sup>H182R</sup>, or MERS-NS4b<sup>NLSmut</sup>. 24 hours post-infection, media was replaced with fresh media + 5  $\mu$ g/ml actinomycin D. I then waited one hour to ensure full transcriptional arrest, and lysed cells for RNA extraction and designated this as time 0. 8 hours later, a second set of cells were lysed for RNA extraction. The abundance of indicated RNAs was analyzed by qRT-PCR. To calculate RNA abundance for experiments measuring mRNA decay, I first calculated the amount of RNA relative to the highly stable 18S mRNA using the formula  $2^{-\Delta Ct}$ , with the 0 hour time point set as 1 (or 100%). The fraction of mRNA remaining after 8 hours was calculated by dividing the relative mRNA level (to 18S) at later time points by the relative RNA level at the 0 hour time point.

deadenylating activity of eukaryotic

2H-PE USB1(34), we sought to

determine whether NS4b destabilizes

host antiviral mRNAs. I infected

A549<sup>DPP4</sup> cells with either WT MERS-

CoV, MERS-NS4b<sup>H182R</sup>, and

MERS-NS4b<sup>NLSmut</sup> at MOI=5 and

at 24 hpi treated the cells with 5

$\mu$ g/ml actinomycin D to arrest

transcription as described in the

literature. (41, 42). At 0 and 8

hours post-actinomycin D

treatment I harvested RNA from infected cells. I then used qRT-PCR to quantify

the amounts of indicated antiviral mRNA relative to the first RNA harvest time

point to assay for the percentage amount of mRNA remaining as an indirect

measure of mRNA degradation. At 8 hours post-treatment I compared the percentage of mRNA remaining between WT MERS-CoV, MERS-NS4b<sup>H182R</sup>, and MERS-NS4b<sup>NLSmut</sup>. I did not observe any apparent difference in antiviral mRNA decay during infection with the WT or NS4b mutant viruses (Fig 4.3), suggesting that MERS-CoV NS4b does not induce accelerated decay of antiviral mRNAs, and thus this putative mechanism does not likely account for the previously observed increase in the abundance of such mRNAs during infection with MERS-NS4b<sup>H182R</sup> and MERS-NS4b<sup>NLSmut</sup>.

**Ablation of MERS-CoV NS4b catalytic activity results in increased abundance of intronic RNA.** After I did not observe any changes in mature

mRNA stability due to mutation of NS4b, I sought to determine if NS4b is involved in post-transcriptional RNA processing during or after splicing. To do so, I utilized two schemes for qRT-PCR analysis. The first aimed at quantification of mature antiviral mRNA using primers amplifying across exon-exon junctions, as described in Chapter 3 and typically used for gene expression

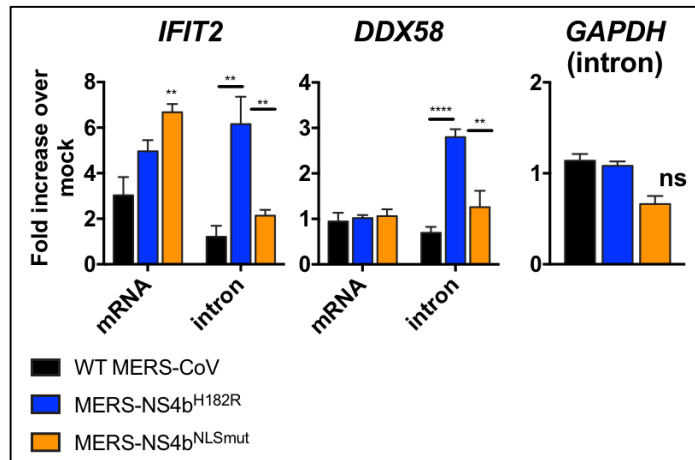


**Figure 4.4. Ablation of MERS-CoV NS4b catalytic activity results in increased abundance of intron-derived RNA.** A549<sup>DPP4</sup> cells were infected at MOI=5 with WT MERS-CoV, MERS-NS4b<sup>H182R</sup>, or MERS-NS4b<sup>NLSmut</sup>. 24 hours post-infection cells were lysed and RNA extracted for analysis by qRT-PCR. RNA harvested at the indicated times post-infection. Gene expression over mock-infected cells was measured by RT-qPCR and calculated over mock-infected cells using the  $2^{-\Delta(\Delta CT)}$  formula. Data are from one representative of three independent experiments and expressed as mean  $\pm$  SEM. Statistical significance was determined by unpaired student's t-test; \* p  $\leq$  0.05, \*\* p  $\leq$  0.01, \*\*\* p  $\leq$  0.001, \*\*\*\* p  $\leq$  0.0001.

quantification. For the second, I used primers targeting introns, which can detect both unspliced pre-mRNAs and introns excised during the splicing reaction but not yet debranched and degraded (Fig 4.4).

I infected A549<sup>DPP4</sup> cells with WT MERS-CoV, MERS-NS4b<sup>H182R</sup>, MERS-NS4b<sup>NLSmut</sup> at MOI=5 and harvested RNA 24 and 36 hpi. I then used qRT-PCR with primers targeting exonic and intronic regions of RNAs transcribed from the ISGs *IFIT2* and *DDX58*, as well as an intron of the metabolic gene *GAPDH*. As seen during previous experiments (Fig 3.6), the abundance of mature *IFIT2* mRNA was elevated during MERS-NS4b<sup>H182R</sup> and MERS-NS4b<sup>NLSmut</sup> infection relative to during WT MERS-CoV infection, while *DDX58* mature mRNA levels were generally not induced by MERS-CoV infection (Fig 4.4), though *DDX58* can be induced in these cells by treatment with high concentrations of recombinant IFN (not shown). *GAPDH* intron RNA levels did not differ between infection with WT or NS4b mutant MERS-CoV (Fig 4.4). In contrast, *IFIT2* and *DDX58* intronic RNA was more abundant during MERS-NS4b<sup>H182R</sup> infection than during infection with WT MERS-CoV or MERS-NS4b<sup>NLSmut</sup> (Fig 4.4). It remains unclear where the targeted intron is more abundant because it is retained in the mRNA are increased frequencies or if the excised lariat is more stable, as attempts to quantify *IFIT2* and *DDX58* pre-mRNA were unsuccessful.

## Discussion

I did not find that mutation of the MERS-CoV NS4b catalytic site or NLS resulted in increased activation of the critical antiviral transcription factor IRF3 (Fig 4.1). Previous studies found that ectopically expressed NS4b inhibits nuclear translocation of IRF3 (7, 40). A later study likewise showed that NS4b blocks IRF3 nuclear translocation, as well as IRF3 phosphorylation and prevented luciferase expression from an *IFNB* promoter following ectopic expression of IRF3 (8). Notably, this study found that removal of the NS4b NLS abrogated the ability of NS4b to block IRF3-induced *IFNB* promoter expression.

The apparent conflict between these reports and my work may be explained by one or multiple factors. Some differences could be accounted for by the use of ectopically expressed NS4b, which may produce results that do not faithfully recapitulate physiological interactions during infection. Specifically, ectopic expression can result in intracellular concentrations well above physiological levels, which may allow for protein-protein interactions that don't occur during infection but would disrupt signaling pathways. Another possibility is that inhibition of IRF3 activation is mediated by regions of NS4b unaffected by the mutations in the recombinant viruses I used. A 2015 report by Yang *et. al.* suggested that cytoplasmic NS4b interferes with the assembly of the MDA5 signaling complex activated in response to viral dsRNA and upstream of IRF3. This function is unlikely to be affected by mutations deep within the NS4b catalytic domain and was found in that study to be independent of the NLS, as N-

terminal truncated NS4b still disrupted MDA5 signaling (8). If confirmed during MERS-CoV infection, this would suggest yet another immune antagonist function for NS4b, which has already been identified as inhibiting RNase L activation (1), NF $\kappa$ B nuclear translocation (43), and the IFN response through a catalytic mechanism independent of RNase L (Chapter 3).

Two factors drove our hypothesis that NS4b innate immune antagonism likely includes an involvement in RNA processing. One is the extensively documented involvement of cellular 2H-PEs in diverse steps of RNA processing, including splicing (9, 34, 44). The second was our observation that NS4b IFN antagonism is dependent on its catalytic activity, suggesting its interaction with the IFN response goes beyond any protein-protein interaction (Fig 3.5). We previously described MERS-CoV NS4b as exhibiting 2',5' PDE activity (1), but the question of whether it can bind to and cleave other substrates remains under investigation. The AKAP7 PDE similarly binds to and cleaves the linear 2-5A molecule, but also binds cAMP (26, 27, 45). The eukaryotic 2H-PE USB1 exhibits 3',5' PDE activity and removes uridines and adenosines from the 3' end of the U6 snRNA (31, 34, 44). Assessing that NS4b might exhibit similar 3',5' exonuclease activity, we tested whether it accelerates mRNA decay, which could occur as a result of 3' deadenylation. My experiments testing this hypothesis did not demonstrate any effect of NS4b on mRNA turnover, and whether NS4b can target substrates other than 2-5A, such as 3',5' phosphodiester bonds, remains an area of active inquiry with our collaborator Robert Silverman of the Cleveland

Clinic. Should NS4b prove to have 3',5' PDE activity, it would be worthwhile to re-examine whether it can target mRNAs

Noting the demonstrated 2',5' PDE activity of MERS-CoV NS4b, we considered that it might act on 2',5' linked substrates other than 2-5A. One such cellular substrate is the intronic lariat formed as a byproduct of the splicing reaction (36). I found that intronic RNA is more abundant during MERS-NS4b<sup>H182R</sup> infection than during infection with WT MERS-CoV or MERS-NS4b<sup>NLSmut</sup> (Fig 4.4), specifically the sole intron from *IFIT2*, and the first intron from the much larger *DDX58* gene. One possible explanation is that NS4b disrupts splicing in some way and that the introns are retained within the mRNA. Retained introns within the gene body typically lead to nonsense mediated decay (NMD) of the mRNA (46-48), so in this scenario the *IFIT2* and *DDX58* mRNAs are unlikely to be translated. My attempts to quantify *IFIT2* and *DDX58* mRNAs with retained introns (or pre-mRNA) using primers spanning exon-intron boundaries were unsuccessful due to apparent low abundance of such transcripts, but this explanation for the increased intron signal during MERS-NS4b<sup>H182R</sup> infection seems unlikely. One reason for this is my inability to reliably quantify intron-containing mRNAs even during viral infection, in contrast with the robust signal obtained by using primers targeted solely within the intron. A second reason is that if intron retention explained the observation, it would mean mutation of an innate immune antagonist results in an increase in non-functional mRNA, while selective pressure seems more likely to result in a scenario wherein

NS4b mutation would lead to a more effective immune response. Nevertheless, it remains important that future studies be designed to test this possibility.

A second, more likely possibility, is that the elevated intron signal is due to slower lariat degradation during MERS-NS4b<sup>H182R</sup> infection than during infection with WT MERS-CoV or MERS-NS4b<sup>NLSmut</sup>. Lariat degradation is initiated by the cellular 2',5' PDE DBR1 (36, 37), but some recent evidence suggests a significant number of lariats can escape debranching and accumulate in the cytoplasm (37). The physiological consequence of circular RNA accumulation, intron-derived or not, remains unclear. However, it is widely recognized that the accumulation of unusual nucleic acid molecules can trigger a variety of antiviral pathways via sensors such as cGAS (49-51), RIG-I (52, 53), and MDA5 (54-56). It is possible that unusual accumulation of lariats may serve as a yet-uncharacterized signal or amplifier of innate immune activation, though such a hypothesis lacks preliminary supportive data and requires significant work to substantiate. Our ongoing efforts to identify a physiological impact of lariat accumulation and the role of NS4b in determining intron fate, before or after splicing, will be further discussed in the General Discussion (Chapter 5).

Although we have not yet elucidated the mechanisms of NS4b interactions with the IFN response, my work described in Chapter 3 and this chapter demonstrates a novel role for viral 2H-PEs. Notably, while NS4b has been previously described as inhibiting elements of the innate immune response other

than RNase L such as NF $\kappa$ B (43) and IFN induction (7, 8, 40, 57), a role for the NS4b catalytic PDE domain, or that of any viral 2H-PE, outside of antagonizing RNase L was previously unknown. Through the unpublished work described in this chapter I have generated preliminary mechanistic insights into this novel role, in that NS4b appears to affect the fate of host introns which is consistent with the recognized role of cellular 2H-PEs in RNA processing. Future work, discussed in Chapter 5, will focus on fully characterizing this interaction and exploring the consequences of lariat accumulation.

## References

1. **Thornbrough JM, Jha BK, Yount B, Goldstein SA, Li Y, Elliott R, Sims AC, Baric RS, Silverman RH, Weiss SR.** 2016. Middle East Respiratory Syndrome Coronavirus NS4b Protein Inhibits Host RNase L Activation. *mBio* **7**:e00258–16.
2. **Zhao L, Jha BK, Wu A, Elliott R, Ziebuhr J, Gorbalenya AE, Silverman RH, Weiss SR.** 2012. Antagonism of the Interferon-Induced OAS-RNase L Pathway by Murine Coronavirus ns2 Protein Is Required for Virus Replication and Liver Pathology. *Cell Host and Microbe* **11**:607–616.
3. **Zhang R, Jha BK, Ogden KM, Dong B, Zhao L, Elliott R, Patton JT, Silverman RH, Weiss SR.** 2013. Homologous 2',5'-phosphodiesterases from disparate RNA viruses antagonize antiviral innate immunity. *Proceedings of the National Academy of Sciences* **110**:13114–13119.
4. **Goldstein SA, Thornbrough JM, Zhang R, Jha BK, Li Y, Elliott R, Quiroz-Figueroa K, Chen AI, Silverman RH, Weiss SR.** 2016. Lineage A Betacoronavirus NS2 proteins and homologous Torovirus Berne pp1a-carboxyterminal domain are phosphodiesterases that antagonize activation of RNase L. *Journal of Virology* **JVI.02201–16**.
5. **Silverman RH.** 2007. Viral encounters with 2',5'-oligoadenylate synthetase and RNase L during the interferon antiviral response. *Journal of Virology* **81**:12720–12729.

6. **Silverman RH, Weiss SR.** 2014. Viral Phosphodiesterases That Antagonize Double-Stranded RNA Signaling to RNase L by Degrading 2-5A. *Journal of Interferon & Cytokine Research* **34**:455–463.
7. **Matthews KL, Coleman CM, van der Meer Y, Snijder EJ, Frieman MB.** 2014. The ORF4b-encoded accessory proteins of Middle East respiratory syndrome coronavirus and two related bat coronaviruses localize to the nucleus and inhibit innate immune signalling. *Journal of General Virology* **95**:874–882.
8. **Yang Y, Ye F, Zhu N, Wang W, Deng Y, Zhao Z, Tan W.** 2015. Middle East respiratory syndrome coronavirus ORF4b protein inhibits type I interferon production through both cytoplasmic and nuclear targets. *Sci Rep* **5**.
9. **Mazumder R, Iyer LM, Vasudevan S, Aravind L.** 2002. Detection of novel members, structure–function analysis and evolutionary classification of the 2H phosphoesterase superfamily. *Nucleic Acids Research* **30**:5229–5243.
10. **Sprinkle TJ.** 1989. 2',3'-cyclic nucleotide 3'-phosphodiesterase, an oligodendrocyte-Schwann cell and myelin-associated enzyme of the nervous system. *Crit Rev Neurobiol* **4**:235–301.
11. **Hofmann A, Tarasov S, Grella M, Ruvinov S, Nasr F, Filipowicz W, Wlodawer A.** 2002. Biophysical characterization of cyclic nucleotide phosphodiesterases. *Biochemical and Biophysical Research Communications* **291**:875–883.
12. **Mylykoski M, Kursula P.** 2017. Structural aspects of nucleotide ligand binding by a bacterial 2H phosphoesterase. *PLoS ONE* **12**:e0170355.
13. **Greer CL, Javor B, Abelson J.** 1983. RNA ligase in bacteria: formation of a 2',5' linkage by an *E. coli* extract. *Cell* **33**:899–906.
14. **Arn EA, Abelson JN.** 1996. The 2'-5' RNA Ligase of *Escherichia coli* PURIFICATION, CLONING, AND GENOMIC DISRUPTION. *Journal of Biological Chemistry* **271**:31145–31153.
15. **Kanai A, Sato A, Fukuda Y, Okada K, Matsuda T, Sakamoto T, Muto Y, Yokoyama S, Kawai G, Tomita M.** 2009. Characterization of a heat-stable enzyme possessing GTP-dependent RNA ligase activity from a hyperthermophilic archaeon, *Pyrococcus furiosus*. *RNA* **15**:420–431.
16. **Wolf YI, Kazlauskas D, Iranzo J, Lucía-Sanz A, Kuhn JH, Krupovic M, Dolja VV, Koonin EV.** 2018. Origins and Evolution of the Global RNA Virome. *mBio* **9**:e02329–18.
17. **Coyle MC, Elya CN, Bronski MJ, Eisen MB.** 2018. Entomophthovirus: An

insect-derived iflavirus that infects a behavior manipulating fungal pathogen of dipterans. *bioRxiv* 371526.

18. **Culver GM, Consaul SA, Tycowski KT, Filipowicz W, Phizicky EM.** 1994. tRNA splicing in yeast and wheat germ. A cyclic phosphodiesterase implicated in the metabolism of ADP-ribose 1“,2-”cyclic phosphate. *Journal of Biological Chemistry* **269**:24928–24934.
19. **Koonin EV, Gorbalenya AE.** 1990. Related domains in yeast tRNA ligase, bacteriophage T4 polynucleotide kinase and RNA ligase, and mammalian myelin 2“,3-”cyclic nucleotide phosphohydrolase revealed by amino acid sequence comparison. *FEBS Lett* **268**:231–234.
20. **Hofmann A, Zdanov A, Genschik P, Ruvinov S, Filipowicz W, Wlodawer A.** 2000. Structure and mechanism of activity of the cyclic phosphodiesterase of Appr>p, a product of the tRNA splicing reaction. *EMBO J* **19**:6207–6217.
21. **Kim H-J, Yi J-Y, Sung H-S, Moore DD, Jhun BH, Lee YC, Lee JW.** 1999. Activating Signal Cointegrator 1, a Novel Transcription Coactivator of Nuclear Receptors, and Its Cytosolic Localization under Conditions of Serum Deprivation. *Molecular and Cellular Biology* **19**:6323–6332.
22. **Jung D-J, Sung H-S, Goo Y-W, Lee HM, Park OK, Jung S-Y, Lim J, Kim H-J, Lee S-K, Kim TS, Lee JW, Lee YC.** 2002. Novel Transcription Coactivator Complex Containing Activating Signal Cointegrator 1. *Molecular and Cellular Biology* **22**:5203–5211.
23. **Torices S, Alvarez-Rodríguez L, Grande L, Varela I, Muñoz P, Pascual D, Balsa A, López-Hoyos M, Martínez-Taboada V, Fernández-Luna JL.** 2015. A Truncated Variant of ASCC1, a Novel Inhibitor of NF-κB, Is Associated with Disease Severity in Patients with Rheumatoid Arthritis. *The Journal of Immunology* **195**:5415–5420.
24. **Böhm J, Malfatti E, Oates E, Jones K, Brochier G, Boland A, Deleuze J-F, Romero NB, Laporte J.** 2018. Novel ASCC1 mutations causing prenatal-onset muscle weakness with arthrogryposis and congenital bone fractures. *J Med Genet jmedgenet*–2018–105390.
25. **Soll JM, Brickner JR, Mudge MC, Mosammaparast N.** 2018. RNA ligase-like domain in activating signal cointegrator 1 complex subunit 1 (ASCC1) regulates ASCC complex function during alkylation damage. *The Journal of Biological Chemistry* **293**:13524–13533.
26. **Gold MG, Smith FD, Scott JD, Barford D.** 2008. AKAP18 Contains a Phosphoesterase Domain that Binds AMP. *Journal of Molecular Biology* **375**:1329–1343.

27. **Gusho E, Zhang R, Jha BK, Thornbrough JM, Dong B, Gaughan C, Elliott R, Weiss SR, Silverman RH.** 2014. Murine AKAP7 Has a 2',5'-Phosphodiesterase Domain That Can Complement an Inactive Murine Coronavirus ns2 Gene. *mBio* **5**.
28. **Sui B, Huang J, Jha BK, Yin P, Zhou M, Fu ZF, Silverman RH, Weiss SR, Peng G, Zhao L.** 2016. Crystal structure of the mouse hepatitis virus ns2 phosphodiesterase domain that antagonizes RNase L activation. *J Gen Virol* **97**:880–886.
29. **Singh A, Redden JM, Kapiloff MS, Dodge-Kafka KL.** 2011. The large isoforms of A-kinase anchoring protein 18 mediate the phosphorylation of inhibitor-1 by protein kinase A and the inhibition of protein phosphatase 1 activity. *Mol Pharmacol* **79**:533–540.
30. **Diviani D, Dodge-Kafka KL, Li J, Kapiloff MS.** 2011. A-kinase anchoring proteins: scaffolding proteins in the heart. *Am J Physiol Heart Circ Physiol* **301**:H1742–53.
31. **Didychuk AL, Montemayor EJ, Carrocci TJ, DeLaitsch AT, Lucarelli SE, Westler WM, Brow DA, Hoskins AA, Butcher SE.** 2017. Usb1 controls U6 snRNP assembly through evolutionarily divergent cyclic phosphodiesterase activities. *Nat Commun* **8**:497.
32. **Mroczek S, Krwawicz J, Kutner J, Lazniewski M, Kuciński I, Ginalski K, Dziembowski A.** 2012. C16orf57, a gene mutated in poikiloderma with neutropenia, encodes a putative phosphodiesterase responsible for the U6 snRNA 3' end modification. *Genes & Development* **26**:1911–1925.
33. **Shchepachev V, Azzalin CM.** 2013. The Mpn1 RNA exonuclease: Cellular functions and implication in disease. *FEBS Lett* **587**:1858–1862.
34. **Nomura Y, Roston D, Montemayor EJ, Cui Q, Butcher SE.** 2018. Structural and mechanistic basis for preferential deadenylation of U6 snRNA by Usb1. *Nucleic Acids Research* **46**:11488–11501.
35. **Shchepachev V, Wischnewski H, Soneson C, Arnold AW, Azzalin CM.** 2015. Human Mpn1 promotes post-transcriptional processing and stability of U6atac. *FEBS Lett* **589**:2417–2423.
36. **Kim JW, Kim HC, Kim GM, Yang JM, Boeke JD, Nam K.** 2000. Human RNA lariat debranching enzyme cDNA complements the phenotypes of *Saccharomyces cerevisiae* dbr1 and *Schizosaccharomyces pombe* dbr1 mutants. *Nucleic Acids Research* **28**:3666–3673.
37. **Talhouarne GJS, Gall JG.** 2018. Lariat intronic RNAs in the cytoplasm of vertebrate cells. *Proc Natl Acad Sci USA* **115**:E7970–E7977.

38. **Scobey T, Yount BL, Sims AC, Donaldson EF, Agnihothram SS, Menachery VD, Graham RL, Swanstrom J, Bove PF, Kim JD, Grego S, Randell SH, Baric RS.** 2013. Reverse genetics with a full-length infectious cDNA of the Middle East respiratory syndrome coronavirus. *Proceedings of the National Academy of Sciences* **110**:16157–16162.
39. **Li Y, Banerjee S, Wang Y, Goldstein SA, Dong B, Gaughan C, Silverman RH, Weiss SR.** 2016. Activation of RNase L is dependent on OAS3 expression during infection with diverse human viruses. *Proc Natl Acad Sci USA* 201519657.
40. **Yang Y, Zhang L, Geng H, Deng Y, Huang B, Guo Y, Zhao Z, Tan W.** 2013. The structural and accessory proteins M, ORF 4a, ORF 4b, and ORF 5 of Middle East respiratory syndrome coronavirus (MERS-CoV) are potent interferon antagonists. *Protein & Cell* **4**:951–961.
41. **Sobell HM.** 1985. Actinomycin and DNA transcription. *Proc Natl Acad Sci USA* **82**:5328–5331.
42. **Leclerc GJ, Leclerc GM, Barredo JC.** 2002. Real-time RT-PCR analysis of mRNA decay: half-life of Beta-actin mRNA in human leukemia CCRF-CEM and Nalm-6 cell lines. *Cancer Cell Int* **2**:1.
43. **Canton J, Fehr AR, Fernandez-Delgado R, Gutierrez-Alvarez FJ, Sanchez-Aparicio MT, Garcia-Sastre A, Perlman S, Enjuanes L, Sola I.** 2018. MERS-CoV 4b protein interferes with the NF- $\kappa$ B-dependent innate immune response during infection. *PLOS Pathogens* **14**:e1006838.
44. **Hilcenko C, Simpson PJ, Finch AJ, Bowler FR, Churcher MJ, Jin L, Packman LC, Shlien A, Campbell P, Kirwan M, Dokal I, Warren AJ.** 2013. Aberrant 3' oligoadenylation of spliceosomal U6 small nuclear RNA in poikiloderma with neutropenia. *Blood* **121**:1028–1038.
45. **Frasher IDC, Tavalin SJ, Lester LB, Langeberg LK, Westphal AM, Dean RA, Marrion NV, Scott JD.** 1998. A novel lipid-anchored A-kinase Anchoring Protein facilitates cAMP-responsive membrane events. *The EMBO Journal* **17**:2261–2272.
46. **Jacob AG, Smith CWJ.** 2017. Intron retention as a component of regulated gene expression programs. *Human Genetics* **136**:1043–1057.
47. **Wong JJ-L, Au AYM, Ritchie W, Rasko JEJ.** 2015. Intron retention in mRNA: No longer nonsense. *Bioessays* **38**:41–49.
48. **Braunschweig U, Barbosa-Morais NL, Pan Q, Nachman EN, Alipanahi B, Gonatopoulos-Pournatzis T, Frey B, Irimia M, Blencowe BJ.** 2014. Widespread intron retention in mammals functionally tunes transcriptomes. *Genome Research* **24**:1774–1786.

49. **Li X-D, Wu J, Gao D, Wang H, Sun L, Chen ZJ.** 2013. Pivotal roles of cGAS-cGAMP signaling in antiviral defense and immune adjuvant effects. *Science* **341**:1390–1394.
50. **Sun L, Wu J, Du F, Chen X, Chen ZJ.** 2013. Cyclic GMP-AMP synthase is a cytosolic DNA sensor that activates the type I interferon pathway. *Science* **339**:786–791.
51. **Du M, Chen ZJ.** 2018. DNA-induced liquid phase condensation of cGAS activates innate immune signaling. *Science* **361**:704–709.
52. **Yoneyama M, Kikuchi M, Natsukawa T, Shinobu N, Imaizumi T, Miyagishi M, Taira K, Akira S, Fujita T.** 2004. The RNA helicase RIG-I has an essential function in double-stranded RNA-induced innate antiviral responses. *Nat Immunol* **5**:730–737.
53. **Ren X, Linehan MM, Iwasaki A, Pyle AM.** 2019. RIG-I Selectively Discriminates against 5'-Monophosphate RNA. *Cell Reports* **26**:2019–2027.e4.
54. **Kang D-C, Gopalkrishnan RV, Wu Q, Jankowsky E, Pyle AM, Fisher PB.** 2002. mda-5: An interferon-inducible putative RNA helicase with double-stranded RNA-dependent ATPase activity and melanoma growth-suppressive properties. *Proc Natl Acad Sci USA* **99**:637–642.
55. **Bruns AM, Horvath CM.** 2015. LGP2 synergy with MDA5 in RLR-mediated RNA recognition and antiviral signaling. *Cytokine* **74**:198–206.
56. **Yoneyama M, Kikuchi M, Matsumoto K, Imaizumi T, Miyagishi M, Taira K, Foy E, Loo Y-M, Gale M, Akira S, Yonehara S, Kato A, Fujita T.** 2005. Shared and unique functions of the DExD/H-box helicases RIG-I, MDA5, and LGP2 in antiviral innate immunity. *J Immunol* **175**:2851–2858.
57. **Chu DKW, Hui KPY, Perera RAPM, Miguel E, Niemeyer D, Zhao J, Channappanavar R, Dudas G, Oladipo JO, Traore A, Fassi-Fihri O, Ali A, Demissié GF, Muth D, Chan MCW, Nicholls JM, Meyerholz DK, Kuranga SA, Mamo G, Zhou Z, So RTY, Hemida MG, Webby RJ, Roger F, Rambaut A, Poon LLM, Perlman S, Drosten C, Chevalier V, Peiris M.** 2018. MERS coronaviruses from camels in Africa exhibit region-dependent genetic diversity. *Proceedings of the National Academy of Sciences* **115**:3144–3149.

## **Chapter 5**

# **GENERAL DISCUSSION**

## Introduction

Through my thesis work I have both expanded the Weiss laboratory's previous contributions to our understanding of virus-RNase L interactions, and expanded our knowledge of how viral phosphodiesterases regulate antiviral responses more broadly. RNase L-mediated cleavage of viral and cellular RNA is a long-known, critical mechanism of antiviral defense against such diverse pathogens as picornaviruses, orthomyxoviruses, reoviruses, togaviruses, flaviviruses, poxviruses, and retroviruses (1). Not unexpectedly, many of these viruses encode proteins that potently inhibit RNase L activation such as poxvirus E3L and D9 (2-4), influenza A virus NS1 (5), and Theiler's murine encephalomyelitis L\* (6, 7). Other viruses targeted by RNase L, such as Sindbis virus and West Nile virus lack a known RNase L antagonist and their replication is significantly enhanced when RNase L is not present (8-10). Coronavirus interactions with the OAS-RNase L pathway were largely unknown prior to a 2012 Weiss laboratory study by Zhao *et. al.* (11). The mouse hepatitis virus (MHV) NS2 protein, the prototypical coronavirus RNase L antagonist, was computationally assessed as a phosphodiesterase in 2002 (12), though its importance for MHV innate immune antagonism was discovered later (13) and its specific inhibition of RNase L later still (11). This characterization included biochemical studies that revealed MHV NS2 as an unusual 2',5'-specific phosphodiesterase (11), setting the stage for the continued studies of coronavirus-RNase L interactions that constituted my early dissertation studies.

## Coronavirus phosphodiesterases and RNase L

Chapter 2 of this thesis describes work involving several members of the Weiss laboratory that significantly expand the scope of interactions between coronaviruses and the OAS-RNase L pathway. The first such interaction to be characterized was that mediated by MHV NS2. Initially, NS2 was believed dispensable for coronavirus replication (14) due to studies being conducted in cell lines that generally lack effective antiviral responses, or in the central nervous system where RNase L is also not active. Once recombinant MHV studies were conducted in bone marrow-derived macrophages (BMMs) with robust antiviral responses, it became clear that NS2 is an essential protein in the face of the innate immune response (15), with the OAS-RNase L pathway as its specific target (11). It is notable that the essential nature of NS2 is not ubiquitous among different sites of infection. NS2 is particularly important for viral replication and pathogenesis in the liver (13) where both Kupffer cells (liver resident macrophages) and liver sinusoidal endothelial cells mount robust OAS-RNase L responses, but not in hepatocytes, which do not (16). Similarly, NS2 is entirely unnecessary for MHV replication and pathogenesis in the brain (13), likely due to low basal levels of OAS expression (17, 18). These discoveries highlight the organ and cell type-specific nature of viral virulence factors, and demonstrate why some *in vitro* systems may not recapitulate natural infection or reveal important virus-host interactions. Additionally, important viral genes may become non-essential if viruses undergo a host-switch that results in tropism for a cell type that lacks robust RNase L activity. Such cross-species transmissions are

best understood in the context of zoonotic infections (19), but have surely played a significant role throughout the evolutionary history of RNA viruses (20, 21). Such a dynamic may underlie observations about the NS2 protein of porcine hemagglutinating encephalomyelitis virus (PHEV), which seems to have lost some of its catalytic activity as described in Chapter 2, and the total loss of NS2 by HCoV-HKU1.

The work described in Chapter 2 strongly suggests that coronavirus PDEs are significant factors in promoting viral replication and fitness, given their near fixation in the *Embecovirus* genome. The identical position of the PDE in these genomes supports the idea that the gene was acquired a single time in the common ancestor of these viruses. The absence of a PDE NS2 gene in HCoV-HKU1 further supports the importance of this gene, suggesting the gene may be disposed of if it becomes unnecessary. It is interesting, however, that HCoV-OC43 and HCoV-HKU1, both respiratory viruses that infect the upper airway, differ in the presence of an NS2 gene. The difference may well be explained by differing cell tropisms that have not yet been identified. Studies using primary human airway epithelial cell cultures have found that HCoV-OC43 and HCoV-HKU1 both exhibit a tropism for ciliated cells (22, 23), but it still is not known if they have identical tropisms during natural infection. We do know from studies of MHV that cell types differ dramatically in their ability to activate RNase L (13, 16).

A critical outstanding question concerns what role the PDEs described in Chapter 2 play during natural infection. The chimeric MHV system we used to study these proteins is powerful but can only determine the capacity of PDEs to antagonize RNase L, not tell us how important the PDE is to promoting viral replication in their native context. The presence of a viral PDE alone is not sufficient to make inferences about the importance of the protein. PHEV, for example, encodes an NS2 PDE, but the PHEV NS2 is significantly less active in degrading 2-5A than the PDEs of MHV, HCoV-OC43 or Berne virus (BEV) despite no defects being obvious from its amino acid sequence (24). This suggests that NS2 is likely not required to promote viral fitness in PHEV target cells, while the presence of an RNase L antagonist in transmissible gastroenteritis virus (TGEV), indicates that porcine hosts do mount an RNase L response in the cells targeted by this virus (25). Fully characterizing the role of the PDEs described in Chapter 2 will require the development of infectious clones, *in vitro* systems similarly powerful to the use of macrophages for studies of MHV, and perhaps where appropriate, animal models. An infectious clone does exist for HCoV-OC43, but the ATCC isolate it is based on is highly neurotropic following extensive serial passage in suckling mice and replicates poorly in human airway-derived cell lines (data not shown) (26, 27).

In contrast to our work with the viruses described in Chapter 2, we characterized the role of MERS-CoV NS4b in its native context. Thanks to the rapid development of a MERS-CoV infectious clone and a collaboration with Dr.

Ralph Baric (28), we were able to use recombinant MERS-NS4b<sup>H182R</sup> to study the interaction between this protein and the OAS-RNase L pathway (29). Notably, the PDEs encoded by MERS-CoV and similar viruses of the *Betacoronavirus* subgenus *Merbecovirus* appear evolutionarily distinct from the other viral PDEs studied by the Weiss laboratory, as they contain a longer N-terminus with a nuclear localization sequence (NLS), a shorter C-terminus, and are situated differently within the genome. An obvious possibility given these differences is that the *Merbecovirus* and *Embecovirus* PDEs were acquired independently from different hosts following the diversification of the *Betacoronavirus* genus. It is unknown whether these diverse viral PDEs share a host PDE ancestor and diverged following viral acquisition, or derive from different ancestors. Another possibility is that an ancestral virus in one subgenus acquired a host PDE that then diverged following horizontal gene transfer to an ancestral virus of the other subgenus. Unfortunately, the nucleotide and amino acid sequences of the viral PDEs are so highly divergent that constructing phylogenetic trees to identify host and viral ancestors is impossible. Obtaining additional high resolution structures of viral and host LigT-like 2H-PEs may offer a different approach to answering these questions. To date, only the structures of the cellular 2H-PEs AKAP18 (30) and USB1 (31) have been solved, and among viral 2H-PEs, only the rotavirus VP3 (32, 33) and MHV NS2 (34) structures are known. Structural information for other LigT-like 2H-PE family members, while perhaps not as informative as phylogenetic trees would be, could provide additional information on evolutionary relationships between cellular and viral proteins.

The fixation of ORF4b genes among MERS-CoV-like viruses suggest that, like the NS2 protein of MHV-like viruses, the NS4b protein is important for promoting viral fitness. As with the NS2 proteins, however, differences in NS4b proteins encoded by various MERS-CoV-like viruses suggest host or cell-type specific requirements for NS4b. Specifically, a MERS-CoV-like virus identified in European hedgehogs (35) encodes an N-terminal truncated NS4b that lacks an NLS. The ancestral merbecovirus presumably contained the NLS present in the NS4b of all other extant MERS-CoV-like viruses, and evidence suggests the subgenus originated in bats (36). It is probable that the selective pressure for nuclear localization of NS4b was relieved upon the establishment of this virus in a hedgehog host, while the cytoplasmic function of antagonizing RNase L remains necessary. As with PHEV, it seems more likely that the hedgehog coronavirus infects a cell type in which some PDE function is unnecessary, rather than there being a dramatic difference in innate immune repertoire.

These subtle differences between *Merbecovirus* PDEs may offer opportunities for further teasing apart virus-host interactions and how such interactions can change when a virus enters a new ecological space. More immediately interesting to us, however, has been testing the hypothesis that MERS-CoV NS4b and its orthologs mediates additional functions beyond antagonism of OAS-RNase L, a hypothesis rooted in the clear differences between NS4b and MHV NS2. In testing this hypothesis, we have contributed to

an emerging paradigm shift about the function of viral phosphodiesterases, while major mechanistic questions remain unresolved.

### **MERS-CoV NS4b – Phosphodiesterases beyond RNase L**

Aside from my work growing our knowledge of *Embecovirus* NS2 proteins, I have worked to expand our understanding of the role of viral 2H-PEs more broadly in countering innate immune responses. Following the initial discovery that MERS-CoV NS4b was a putative PDE by Dr. Joshua Thornbrough, we quickly recognized differences compared to MHV NS2 that argued for a role beyond antagonizing RNase L. NS4b nuclear localization and description of its NLS had been previously reported (37, 38), but a nuclear viral PDE remained a novel concept. Our collaboration with Dr. Ralph Baric at the University of North Carolina, who engineered and recovered the recombinant MERS-CoV variants I have used (28, 29), MERS-NS4b<sup>H182R</sup> and MERS-NS4b<sup>NLSmut</sup>, has been critical to studying these presumed novel functions.

Although mechanistic questions remain to be answered, I have demonstrated that NS4b does indeed play a role during infection previously unknown for viral 2H-PEs. Mutation of either the NS4b catalytic site or its NLS results in increased activation of the interferon (IFN) antiviral response uncoupled from any activation or inhibition of RNase L, while making the equivalent mutation in MHV NS2 has no effect on IFN gene expression during infection of the same cell type (Fig 3.6). Another study has shown that NS4b inhibits NFκB

nuclear translocation (39), indicating that NS4b is truly a multifunctional antagonist of the innate immune response with an expansive repertoire of functions compared to the other viral PDEs the Weiss laboratory has studied and characterized.

As NS4b exhibits unique functions for a viral PDE, resolving the outstanding mechanistic questions will cement a paradigm shift regarding the function of these proteins. My work in this area provides some preliminary insights into at least some of its underlying mechanisms mediating antagonism of the IFN-driven antiviral response. Some studies have suggested that direct interactions with host proteins underlie NS4b innate immune antagonism. One study, for example, demonstrates that the NS4b NLS binds the same importin- $\alpha$  protein as NF $\kappa$ B, thus competitively inhibiting its nuclear import (39). It is possible that NS4b similarly prevents IRF3 nuclear import via cytoplasmic protein-protein interaction, which has some support in published work (38, 40). Other data, including ours (Fig 3.6) suggest NS4b inhibits IFN activation in the nucleus, downstream of IRF3 (37, 40) through a yet-unknown mechanism. Uniquely, our data suggests that IFN antagonism by NS4b is mediated at least in part by its catalytic activity (Fig 3.6), though we cannot determine whether this occurs in the nucleus or cytoplasm. In fact, our observation of elevated IFN transcript levels induced by MERS-NS4b<sup>H182R</sup> and MERS-NS4b<sup>NLSmut</sup>, though of similar magnitude, may be a result of distinct mechanisms.

Preliminary data suggests that NS4b, through its catalytic activity, reduces the abundance of intronic RNA during infection (Fig 4.4) which is likely though not certain to occur in the nucleus, as intronic lariats have been observed to accumulate in the cytoplasm of mammalian cells (41). The most obvious confounding factor in these data is that if NS4b mediates this effect in the nucleus, then mutation of the NLS should produce the same effect as mutation of the catalytic site, but does not. Two possibilities might explain this problem. The first is the possibility that despite mutation of the NLS the nuclear concentration of NS4b, while reduced, remains sufficiently high to reduce intronic RNA abundance. Two published studies suggest that mutation of the downstream basic motif (KRR) of the NS4b NLS is less potent at abrogating nuclear localization than mutation of the first motif (RKR) (37, 39). I have not done quantitative analysis of NS4b localization, but these reports are consistent with my general observations. Nevertheless, this remains a worthwhile line of inquiry as mechanistic studies of NS4b proceed. The second possibility may be that while NS4b normally acts to reduce the abundance of intronic RNA in the nucleus, that when NS4b is excluded from the nucleus, such RNA escapes to the cytoplasm, where it might still be targeted by NS4b. Mutating the first basic motif of the NS4b NLS is impossible in recombinant MERS-CoV without inducing non-synonymous mutation in NS4a or splitting ORF4a and ORF4b as was done in a recent study (39), but which we chose not to do with the understanding that NS4b expressed by MERS-NS4b<sup>NLSmut</sup> might not be entirely excluded from the nucleus. One possible approach for resolving this issue would be to develop a

system in which different NS4b constructs are expressed outside the context of infection but which would recapitulate the observation of increased intronic signal upon mutation of the NS4b catalytic site. In such a system, various NS4b constructs could be expressed such as mutation of the first basic motif or mutations that enhance the strength of the NLS alone or in combination with the catalytic mutation. I attempted to generate A549 cell lines stably or inducibly expressing some of these proteins, but was not able to detect expression of NS4b. It is possible that another cell line would be more amenable to generating such a system.

The most significant outstanding question is what accounts for the increased intronic RNA when MERS-CoV NS4b is catalytically inactive. I have made this observation from introns of two interferon stimulated genes (ISGs), *IFIT2* and *DDX58*, which encodes the dsRNA sensor RIG-I. *IFIT2* has a single intron and I have confirmed this phenomenon with multiple primer sets, while *DDX58* is a large gene with over a dozen introns, the first of which is represented in my data. Our preliminary hypothesis is that the increased signal reflects a greater abundance of intronic lariats, suggesting wild-type NS4b enhances lariat turnover (Fig 5.1). We find this possibility particularly intriguing because of the 2',5' phosphodiester bond that forms the lariat structure (41-43). 2',5' phosphodiester bonds are relatively rare, with the two most obvious occurrences being in 2-5A and intronic lariats.

Determining whether there is in fact an accumulation of lariats during MERS-NS4b<sup>H182R</sup> infection is a necessary and immediate priority. Initially, these experiments should focus on *IFIT2* and *DDX58*. The first *GAPDH* intron does not

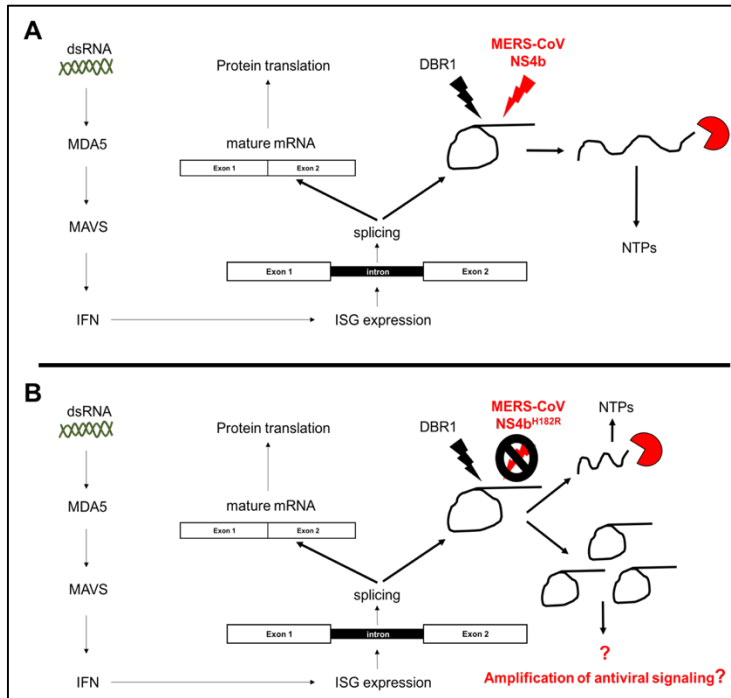


**Figure 5.1 Hypothesized model for NS4b acceleration of lariat debranching.** A) We hypothesize that WT NS4b accelerates debranching to prevent the accumulation of lariats during infection, which may induce increased transcriptional activity B) In this scenario NS4b<sup>H182R</sup> fails to accelerate debranching, leading to an accumulation of lariats due to escape from or saturation of the constitutive debranching machinery. The aberrant accumulation of nucleic acids may promote antiviral signaling, particularly if they escape to the cytoplasm.

exhibit increased abundance due to NS4b catalytic mutation, but otherwise trying to predict which introns might be affected and should therefore be studied in a targeted fashion is exceedingly cumbersome.

I have attempted to determine whether circular *IFIT2* intron accumulates during MERS-NS4b<sup>H182R</sup>

infection by northern blot, as circular RNAs, like circular DNA, will appear on a gel to be larger than its actual size (41). However, I was not able to detect even the mature *IFIT2* mRNA, likely to be more abundant than any intronic *IFIT2* mRNA, presumably because during MERS-CoV infection it remains a low abundance transcript. As an alternative and likely more sensitive approach, I propose RNase R digestion (41) of linear RNA from A549<sup>DPP4</sup> cells infected with

WT MERS-CoV, MERS-NS4b<sup>H182R</sup>, and MERS-NS4b<sup>NLSmut</sup>, followed by the same RT-qPCR analysis as described in Figure 4.4. If the enhanced intronic RNA signal is due to increased abundance of *IFIT2*-derived circular intronic RNA, this signal should persist even after RNase R digestion. Should we obtain this finding, high-throughput RNA sequencing would enable a more complete understanding of how inactivation of the NS4b catalytic site affects intron turnover, including determining whether the accumulation of intronic RNA represents persistent lariats or re-circularized, debranched introns (41, 44).

Biochemical approaches must also be utilized in testing this hypothesis and would benefit from extensive collaboration as they fall outside the Weiss laboratory area of expertise. We have previously demonstrated that NS4b has 2',5' phosphodiesterase activity, but it is unclear whether it is able to debranch introns, a critical piece of information towards supporting or refuting our hypothesis. Therefore, NS4b could be included in an *in vitro* debranching assay with the cellular debranching enzyme DBR1 as a positive control (45). Additionally, solving the NS4b structure in complex with known (2-5A) or possible (lariat) substrates would prove informative as to whether NS4b has the capacity to debranch introns (46) as DBR1, a phosphoesterase of a distinct family, does. Although no 2H-PE has yet been shown to bind and debranch introns, to our knowledge no one has looked, the cellular 2H-PE USB1 sets a clear precedent for such proteins to associate with components of the spliceosome.

The possible biological significance of intron accumulation is difficult to predict. Although the field studying stable intronic RNAs is expanding, there is still little agreement on their function, or if there is one. In the context of virus infection, we can presume that if MERS-CoV has acquired a means of preventing lariat accumulation, then such accumulation is likely to prove detrimental to the virus in some way. The accumulation of unusual types of nucleic acid in unexpected cellular compartments is a classic trigger of antiviral responses. Examples include activation of cGAS by cytoplasmic DNA of mitochondrial or viral origin (47-50), and of RIG-I and MDA-5 by cytoplasmic dsRNA (51, 52). With some evidence now available that introns which escape debranching by the endogenous cellular machinery can accumulate in the cytoplasm (41), it is possible to consider that such accumulation might trigger or enhance antiviral responses (Fig 5.1). However, the literature surrounding this remains limited and our data is preliminary. Much work remains to be done before any conclusions should be considered.

A second possibility, in contrast to the hypothesis that NS4b mutation slows intron turnover, is that the elevated intron signal is due to intron retention. Intron retention is a well-recognized mechanism of gene expression and translational regulation (53-55). Typically, intron retention between exons will result in nonsense mediated decay (NMD) of the mRNA, which can regulate protein levels post-transcriptionally (55). In contrast, intron retention in other regions of an mRNA, such as in untranslated regions, can actually enhance

translation (56). Since the increased intron signal from *IFIT2* and *DDX58* comes from an intron between exons, if it is due to a failure to excise the intron during splicing the mRNA is likely directed towards degradation by NMD. I have attempted to quantitatively assay for intron retention by RT-qPCR, but low abundance of transcripts containing an intact exon-intron junction has precluded success so far. It may be possible to induce sufficiently high levels of *IFIT2* or *DDX58* pre-mRNA by stimulation with high levels of IFN, but prospects for quantifying such transcripts during MERS-CoV infection remain remote. The best opportunity to determine whether mutation of NS4b results in more frequent intron retention will be during analysis of the RNA sequencing experiment described above using established computational pipelines for quantifying intron retention (44). If my data does reflect intron retention, it would seem likely this results in a higher percentage of less functional ISG mRNA, and therefore a dampened innate immune response. Given that NS4b is an innate immune antagonists, I would expect that mutation of NS4b would result in a more effective antiviral response. This is one reason I consider it more likely that NS4b participates in intron turnover, rather than promoting correct splicing of cellular mRNAs, including those transcribed from antiviral genes.

Conducting the experiments described above will not be exhaustive, as even if our hypothesis is correct new questions and challenges will surely arise. However, this should constitute a roadmap for pushing forward with the exploration of novel viral phosphodiesterase interactions with the host. One

critically important question is not addressed because we lack preliminary data supporting any particular hypothesis. Specifically, we still do not know how NS4b inhibits the expression of *IFNL1*. That it does so is widely reported in the literature (37, 38, 40, 57) but we uniquely found that it does so via its catalytic activity. It is possible that, at least in the case of MERS-NS4b<sup>H182R</sup>, the increased *IFNL1* transcript abundance is actually downstream of intron accumulation, but support for such a mechanism requires more experimental evidence of intron accumulation during MERS-NS4b<sup>H182R</sup> infection and of such accumulation triggering antiviral signaling. It has previously been reported that nuclear NS4b blocks IFN gene expression downstream of IRF3 activation (40). The mechanism for doing so is unknown. Although I did not detect IRF3 activation during MERS-CoV infection there is likely a low level of activation underlying the modest IFN expression that does occur. There also remains the issue that the full picture of NS4b interactions with the host antiviral response continues to increase in complexity. It has now been identified during infection as an RNase L antagonist (29), an inhibitor of NFκB nuclear translocation (39), and an IFN antagonist (Chapter 3) (57). Additional layers of complexity may be surprising, but are supported by preliminary data and can only be demonstrated or dispensed with through further experimentation. These experiments have the potential to mechanistically characterize an entirely novel function for viral phosphodiesterases, expanding our understanding of how viruses interact with their hosts using host genes repurposed to their own ends.

## Conclusion

The work described in this thesis covers a broad array of virus-host interactions mediated by viral phosphodiesterases. The understanding of these proteins as modulators of innate immunity has accelerated over the last decade after the prototype, MHV NS2, was initially considered dispensable (14). NS2 was computationally characterized in 2002 (12), but its full importance has only been recognized in a series of much later studies (11, 13, 16). A parallel body of work has begun to illuminate the function of cellular 2H-PEs in intracellular signaling (30, 58) and RNA processing (31, 59-61). I have been able to expand the range of viral PDEs known to interact with OAS-RNase L (24) and initiated what may develop into a paradigm shift in the range of known functions mediated by these proteins. We have shown for the first time that viral phosphodiesterase activity modulates an element of the innate immune response apart from the OAS-RNase L pathway. Yet, much opportunity remains for elucidating potential interactions and mechanisms underlying this phenomenon. These opportunities and the potential experiments described herein can serve as the basis of continued research into this previously unrecognized role of 2H-PEs. In addition, fundamental questions about intron fate and its biological consequences may be addressed as well. Therefore, the work described in this thesis has both advanced our scientific knowledge of coronavirus-host interactions and generated even more new questions in this area, creating exciting prospects for future research.

## References

1. **Silverman RH.** 2007. Viral encounters with 2',5'-oligoadenylate synthetase and RNase L during the interferon antiviral response. *Journal of Virology* **81**:12720–12729.
2. **Rivas C, Gil J, Mělková Z, Esteban M, Díaz-Guerra M.** 1998. Vaccinia Virus E3L Protein Is an Inhibitor of the Interferon (IFN)-Induced 2-5A Synthetase Enzyme. *Virology* **243**:406–414.
3. **Liu S-W, Katsafanas GC, Liu R, Wyatt LS, Moss B.** 2015. Poxvirus Decapping Enzymes Enhance Virulence by Preventing the Accumulation of dsRNA and the Induction of Innate Antiviral Responses. *Cell Host and Microbe* **17**:320–331.
4. **Liu R, Moss B.** 2016. Opposing Roles of Double-Stranded RNA Effector Pathways and Viral Defense Proteins Revealed with CRISPR-Cas9 Knockout Cell Lines and Vaccinia Virus Mutants. *Journal of Virology* **90**:7864–7879.
5. **Min JY, Krug RM.** 2006. The primary function of RNA binding by the influenza A virus NS1 protein in infected cells: Inhibiting the 2'-5' oligo (A) synthetase/RNase L pathway. *Proc Natl Acad Sci USA* **103**:7100–7105.
6. **Drappier M, Jha BK, Stone S, Elliott R, Zhang R, Vertommen D, Weiss SR, Silverman RH, Michiels T.** 2018. A novel mechanism of RNase L inhibition: Theiler's virus L\* protein prevents 2-5A from binding to RNase L. *PLOS Pathogens* **14**:e1006989.
7. **Sorgeloos F, Jha BK, Silverman RH, Michiels T.** 2013. Evasion of antiviral innate immunity by Theiler's virus L\* protein through direct inhibition of RNase L. *PLOS Pathogens* **9**:e1003474.
8. **Samuel MA, Whitby K, Keller BC, Marri A, Barchet W, Williams BRG, Silverman RH, Gale M, Diamond MS.** 2006. PKR and RNase L contribute to protection against lethal West Nile Virus infection by controlling early viral spread in the periphery and replication in neurons. *Journal of Virology* **80**:7009–7019.
9. **Scherbik SV, Paranjape JM, Stockman BM, Silverman RH, Brinton MA.** 2006. RNase L plays a role in the antiviral response to West Nile virus. *Journal of Virology* **80**:2987–2999.
10. **Li Y, Banerjee S, Wang Y, Goldstein SA, Dong B, Gaughan C, Silverman RH, Weiss SR.** 2016. Activation of RNase L is dependent on OAS3 expression during infection with diverse human viruses.

Proc Natl Acad Sci USA 2015;112:19657.

11. **Zhao L, Jha BK, Wu A, Elliott R, Ziebuhr J, Gorbalenya AE, Silverman RH, Weiss SR.** 2012. Antagonism of the Interferon-Induced OAS-RNase L Pathway by Murine Coronavirus ns2 Protein Is Required for Virus Replication and Liver Pathology. *Cell Host and Microbe* **11**:607–616.
12. **Mazumder R, Iyer LM, Vasudevan S, Aravind L.** 2002. Detection of novel members, structure–function analysis and evolutionary classification of the 2H phosphoesterase superfamily. *Nucleic Acids Research* **30**:5229–5243.
13. **Roth-Cross JK, Stokes H, Chang G, Chua MM, Thiel V, Weiss SR, Gorbalenya AE, Siddell SG.** 2009. Organ-specific attenuation of murine hepatitis virus strain A59 by replacement of catalytic residues in the putative viral cyclic phosphodiesterase ns2. *Journal of Virology* **83**:3743–3753.
14. **Schwarz B, Routledge E, Siddell SG.** 1990. Murine coronavirus nonstructural protein ns2 is not essential for virus replication in transformed cells. *Journal of Virology* **64**:4784–4791.
15. **Roth-Cross JK, Stokes H, Chang G, Chua MM, Thiel V, Weiss SR, Gorbalenya AE, Siddell SG.** 2009. Organ-Specific Attenuation of Murine Hepatitis Virus Strain A59 by Replacement of Catalytic Residues in the Putative Viral Cyclic Phosphodiesterase ns2. *Journal of Virology* **83**:3743–3753.
16. **Li Y, Weiss SR.** 2016. Antagonism of RNase L Is Required for Murine Coronavirus Replication in Kupffer Cells and Liver Sinusoidal Endothelial Cells but Not in Hepatocytes. *Journal of Virology* **90**:9826–9832.
17. **Zhao L, Birdwell LD, Wu A, Elliott R, Rose KM, Phillips JM, Li Y, Grinspan J, Silverman RH, Weiss SR.** 2013. Cell-Type-Specific Activation of the Oligoadenylate Synthetase-RNase L Pathway by a Murine Coronavirus. *Journal of Virology* **87**:8408–8418.
18. **Birdwell LD, Zalinger ZB, Li Y, Wright PW, Elliott R, Rose KM, Silverman RH, Weiss SR.** 2016. Activation of RNase L by Murine Coronavirus in Myeloid Cells Is Dependent on Basal Oas Gene Expression and Independent of Virus-Induced Interferon. *Journal of Virology* **90**:3160–3172.
19. **Geldenhuys M, Mortlock M, Weyer J, Bezuidt O, Seamark ECJ, Kearney T, Gleasner C, Erkkila TH, Cui H, Markotter W.** 2018. A metagenomic viral discovery approach identifies potential zoonotic

- and novel mammalian viruses in Neoromicia bats within South Africa. PLoS ONE 13:e0194527.
20. **Wolf YI, Kazlauskas D, Iranzo J, Lucía-Sanz A, Kuhn JH, Krupovic M, Dolja VV, Koonin EV.** 2018. Origins and Evolution of the Global RNA Virome. *mBio* 9:e02329–18.
  21. **Shi M, Lin X-D, Chen X, Tian J-H, Chen L-J, Li K, Wang W, Eden J-S, Shen J-J, Liu L, Holmes EC, Zhang Y-Z.** 2018. The evolutionary history of vertebrate RNA viruses. *Nature*.
  22. **Dijkman R, Jebbink MF, Koekkoek SM, Deijs M, Jonsdottir HR, Molenkamp R, Ieven M, Goossens H, Thiel V, van der Hoek L.** 2013. Isolation and Characterization of Current Human Coronavirus Strains in Primary Human Epithelial Cell Cultures Reveal Differences in Target Cell Tropism. *Journal of Virology* 87:6081–6090.
  23. **Pyrk K, Sims AC, Dijkman R, Jebbink M, Long C, Deming D, Donaldson E, Vabret A, Baric R, van der Hoek L, Pickles R.** 2010. Culturing the unculturable: human coronavirus HKU1 infects, replicates, and produces progeny virions in human ciliated airway epithelial cell cultures. *Journal of Virology* 84:11255–11263.
  24. **Goldstein SA, Thornbrough JM, Zhang R, Jha BK, Li Y, Elliott R, Quiroz-Figueroa K, Chen AI, Silverman RH, Weiss SR.** 2016. Lineage A Betacoronavirus NS2 proteins and homologous Torovirus Berne pp1a-carboxyterminal domain are phosphodiesterases that antagonize activation of RNase L. *Journal of Virology* JVI.02201–16.
  25. **Cruz JLG, Sola I, Becares M, Alberca B, Plana J, Enjuanes L, Zuniga S.** 2011. Coronavirus Gene 7 Counteracts Host Defenses and Modulates Virus Virulence. *PLOS Pathogens* 7:1–25.
  26. **Butler N, Pewe L, Trandem K, Perlman S.** 2006. Murine encephalitis caused by HCoV-OC43, a human coronavirus with broad species specificity, is partly immune-mediated. *Virology* 347:410–421.
  27. **Jacomy H, Talbot PJ.** 2003. Vacuolating encephalitis in mice infected by human coronavirus \OC43\. *Virology* 315:20–33.
  28. **Scobey T, Yount BL, Sims AC, Donaldson EF, Agnihothram SS, Menachery VD, Graham RL, Swanstrom J, Bove PF, Kim JD, Grego S, Randell SH, Baric RS.** 2013. Reverse genetics with a full-length infectious cDNA of the Middle East respiratory syndrome coronavirus. *Proceedings of the National Academy of Sciences* 110:16157–16162.
  29. **Thornbrough JM, Jha BK, Yount B, Goldstein SA, Li Y, Elliott R,**

- Sims AC, Baric RS, Silverman RH, Weiss SR.** 2016. Middle East Respiratory Syndrome Coronavirus NS4b Protein Inhibits Host RNase L Activation. *mBio* **7**:e00258–16.
30. **Gold MG, Smith FD, Scott JD, Barford D.** 2008. AKAP18 Contains a Phosphoesterase Domain that Binds AMP. *Journal of Molecular Biology* **375**:1329–1343.
31. **Hilcenko C, Simpson PJ, Finch AJ, Bowler FR, Churcher MJ, Jin L, Packman LC, Shlien A, Campbell P, Kirwan M, Dokal I, Warren AJ.** 2013. Aberrant 3' oligoadenylation of spliceosomal U6 small nuclear RNA in poikiloderma with neutropenia. *Blood* **121**:1028–1038.
32. **Brandmann T, Jinek M.** 2015. Crystal structure of the C-terminal 2',5'-phosphodiesterase domain of group a rotavirus protein VP3. *Proteins* **83**:997–1002.
33. **Ogden KM, Hu L, Jha BK, Sankaran B, Weiss SR, Silverman RH, Patton JT, Prasad BVV.** 2015. Structural Basis for 2'-5'-Oligoadenylate Binding and Enzyme Activity of a Viral RNase L Antagonist. *Journal of Virology* **89**:6633–6645.
34. **Sui B, Huang J, Jha BK, Yin P, Zhou M, Fu ZF, Silverman RH, Weiss SR, Peng G, Zhao L.** 2016. Crystal structure of the mouse hepatitis virus ns2 phosphodiesterase domain that antagonizes RNase L activation. *J Gen Virol* **97**:880–886.
35. **Corman VM, Kallies R, Philipps H, Göpner G, Müller MA, Eckerle I, Brünink S, Drosten C, Drexler JF.** 2014. Characterization of a novel betacoronavirus related to middle East respiratory syndrome coronavirus in European hedgehogs. *Journal of Virology* **88**:717–724.
36. **Anthony SJ, Johnson CK, Greig DJ, Kramer S, Che X, Wells H, Hicks AL, Joly DO, Wolfe ND, Daszak P, Karesh W, Lipkin WI, Morse SS, Mazet JAK, Goldstein T.** 2017. Global patterns in coronavirus diversity. *Virus Evol* **3**:vex012–vex012.
37. **Matthews KL, Coleman CM, van der Meer Y, Snijder EJ, Frieman MB.** 2014. The ORF4b-encoded accessory proteins of Middle East respiratory syndrome coronavirus and two related bat coronaviruses localize to the nucleus and inhibit innate immune signalling. *Journal of General Virology* **95**:874–882.
38. **Yang Y, Zhang L, Geng H, Deng Y, Huang B, Guo Y, Zhao Z, Tan W.** 2013. The structural and accessory proteins M, ORF 4a, ORF 4b, and ORF 5 of Middle East respiratory syndrome coronavirus (MERS-CoV) are potent interferon antagonists. *Protein & Cell* **4**:951–961.

39. **Canton J, Fehr AR, Fernandez-Delgado R, Gutierrez-Alvarez FJ, Sanchez-Aparicio MT, Garcia-Sastre A, Perlman S, Enjuanes L, Sola I.** 2018. MERS-CoV 4b protein interferes with the NF- $\kappa$ B-dependent innate immune response during infection. *PLOS Pathogens* **14**:e1006838.
40. **Yang Y, Ye F, Zhu N, Wang W, Deng Y, Zhao Z, Tan W.** 2015. Middle East respiratory syndrome coronavirus ORF4b protein inhibits type I interferon production through both cytoplasmic and nuclear targets. *Sci Rep* **5**.
41. **Talhouarne GJS, Gall JG.** 2018. Lariat intronic RNAs in the cytoplasm of vertebrate cells. *Proc Natl Acad Sci USA* **115**:E7970–E7977.
42. **Côté F, Lévesque D, Perreault JP.** 2001. Natural 2',5'-phosphodiester bonds found at the ligation sites of peach latent mosaic viroid. *Journal of Virology* **75**:19–25.
43. **Li X, Yang L, Chen L-L.** 2018. The Biogenesis, Functions, and Challenges of Circular RNAs. *Mol Cell* **71**:428–442.
44. **Zhang AY, Su S, Ng AP, Holik AZ, Asselin-Labat M-L, Ritchie ME, Law CW.** 2018. A data-driven approach to characterising intron signal in RNA-seq data. *bioRxiv* 1–15.
45. **Khalid MF, Damha MJ, Shuman S, Schwer B.** 2005. Structure-function analysis of yeast RNA debranching enzyme (Dbr1), a manganese-dependent phosphodiesterase. *Nucleic Acids Research* **33**:6349–6360.
46. **Montemayor EJ, Katolik A, Clark NE, Taylor AB, Schuermann JP, Combs DJ, Johnsson R, Holloway SP, Stevens SW, Damha MJ, Hart PJ.** 2014. Structural basis of lariat RNA recognition by the intron debranching enzyme Dbr1. *Nucleic Acids Research* **42**:10845–10855.
47. **Du M, Chen ZJ.** 2018. DNA-induced liquid phase condensation of cGAS activates innate immune signaling. *Science* **361**:704–709.
48. **Li X-D, Wu J, Gao D, Wang H, Sun L, Chen ZJ.** 2013. Pivotal roles of cGAS-cGAMP signaling in antiviral defense and immune adjuvant effects. *Science* **341**:1390–1394.
49. **Sun L, Wu J, Du F, Chen X, Chen ZJ.** 2013. Cyclic GMP-AMP synthase is a cytosolic DNA sensor that activates the type I interferon pathway. *Science* **339**:786–791.
50. **Sun B, Sundström KB, Chew JJ, Bist P, Gan ES, Tan HC, Goh**

- KC, Chawla T, Tang CK, Ooi EE.** 2017. Dengue virus activates cGAS through the release of mitochondrial DNA. *Sci Rep* **7**:3594.
51. **Yoneyama M, Kikuchi M, Matsumoto K, Imaizumi T, Miyagishi M, Taira K, Foy E, Loo Y-M, Gale M, Akira S, Yonehara S, Kato A, Fujita T.** 2005. Shared and unique functions of the DExD/H-box helicases RIG-I, MDA5, and LGP2 in antiviral innate immunity. *J Immunol* **175**:2851–2858.
52. **Dhir A, Dhir S, Borowski LS, Jimenez L, Teitell M, Rötig A, Crow YJ, Rice GI, Duffy D, Tamby C, Nojima T, Munnich A, Schiff M, de Almeida CR, Rehwinkel J, Dziembowski A, Szczesny RJ, Proudfoot NJ.** 2018. Mitochondrial double-stranded RNA triggers antiviral signalling in humans. *Nature* **560**:238–242.
53. **Jacob AG, Smith CWJ.** 2017. Intron retention as a component of regulated gene expression programs. *Human Genetics* **136**:1043–1057.
54. **Middleton R, Gao D, Thomas A, Singh B, Au A, Wong JJ-L, Bomane A, Cosson B, Eyraas E, Rasko JEJ, Ritchie W.** 2017. IRFinder: assessing the impact of intron retention on mammalian gene expression. *Genome Biol* **18**:51.
55. **Braunschweig U, Barbosa-Morais NL, Pan Q, Nachman EN, Alipanahi B, Gonatopoulos-Pournatzis T, Frey B, Irimia M, Blencowe BJ.** 2014. Widespread intron retention in mammals functionally tunes transcriptomes. *Genome Research* **24**:1774–1786.
56. **Wong JJ-L, Au AYM, Ritchie W, Rasko JEJ.** 2015. Intron retention in mRNA: No longer nonsense. *Bioessays* **38**:41–49.
57. **Chu DKW, Hui KPY, Perera RAPM, Miguel E, Niemeyer D, Zhao J, Channappanavar R, Dudas G, Oladipo JO, Traore A, Fassi-Fihri O, Ali A, Demissié GF, Muth D, Chan MCW, Nicholls JM, Meyerholz DK, Kuranga SA, Mamo G, Zhou Z, So RTY, Hemida MG, Webby RJ, Roger F, Rambaut A, Poon LLM, Perlman S, Drosten C, Chevalier V, Peiris M.** 2018. MERS coronaviruses from camels in Africa exhibit region-dependent genetic diversity. *Proceedings of the National Academy of Sciences* **115**:3144–3149.
58. **Welch EJ, Jones BW, Scott JD.** 2010. Networking with AKAPs: context-dependent regulation of anchored enzymes. *Mol Interv* **10**:86–97.
59. **Didychuk AL, Montemayor EJ, Carrocci TJ, DeLaitsch AT, Lucarelli SE, Westler WM, Brow DA, Hoskins AA, Butcher SE.** 2017. Usb1 controls U6 snRNP assembly through evolutionarily

divergent cyclic phosphodiesterase activities. *Nat Commun* **8**:497.

60. **Shchepachev V, Wischnewski H, Soneson C, Arnold AW, Azzalin CM.** 2015. Human Mpn1 promotes post-transcriptional processing and stability of U6atac. *FEBS Lett* **589**:2417–2423.
61. **Nomura Y, Roston D, Montemayor EJ, Cui Q, Butcher SE.** 2018. Structural and mechanistic basis for preferential deadenylation of U6 snRNA by Usb1. *Nucleic Acids Research* **46**:11488–11501.